ISSN 1881-7831 Online ISSN 1881-784X

DD&T

Drug Discoveries & Therapeutics

Volume 19, Number 2
April 2025

IRCA BSSA
IACMHR

www.ddtjournal.com

DD&T
Drug Discoveries & Therapeutics

ISSN: 1881-7831
Online ISSN: 1881-784X
CODEN: DDTRBX
Issues/Year: 6
Language: English
Publisher: IACMHR Co., Ltd.

Drug Discoveries & Therapeutics is one of a series of peer-reviewed journals of the International Research and Cooperation Association for Bio & Socio-Sciences Advancement (IRCA-BSSA) Group. It is published bimonthly by the International Advancement Center for Medicine & Health Research Co., Ltd. (IACMHR Co., Ltd.) and supported by the IRCA-BSSA.

Drug Discoveries & Therapeutics publishes contributions in all fields of pharmaceutical and therapeutic research such as medicinal chemistry, pharmacology, pharmaceutical analysis, pharmaceutics, pharmaceutical administration, and experimental and clinical studies of effects, mechanisms, or uses of various treatments. Studies in drug-related fields such as biology, biochemistry, physiology, microbiology, and immunology are also within the scope of this journal.

Drug Discoveries & Therapeutics publishes Original Articles, Brief Reports, Reviews, Policy Forum articles, Case Reports, Communications, Editorials, News, and Letters on all aspects of the field of pharmaceutical research. All contributions should seek to promote international collaboration in pharmaceutical science.

Editorial Board

International Field Chief Editors:

Nobuyoshi AKIMITSU
The University of Tokyo, Tokyo, Japan

Fen-Er CHEN
Fudan University, Shanghai, China

Hiroshi HAMAMOTO
Yamagata University, Yamagata, Japan

Takashi KARAKO
National Center for Global Health and Medicine, JIHS, Tokyo, Japan

Hongzhou LU
National Clinical Research Centre for Infectious Diseases, Shenzhen, Guangdong, China

Sven SCHRÖDER
University Medical Center Hamburg Eppendorf (UKE), Hamburg, Germany

Kazuhisa SEKIMIZU
Teikyo University, Tokyo, Japan

Corklin R. STEINHART
CAN Community Health, FL, USA

Associate Editors:

Feihu CHEN
Anhui Medical University, Hefei, Anhui, China

Jianjun GAO
Qingdao University, Qingdao, Shandong, China

Chikara KAITO
Okayama University, Okayama, Japan

Gagan KAUSHAL
Jefferson College of Pharmacy, Philadelphia, PA, USA

Hironori KAWAKAMI
Sanyo-Onoda City University, Yamaguchi, Japan

Xiao-Kang LI
National Research Institute for Child Health and Development, Tokyo, Japan

Yasuhiko MATSUMOTO
Meiji Pharmaceutical University, Tokyo, Japan

Atsushi MIYASHITA
Teikyo University, Tokyo, Japan

Tomofumi SANTA
The University of Tokyo, Tokyo, Japan

Tianqiang SONG
Tianjin Medical University, Tianjin, China

Sanjay K. SRIVASTAVA
Texas Tech University Health Sciences Center, Abilene, TX, USA

Hongbin SUN
China Pharmaceutical University, Nanjing, Jiangsu, China

Fengshan WANG
Shandong University, Jinan, Shandong, China.

Proofreaders:

Curtis BENTLEY
Roswell, GA, USA
Thomas R. LEBON
Los Angeles, CA, USA

Editorial and Head Office:

Pearl City Koishikawa 603,
2-4-5 Kasuga, Bunkyo-ku,
Tokyo 112-0003, Japan
E-mail: office@ddtjournal.com

Drug Discoveries & Therapeutics

Editorial and Head Office

Pearl City Koishikawa 603, 2-4-5 Kasuga, Bunkyo-ku,
Tokyo 112-0003, Japan

E-mail: office@ddtjournal.com
URL: www.ddtjournal.com

Editorial Board Members

Alex ALMASAN
(Cleveland, OH)
John K. BUOLAMWINI
(Memphis, TN)
Jianping CAO
(Shanghai)
Shousong CAO
(Buffalo, NY)
Jang-Yang CHANG
(Tainan)
Zhe-Sheng CHEN
(Queens, NY)
Zilin CHEN
(Wuhan, Hubei)
Xiaolan CUI
(Beijing)
Saphala DHITAL
(Clemson, SC)
Shaofeng DUAN
(Lawrence, KS)
Hao FANG
(Ji'nan, Shandong)
Marcus L. FORREST
(Lawrence, KS)
Tomoko FUJIYUKI
(Tokyo)
Takeshi FUKUSHIMA
(Funabashi, Chiba)
Harald HAMACHER
(Tübingen, Baden-Württemberg)
Kenji HAMASE
(Fukuoka, Fukuoka)
Junqing HAN
(Ji'nan, Shandong)
Xiaojiang HAO
(Kunming, Yunnan)
Kiyoshi HASEGAWA
(Tokyo)
Waseem HASSAN
(Rio de Janeiro)
Langchong HE
(Xi'an, Shaanxi)
Rodney J. Y. HO
(Seattle, WA)
Hsing-Pang HSIEH
(Zhunan, Miaoli)
Yongzhou HU
(Hangzhou, Zhejiang)
Youcai HU
(Beijing)
Yu HUANG
(Hong Kong)
Zhangjian HUANG
(Nanjing Jiangsu)
Amrit B. KARMARKAR
(Karad, Maharashra)
Toshiaki KATADA
(Tokyo)
Ibrahim S. KHATTAB
(Kuwait)
Shiroh KISHIOKA
(Wakayama, Wakayama)
Robert Kam-Ming KO
(Hong Kong)
Nobuyuki KOBAYASHI
(Nagasaki, Nagasaki)
Toshiro KONISHI
(Tokyo)
Peixiang LAN
(Wuhan, Hubei)
Chun-Guang LI
(Melbourne)
Minyong LI
(Ji'nan, Shandong)
Xun LI
(Ji'nan, Shandong)
Dongfei LIU
(Nanjing, Jiangsu)
Jian LIU
(Hefei, Anhui)
Jikai LIU
(Wuhan, Hubei)
Jing LIU
(Beijing)
Xinyong LIU
(Ji'nan, Shandong)
Yuxiu LIU
(Nanjing, Jiangsu)
Hongxiang LOU
(Jinan, Shandong)
Hai-Bin LUO
(Haikou, Hainan)
Xingyuan MA
(Shanghai)
Ken-ichi MAFUNE
(Tokyo)
Sridhar MANI
(Bronx, NY)
Tohru MIZUSHIMA
(Tokyo)
Jasmin MONPARA
(Philadelphia, PA)
Masahiro MURAKAMI
(Osaka)
Yoshinobu NAKANISHI
(Kanazawa, Ishikawa)
Munehiro NAKATA
(Hiratsuka)
Siriporn OKONOGI
(Chiang Mai)
Weisan PAN
(Shenyang, Liaoning)
Chan Hum PARK
(Eumseong)
Rakesh P. PATEL
(Mehsana, Gujarat)
Shivanand P. PUTHLI
(Mumbai, Maharashtra)
Shafiqur RAHMAN
(Brookings, SD)
Gary K. SCHWARTZ
(New York, NY)
Luqing SHANG
(Tianjin)
Yuemao SHEN
(Ji'nan, Shandong)
Rong SHI
(Shanghai)
Yoshitaka SHIMOTAI
(Yamagata)
Chandan M. THOMAS
(Bradenton, FL)
Michihisa TOHDA
(Sugitani, Toyama)
Li TONG
(Xining, Qinghai)
Murat TURKOGLU
(Istanbul)
Hui WANG
(Shanghai)
Quanxing WANG
(Shanghai)
Stephen G. WARD
(Bath)
Zhun WEI
(Qingdao, Shandong)
Tao XU
(Qingdao, Shandong)
Yuhong XU
(Shanghai)
Yong XU
(Guangzhou, Guangdong)
Bing YAN
(Ji'nan, Shandong)
Chunyan YAN
(Guangzhou, Guangdong)
Xiao-Long YANG
(Chongqing)
Yun YEN
(Duarte, CA)
Yongmei YIN
(Tianjin)
Yasuko YOKOTA
(Tokyo)
Yun YOU
(Beijing)
Rongmin YU
(Guangzhou, Guangdong)
Tao YU
(Qingdao, Shandong)
Guangxi ZHAI
(Ji'nan, Shandong)
Liangren ZHANG
(Beijing)
Lining ZHANG
(Ji'nan, Shandong)
Na ZHANG
(Ji'nan, Shandong)
Ruiwen ZHANG
(Houston, TX)
Xiu-Mei ZHANG
(Ji'nan, Shandong)
Xuebo ZHANG
(Baltimore, MD)
Yingjie ZHANG
(Ji'nan, Shandong)
Yongxiang ZHANG
(Beijing)
Haibing ZHOU
(Wuhan, Hubei)
Jian-hua ZHU
(Guangzhou, Guangdong)

(*As of April 2025*)

CONTENTS

Volume 19, Number 2, 2025

Original Article

Correspondence

Original Article

DOI: 10.5582/ddt.2025.01026

Silkworm (*Bombyx mori*) as a novel infection model for fish-derived *Aeromonas hydrophila*

Atsushi Miyashita[1], Kazuhiro Mikami[1,2], Hiroto Nakajima[1], Yidong Yu[1], Masanobu Miyauchi[1,3], Kazuhisa Sekimizu[4,*]

[1] Institute of Medical Mycology, Teikyo University, Tokyo, Japan;
[2] Graduate School of Medical Care and Technology, Teikyo University, Tokyo, Japan;
[3] Department of Psychology, Faculty of Liberal Arts, Teikyo University, Tokyo, Japan;
[4] School of Pharma-Science, Teikyo University, Tokyo, Japan.

SUMMARY: *Aeromonas hydrophila* is a significant pathogenic bacterium in aquaculture and the ornamental fish industry, causing lethal infections in fish and contributing to rising drug resistance. This leads to substantial economic losses and underscores the urgent need for new treatments and infection controls. However, the lack of a simple, sensitive infection model has hindered studies on the pathogenicity of *A. hydrophila* and therapeutic evaluation. This study introduces the silkworm (*Bombyx mori*) as a highly sensitive and cost-effective infection model for *A. hydrophila*. Using a strain isolated from diseased Wakins (goldfish), the pathogenicity of *A. hydrophila* was confirmed in silkworms, which exhibited a much lower median lethal dose (LD_{50} = 0.3 CFU/larva) compared to Wakins (LD_{50} = 5.1 × 10^6 CFU/g body weight). This demonstrates the silkworm's higher sensitivity to *A. hydrophila*. The *in vivo* efficacy of three antibiotics (gentamicin, kanamycin, and tetracycline) was also tested. Gentamicin and kanamycin prolonged survival in both models, while tetracycline also showed efficacy in both models, though its effect was weaker in the silkworm model. This highlights the silkworm model's utility in evaluating bactericidal agents against *A. hydrophila*. This model addresses key limitations of traditional fish infection models, including low sensitivity, long experimental durations, and high costs. The silkworm-based method enables efficient investigation of *A. hydrophila* pathogenicity and rapid screening of potential treatments, accelerating the development of new therapeutic strategies for aquaculture and beyond.

Keywords: Alternative models, silkworm, *Aeromonas*, fish infection, antibiotics

1. Introduction

Infectious disease research relies heavily on animal models to evaluate pathogenicity and develop therapeutic strategies. Traditionally, mammalian models such as mice and rats have been extensively used. However, they entail high costs, require specialized housing facilities, and raise ethical concerns related to animal welfare (*1,2*). Similarly, fish models like zebrafish are valuable for studies in aquatic toxicology and infectious diseases but necessitate specialized equipment for husbandry, limiting the scalability of experiments (*3,4*). These limitations underscore the urgent need for alternative infection models that are cost-effective, ethically acceptable, and easy to manipulate (*1,5*).

The silkworm (*Bombyx mori*) has emerged as a promising model that meets these criteria (*6-10*). Its large body size (4-5 cm in length) and ease of handling allow for precise experimental manipulations such as pathogen inoculation, drug administration, and tissue sampling (*11*). Moreover, silkworms can be reared inexpensively and in large numbers within a short timeframe, enabling large-scale experiments and the efficient acquisition of statistically significant data. Infection models using silkworms have been successfully established for human pathogens such as *Staphylococcus aureus*, *Pseudomonas aeruginosa*, and *Candida albicans*, facilitating the identification of virulence factors and the evaluation of antimicrobial drug efficacy (*12-14*). Additionally, the innate immune system of the silkworm shares significant similarities with those of mammals and fish, including Toll receptor-mediated responses, production of antimicrobial peptides, and phagocytosis by hemocytes (*15-17*), making it an excellent model for analyzing pathogen-host interactions.

Building on the successful use of silkworms as models for human pathogenic infections, this versatile animal model holds great potential for application to pathogens

affecting the aquaculture and ornamental fish industries. In these sectors, bacteria of the genus *Aeromonas*, particularly *Aeromonas hydrophila*, are responsible for lethal diseases and substantial economic losses (*18-20*). *A. hydrophila* is a Gram-negative bacterium and an opportunistic pathogen in fish (also in humans). It can cause widespread infections, inducing hemorrhagic septicemia and ulcerative diseases in fish, which lead to decreased productivity (*18*). The emergence of drug-resistant *A. hydrophila* strains has become a serious concern in recent years (*21*), highlighting the urgent need for new treatments and effective antimicrobial agents. To date, the pathogenicity of *A. hydrophila* has been evaluated primarily in fish or rodent models, such as channel catfish (*Ictalurus punctatus*) (*22*), rainbow trout (*Oncorhynchus mykiss*) (*23*), zebrafish (*Danio rerio*) (*24*), and mouse (*Mus musculus*) (*25*). However, these models are constrained by the various challenges, including high costs, ethical concerns, and limitations in scalability. While invertebrate models like the mealworm (*Tenebrio molitor*) (*26*) and the American crayfish (*Pacifastacus leniusculus*) (*27,28*) have been explored, assessments of *A. hydrophila* pathogenicity using these organisms have remained largely qualitative, lacking quantitative measures such as median lethal dose (LD_{50}) determinations.

In this study, we aim to establish a silkworm infection model for fish-derived *A. hydrophila*, enabling a quantitative evaluation of its pathogenicity and facilitating the assessment of candidate antimicrobial therapies for fish. To validate this model, we will first confirm whether *A. hydrophila* isolates from diseased Wakin goldfish (*Carassius auratus*) induce lethal infections in the silkworm. We will then quantify the LD_{50} in silkworms as an indicator of pathogenicity, thereby confirming the suitability of the silkworm model for evaluating potential antimicrobial treatments. Additionally, we will administer antibacterial agents to infected silkworms to evaluate therapeutic efficacy and confirm the model's suitability for assessing antimicrobial treatments. This silkworm-based research represents the first quantitative assessment of fish-derived *A. hydrophila* pathogenicity and antimicrobial efficacy using invertebrate alternative models, highlighting the potential of invertebrate model in aquaculture disease research. By establishing the silkworm as an efficient alternative infection model, we aim to enable large-scale experimentation and accelerate the development of new treatments, ultimately supporting more sustainable aquaculture practices.

2. Materials and Methods

2.1. Experimental animals

Wakin goldfish (*C. auratus*, body weight 1.3 g to 2.1 g) were purchased from a local supplier, Yoshida Fish Company, and Yoshida Aquarium Shop (Tokyo, Japan). The goldfish were maintained at 22℃ to 25℃ and were not fed after purchase and used for experiments on the following day. Eggs of the silkworm (*B. mori*) KINSYU × SHOWA strain were purchased from Ehime-Sanshu (Ehime, Japan) and reared as described previously (*8,9,29*).

2.2. Isolation, identification and preparation of *A. hydrophila*

The *A. hydrophila* strain used in the study was isolated from diseased Wakin goldfish (*C. auratus*) in our laboratory using brain heart infusion (BHI) agar plate, which were then subjected to DNA extraction, polymerase chain reaction (PCR) amplification of the 16S rRNA region, and sequencing (by conventional dideoxy method). Species identification was confirmed through BLAST analysis (*https://blast.ncbi.nlm.nih.gov/Blast.cgi*) using the standard nucleotide BLAST. The search databases were the 16S ribosomal RNA sequences for bacteria and archaea database, and the nucleotide collection (nr/nt). We included the nucleotide collection in addition to the 16S ribosomal RNA database, because 16S ribosomal sequences for some bacterial isolates were only registered in the nucleotide collection while not in the 16S ribosomal RNA database.

For experiments in this study, the obtained *A. hydrophila* strain was cultured overnight at 30℃ in BHI medium with shaking at 200 rpm. Afterwards, the bacterial culture was washed with physiological saline (0.9% NaCl) by centrifugation at 8,400 *g* for 5 minutes, and the pellet was resuspended in an equal volume of saline to the original culture medium. The concentrations of the bacterial suspensions utilized in the experiments was determined based on colony counts on agar plates.

2.3. Phylogenetic analysis

The obtained 16S rRNA gene sequence was aligned with reference sequences retrieved from the NCBI GenBank database using Clustal Omega. The phylogenetic analysis included the following reference strains: *A. media* ATCC33907, *A. hydrophila* ATCC49140, *A. hydrophila* subsp. LMG19562T, and *A. caviae* ATCC15468. Branch lengths represent genetic distances.

2.4. Infection experiments

In the infection experiments, prepared bacterial suspensions were used to infect both goldfish and silkworms. For goldfish, 50 μL of the bacterial suspension was injected intraperitoneally using a 1-mL syringe with a 27-gauge needle. Silkworms received the same volume (50 μL), injected into the hemolymph with a 27-gauge needle as described previously (*30,31*). The

control groups were injected with the same volume of physiological saline. The number of surviving individuals was observed at two days post-infection.

2.5. Antimicrobial susceptibility testing

Antimicrobial susceptibility testing involved measuring the minimum inhibitory concentrations (MICs) of antibiotics against *A. hydrophila*. The antibiotics used were gentamicin, kanamycin, tetracycline, and norfloxacin, all of which were purchased from FUJIFILM Wako Pure Chemical Corporation (Osaka, Japan). MICs were measured using the broth microdilution method with twofold serial dilutions as described previously (*14*). Cultures were incubated at 30°C, and bacterial growth was visually inspected after 24 hours.

2.6. Therapeutic efficacy of selected antibiotics in goldfish (Wakin) and silkworm models

Among the four antibiotics, norfloxacin was poorly soluble in physiological saline to deliver in the host animals. Hence, we excluded norfloxacin from the *in vivo* therapeutic efficacy evaluation. The infection doses were set at 1×10^7 CFU/g body weight for goldfish and 1×10^2 CFU/larva for silkworms, based on the earlier pathogenicity assessment. Each of the three antibiotics (*i.e.*, gentamicin, kanamycin, tetracycline) was dissolved in physiological saline at the desired concentration. After bacterial inoculation, Wakin goldfish and silkworms (n = 4 for each dose) received 50 µL of the antibiotic solution, ether intraperitoneally (for Wakin) or into the hemolymph (for silkworms). Control groups were administered an equivalent volume of physiological saline. The number of survivors was recorded two days post-infection.

2.7. Data analysis and figure drawing

Data analysis was conducted using R (version 4.2.2). We used *dplyr* for data manipulation, *ggplot2* for data visualization, *drc* for dose-response curve analysis, and *readxl* for data import. Dose-response curves were fitted with the *drm* function in *drc*, using a four-parameter logistic model (LL.4). The upper and lower limits were fixed at 1 and 0, respectively. Median lethal (LD_{50}) and effective (ED_{50}) doses were estimated using the ED function. Plots of dose-response curves and other visualization were generated with ggplot2. All presentation materials including graphs and photos were organized using Affinity Designer.

3. Results

3.1. Silkworms exhibit an extreme susceptibility to *A. hydrophila* infection

The *A. hydrophila* strain used in this study (Figure 1a) was isolated from diseased Wakin goldfish (*C. auratus*), with the species identification using BLAST analysis of 16S ribosomal RNA gene sequence (see Figure 1b for phylogenetic tree). The pathogenicity of the isolated *A. hydrophila* strain was evaluated by infecting Wakin goldfish and silkworms (*B. mori*) with the pathogen. Infection resulted in mortality in both hosts within two days post-inoculation, and the lethality was dose-dependent (Figures 2a and 2b for goldfish, and Figures 2c and 2d for silkworms). The LD_{50} was determined to be 5.1×10^6 CFU (colony-forming units)/g body weight for goldfish and 0.30 CFU/larva (average body weight of the silkworm is approximately 2 g, giving ca. 0.15 CFU/g body weight) for silkworms. These results suggests that the silkworm (*B. mori*) can be used as an alternative model for *Aeromonas* infection, with a million-fold susceptibility that enables a rapid and efficient screening for antimicrobials.

3.2. Antibiotic susceptibility testing of isolated *A. hydrophila*

To perform a validation study to confirm therapeutic

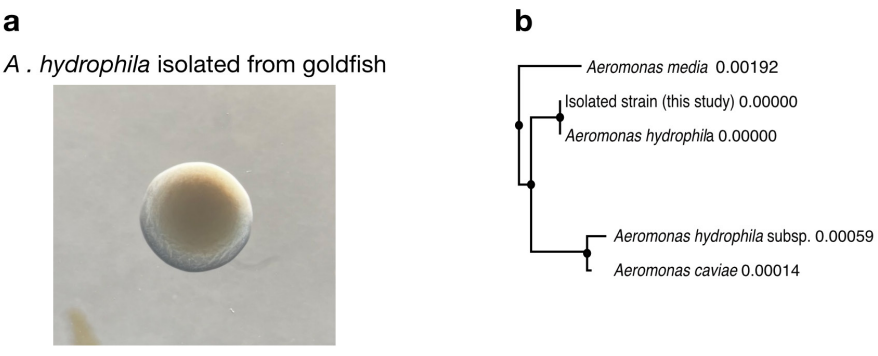

Figure 1. The Aeromonas hydrophila strain isolated in this study. a: Microscopic image of *A. hydrophilia* colony isolated from diseased goldfish. **b**: Phylogenetic tree based on 16S rRNA gene sequences, showing the relationship between the isolated strain and closely related *Aeromonas* species. The isolated strain exhibits 100% identity with the *A. hydrophila*. The phylogenetic analysis includes *A. media* ATCC33907, *A. hydrophila* ATCC49140, *A. hydrophila* subsp. LMG19562T, and *A. caviae* ATCC15468. Branch lengths represent genetic distances.

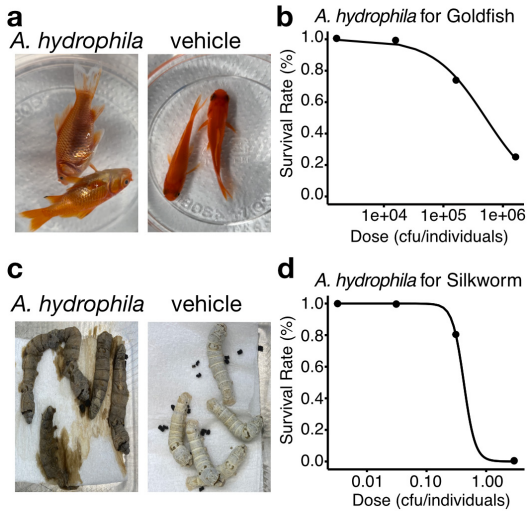

Figure 2. Infection susceptibility of the Wakin goldfish and the silkworm to *A. hydrophila*. **a**: Wakin goldfish succumbed to *A. hydrophila* infection (left panel; infected dose: 6.3×10^6 CFU/g body weight). The right panel shows the control group treated with saline (vehicle). **b**: Dose-response curve showing the survival rate of Wakin goldfish after *A. hydrophila* infection. The x-axis represents the logarithmic bacterial dose, and the y-axis shows the survival rate. Black dots indicate observed survival rates at each dose ($n = 4$). The LD_{50} was calculated as 5.1×10^6 CFU/g body weight. **c**: Silkworms succumbed to *A. hydrophila* infection (left panel; infected dose: 93 CFU/larva). The right panel shows the control group treated with saline (vehicle). **d**: Dose-response curve showing the survival rate of silkworms after *A. hydrophila* infection. The x-axis represents the logarithmic bacterial dose, and the y-axis shows the survival rate. Black dots indicate observed survival rates at each dose ($n = 4$). The LD_{50} was calculated as 0.3 CFU/larva.

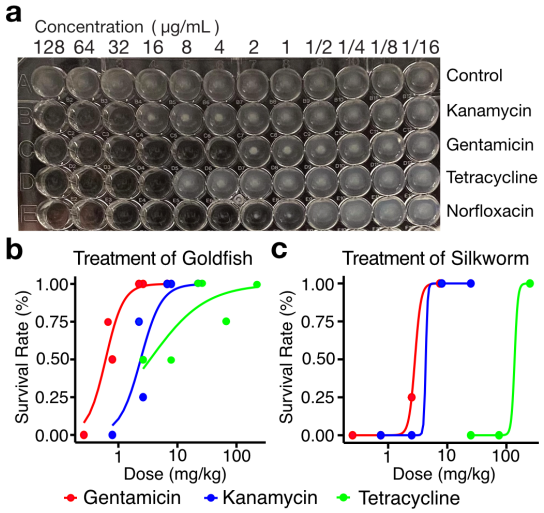

Figure 3. Comparative study on antimicrobial chemotherapy in the goldfish and the silkworm models. **a**: The antimicrobial susceptibility of the isolated *A. hydrophila* strain was evaluated using the broth microdilution method. Bacterial growth was assessed based on turbidity, with clear wells indicating growth inhibition. The MIC values (Table 1) were defined as the lowest antibiotic concentrations that completely inhibited visible bacterial growth. **b**: Therapeutic effects of antimicrobial agents on Wakin goldfish infected with *A. hydrophila*. The y-axis shows survival rates, and the x-axis indicates antibiotic concentration ($n = 4$). ED_{50} values were 0.6 mg/kg for gentamicin, 2.4 mg/kg for kanamycin, and 3.4 mg/kg for tetracycline. **c**. Therapeutic effects of antimicrobial agents on silkworms infected with *A. hydrophila*. The y- axis shows survival rates, and the x-axis indicates antibiotic concentration ($n = 4$). ED_{50} values for these antibiotics were 2.8 mg/kg for gentamicin, 4.3 mg/kg for kanamycin, and 137.6 mg/kg for tetracycline.

efficacy of known antimicrobials using the silkworm-based *A. hydrophila* infection model, we first tested four antimicrobials for their antibacterial activities to the obtained *A. hydrophila* strain. The MICs of the four antibiotics (kanamycin, gentamicin, tetracycline, and norfloxacin) were 32 μg/mL for kanamycin, 4.0 μg/mL for gentamicin, 16 μg/mL for tetracycline, and 1.0 μg/mL for norfloxacin (Figure 3a). These results indicate that the isolated *A. hydrophil*a strain is highly sensitive to gentamicin and norfloxacin but shows lower sensitivity to kanamycin and tetracycline.

3.3. Gentamicin shows the highest therapeutic efficacy against *A. hydrophila* infection in both goldfish and silkworm models

3.3.1. Goldfish

After *A. hydrophila* infection, six different doses of each antibiotic were given to the host animal. All infected goldfish treated with physiological saline died within 24 hours, whereas survival rates in antibiotic-treated groups improved in a dose-dependent manner (Figure 3b). The median ED_{50} for each antimicrobial is listed in Table 1. Gentamicin demonstrated the highest efficacy, with the lowest ED_{50} value of 0.6 mg/kg. In comparison, kanamycin and tetracycline exhibited ED_{50} values of 2.4 mg/kg and 3.4 mg/kg, respectively. These findings highlight gentamicin as the most effective antibiotic against *A. hydrophila* infections in goldfish, requiring the lowest dose to achieve therapeutic effects.

3.3.2. Silkworms

The therapeutic efficacy of the three antibiotics was also evaluated using the silkworm infection model. Following *A. hydrophila* infection, silkworms treated with physiological saline experienced 100% mortality, whereas antibiotic-treated groups (four different doses for each antibiotic, except for tetracycline, which were tested at three doses) showed improved survival in a dose-dependent manner (Figure 3c). The ED_{50} values are presented in Table 1. Gentamicin and kanamycin showed ED_{50} values of 2.8 mg/kg and 4.3 mg/kg, respectively. In contrast, tetracycline exhibited a significantly higher ED_{50} of 138 mg/kg. These results suggest that gentamicin and kanamycin (both bactericidal aminoglycoside antibiotics) are more effective than tetracycline (a bacteriostatic antibiotic) in the silkworm model of *A. hydrophila* infection.

3.3.3. Comparison of the two models

Table 1. Median effective doses (ED_{50}) and ED_{50}/MIC (minimal inhibitory concentration) ratios of antimicrobial agents in the goldfish and silkworm infection models of *A. hydrophila*

Antibiotics	ED_{50} (mg/kg)		MIC (μg/mL)	ED_{50}/MIC ratio	
	Goldfish	Silkworm		Goldfish	Silkworm
Gentamicin	0.6	2.8	4	0.15	0.71
Kanamycin	2.4	4.3	32	0.07	0.14
Tetracycline	3.4	137.6	16	0.21	8.60

The ED_{50}/MIC ratios of gentamicin and kanamycin were relatively small and comparable between the goldfish and silkworm models (0.15 and 0.71 for gentamicin; 0.070 and 0.14 for kanamycin; see Table 1). These findings indicate that gentamicin and kanamycin (bactericidal antibiotics) maintain their efficacy *in vivo*, aligning well with their *in vitro* activity (*12*). In contrast, tetracycline (a bacteriostatic antibiotic) exhibited a markedly higher ED_{50}/MIC ratio in the silkworm model (8.6) compared to the goldfish model (0.21).

4. Discussion

4.1. A silkworm-based novel infection model of *A. hydrophila*

In the present study, we evaluated the pathogenicity and antibiotic susceptibility of *A. hydrophila* using both Wakin goldfish (*C. auratus*) and silkworms (*B. mori*) as infection models. *A. hydrophila* induced lethal infections within two days post-inoculation in both hosts. The median lethal dose (LD_{50}) values were 5.1×10^6 CFU/g body weight for goldfish and only 0.30 CFU/larva for silkworms, underscoring the silkworm model's potential for rapid and efficient *in vivo* screening of anti–*A. hydrophila* compounds.

The use of silkworms offers several advantages over other animal models. Compared with mammalian systems such as mice or rats, silkworms lower both ethical and economic burdens. They also require less specialized maintenance than fish models like zebrafish (*3,4*). Notably, silkworms' pronounced susceptibility to infection enables sensitive and reproducible detection of pathogenicity differences among bacterial strains (*13*), including those with low virulence or lacking key virulence factors. However, because of this extreme sensitivity, the silkworm model may not always distinguish subtle differences in pathogenicity among highly virulent strains. Addressing this issue will require identifying key factors that drive both bacterial pathogenicity and silkworm susceptibility, thereby broadening the utility of this model for analyzing a broader spectrum of pathogenic microbes.

4.2. Correlation of antibacterial effectiveness across models

We next evaluated antibiotic efficacy in both silkworms and goldfish inoculated with *A. hydrophila*. Despite the rapid disease progression in silkworms, dose-dependent therapeutic effects were clearly demonstrated, as survival rates improved with antibiotic administration in both models. These findings confirm that the silkworm model can quantitatively assess antibacterial activity, providing a feasible platform for screening new or existing drugs against fish-associated bacterial pathogens. Because experimental studies can be conducted efficiently and cost-effectively in silkworms, this model has considerable potential for accelerating drug discovery for aquaculture. Moreover, previous reports indicate that the pharmacokinetics (ADME: Absorption, Distribution, Metabolism, Excretion) of many antibiotics in silkworms correlate well with those in mammals (*32*). Therefore, results obtained from the silkworm model may have broader relevance for treating infections in both fish and mammalian systems. Further investigation into pharmacokinetic and pharmacodynamic parameters in silkworms and fish will enhance confidence in the model's translational value for aquaculture and beyond.

Among the three antibiotics tested (gentamicin, kanamycin, and tetracycline), the aminoglycosides (gentamicin and kanamycin) exhibited particularly high efficacy in both goldfish and silkworms. A potential explanation for this finding is linked to the exceptionally high susceptibility of silkworms to *A. hydrophila*, which may reflect a relative lack of immune mechanisms against this pathogen. In other words, silkworms could be considered in an "immunosuppressed" state regarding *A. hydrophila* infection. Because bactericidal antibiotics like aminoglycosides directly kill bacteria, they do not rely as heavily on the host's immune system to clear infection; thus, they provided a marked therapeutic benefit in silkworms. In contrast, bacteriostatic antibiotics such as tetracycline primarily inhibit bacterial growth; full clearance typically requires an intact host immune response to remove nonreplicating microbes. When the host's defense mechanisms are weakened or insufficient (*e.g.*, in silkworms lacking certain vertebrate-like adaptive immune components), bacteriostatic agents may not achieve a sufficient therapeutic effect. This distinction underscores the importance of understanding the host's immune capacity when evaluating antibiotic efficacy, particularly in model organisms with reduced or simplified immune systems.

4.3. Limitation of the study

Despite our findings, the underlying reason for silkworms' extreme susceptibility to *A. hydrophila* remains unclear. One possibility is that, unlike vertebrates, silkworms lack an adaptive immune system, potentially reducing their ability to control bacterial proliferation. Moreover, *A. hydrophila* may produce specific factors that evade or suppress innate immune responses, making silkworms (reliant solely on innate immunity) especially vulnerable to infection. Alternatively, silkworm physiology may offer conditions highly conducive to rapid bacterial growth. Elucidating these mechanisms will provide deeper insights into the virulence strategies of *A. hydrophila* and may inform novel approaches to preventing and treating infections in other hosts.

5. Conclusion

This study demonstrates that both silkworms (*B. mori*) and Wakin goldfish (*C. auratus*) can serve as valuable infection models for evaluating the pathogenicity of *A. hydrophila* and assessing antibiotic efficacy. Silkworms exhibited extreme sensitivity to *A. hydrophila* (an LD_{50} of 0.30 CFU/larva), making them particularly useful for detecting low-pathogenicity strains, compared with goldfish (an LD_{50} of 5.1×10^6 CFU/g body weight). Among the antibiotics tested, aminoglycosides (gentamicin and kanamycin) showed dose-dependent therapeutic effects in both models, highlighting the potential of silkworms for cost-effective, large-scale antibiotic screening. Moreover, the simplicity of silkworm husbandry and reduced ethical concerns further underscore their suitability for infection research. Future studies focusing on pharmacokinetic and pharmacodynamic correlations between silkworms and fish will likely expand the applicability and reliability of the silkworm model, contributing to improved infectious disease control in aquaculture and the development of novel therapeutic strategies.

Acknowledgements

We thank Genome Pharmaceuticals Institute, Inc., for technical assistance for the study. This work was supported by JSPS KAKENHI (Grant# 22K15461, AM), the Research and implementation promotion program through open innovation grants (Grant# JPJ011937, to the consortium where AM serves as a member) from the Project of the Bio-oriented Technology Research Advancement Institution (BRAIN), and a Teikyo University Team Research Grant (Grant# 22–24, AM).

Funding: None.

Conflict of Interest: The authors have no conflicts of interest to disclose.

References

1. Kaito C, Murakami K, Imai L, Furuta K. Animal infection models using non-mammals. Microbiol Immunol. 2020; 64:585-592.
2. Walker RL, Eggel M. From mice to monkeys? Beyond orthodox approaches to the ethics of animal model choice. Animals (Basel). 2020; 10:77.
3. Ribas L, Piferrer F. The zebrafish (*Danio rerio*) as a model organism, with emphasis on applications for finfish aquaculture research. Rev Aquac. 2014; 6:209-240.
4. Li H, Liu Y, Chen Q, Jin L, Peng R. Research progress of zebrafish model in aquatic ecotoxicology. Water. 2023; 15:1735.
5. Rees DA, Alcolado JC. Animal models of diabetes mellitus. Diabet Med. 2005; 22:359-370.
6. Tabuchi F, Mikami K, Miyauchi M, Sekimizu K, Miyashita A. Discovery of new AMR drugs targeting modulators of antimicrobial activity using *in vivo* silkworm screening systems. Antibiot (Tokyo). 2025; 78:69-77.
7. Miyashita A, Kataoka K, Tsuchida T, Ogasawara AA, Nakajima H, Takahashi M, Sekimizu K. High molecular weight glucose homopolymer of broccoli (*Brassica oleracea* var. *italica*) stimulates both invertebrate and mammalian immune systems. Front Food Sci Technol. 2023; 3. DOI: 10.3389/frfst.2023.1012121
8. Miyashita A, Mitsutomi S, Mizushima T, Sekimizu K. Repurposing the PDMA-approved drugs in Japan using an insect model of staphylococcal infection. FEMS Microbes. 2022; 3:xtac014.
9. Li W, Miyashita A, Sekimizu K. Peanut triacylglycerols activate innate immunity both in insects and mammals. Sci Rep. 2022; 12:1-9.
10. Miyashita A, Sekimizu K. Using silkworms to search for lactic acid bacteria that contribute to infection prevention and improvement of hyperglycemia. Drug Discov Ther. 2021; 15:51-54.
11. Kaito C, Akimitsu N, Watanabe H, Sekimizu K. Silkworm larvae as an animal model of bacterial infection pathogenic to humans. Microb Pathog. 2002; 32:183-190.
12. Hamamoto H, Kurokawa K, Kaito C, Kamura K, Manitra Razanajatovo I, Kusuhara H, Santa T, Sekimizu K. Quantitative evaluation of the therapeutic effects of antibiotics using silkworms infected with human pathogenic microorganisms. Antimicrob Agents Chemother. 2004; 48:774-779.
13. Kaito C, Sekimizu K. A silkworm model of pathogenic bacterial infection. Drug Discov Ther. 2007; 1:89-93.
14. Hamamoto H, Urai M, Ishii K, *et al*. Lysocin E is a new antibiotic that targets menaquinone in the bacterial membrane. Nat Chem Biol. 2015; 11:127-133.
15. Taniai K, Wago H, Yamakawa M. *In vitro* phagocytosis of *Escherichia coli* and release of lipopolysaccharide by adhering hemocytes of the silkworm, *Bombyx mori*. Biochem Biophys Res Commun. 1997; 231:623-627.
16. Wu S, Zhang X, Chen X, Cao P, Beerntsen BT, Ling E. BmToll9, an Arthropod conservative Toll, is likely involved in the local gut immune response in the silkworm, *Bombyx mori*. Dev Comp Immunol. 2010;

34:93-96.
17. Cheng T, Zhao P, Liu C, Xu P, Gao Z, Xia Q, Xiang Z. Structures, regulatory regions, and inductive expression patterns of antimicrobial peptide genes in the silkworm *Bombyx mori*. Genomics. 2006; 87:356-365.
18. Chakraborty N, Das BK, Bera AK, Borah S, Mohanty D, Yadav AK, Kumar J, Koushlesh SK, Chanu TN, Panda SP, Vallangi R. Co-prevalence of virulence and pathogenic potential in multiple antibiotic resistant *Aeromonas* spp. from diseased fishes with *in silico* insight on the virulent protein network. Life. 2022; 12:1979.
19. Beaz-Hidalgo R, Figueras MJ. *Aeromonas* spp. whole genomes and virulence factors implicated in fish disease. J Fish Dis. 2013; 36:371-388.
20. Hossain S, Dahanayake PS, De Silva BCJ, Wickramanayake M, Wimalasena S, Heo GJ. Multidrug resistant *Aeromonas* spp. isolated from zebrafish (*Danio rerio*): antibiogram, antimicrobial resistance genes and class 1 integron gene cassettes. Lett Appl Microbiol. 2019; 68:370-377.
21. Hossain S, Heo GJ. Ornamental fish: a potential source of pathogenic and multidrug-resistant motile *Aeromonas* spp. Lett Appl Microbiol. 2021; 72:2-12.
22. De Figueiredo J, Plumb JA. Virulence of different isolates of *Aeromonas hydrophila* in channel catfish. Aquaculture. 1977; 11:349-354.
23. Newaj-Fyzul A, Adesiyun AA, Mutani A, Ramsubhag A, Brunt J, Austin B. Bacillus subtilis AB1 controls Aeromonas infection in rainbow trout (Oncorhynchus mykiss, Walbaum). J Appl Microbiol. 2007; 103:1699-706.
24. Romero A, Saraceni PR, Merino S, Figueras A, Tomás JM, Novoa B. The animal model determines the results of *Aeromonas* virulence factors. Front Microbiol. 2016; 7.
25. Wong CYF, Heuzenroeder MW, Flower RLP. Inactivation of two haemolytic toxin genes in *Aeromonas hydrophila* attenuates virulence in a suckling mouse model. Microbiology (Reading). 1998; 144 (Pt 2):291-298.
26. Noonin C, Jiravanichpaisal P, Söderhäll I, Merino S, Tomás JM, Söderhäll K. Melanization and pathogenicity in the insect, *Tenebrio molitor*, and the crustacean, *Pacifastacus leniusculus*, by *Aeromonas hydrophila* AH-3. PLoS One. 2011; 5:e15728.
27. Jiravanichpaisal P, Roos S, Edsman L, Liu H, Söderhäll K. A highly virulent pathogen, *Aeromonas hydrophila*, from the freshwater crayfish *Pacifastacus leniusculus*. J Invertebr Pathol. 2009; 101:56-66.
28. Zeng Y. *Aeromonas hydrophila*, one reason causing the death of freshwater crayfish *Procambarus clarkii* (Girard, 1852). Iran J Fish Sci. 2020; 19:1770-1779.
29. Miyashita A, Hamamoto H, Sekimizu K. Applying the silkworm model for the search of immunosuppressants. Drug Discov Ther. 2021; 15:139-142.
30. Miyashita A, Kizaki H, Kawasaki K, Sekimizu K, Kaito C. Primed immune responses to gram-negative peptidoglycans confer infection resistance in silkworms. J Biol Chem. 2014; 289:14412-14421.
31. Miyashita A, Iyoda S, Ishii K, Hamamoto H, Sekimizu K, Kaito C. Lipopolysaccharide O-antigen of enterohemorrhagic *Escherichia coli* O157:H7 is required for killing both insects and mammals. FEMS Microbiol Lett. 2012; 333:59-68.
32. Panthee S, Paudel A, Hamamoto H, Sekimizu K. Advantages of the silkworm as an animal model for developing novel antimicrobial agents. Front Microbiol. 2017; 8:373.

Received March 27, 2025; Accepted April 15, 2025.

*Address correspondence to:
Kazuhisa Sekimizu, School of Pharma-Science, Teikyo University, Tokyo, Japan.
E-mail: sekimizu@main.teikyo-u.ac.jp

Released online in J-STAGE as advance publication April 27, 2025.

Original Article

DOI: 10.5582/ddt.2025.01025

Practical training reduces aspiration-linked gaps in pressure ulcer education for pharmacy students

Shingo Kondo[1,2], Ririka Mima[1], Rira Okui[1], Hiroki Iwata[1,2], Yoshiko Kawamoto[2], Noriko Kobayashi[1,2], Katsunori Furuta[3], Katsunori Yamaura[1,2,*]

[1] Division of Social Pharmacy, Center for Social Pharmacy and Pharmaceutical Sciences, Faculty of Pharmacy, Keio University, Tokyo, Japan;
[2] Keio University Community Pharmacy, Tokyo, Japan;
[3] Department of Pressure Ulcer Care, Kobayashi Memorial Hospital, Aichi, Japan.

SUMMARY: Expectations for pharmacists' contribution and involvement in pressure ulcer pharmacotherapy are growing. This study aimed to not only clarify the effects of incorporating practical training on the use of topical medications into clinical preparatory education but also examine the relationship between students' aspiration—or lack thereof—to pursue a career as a pharmacist. The percentage of positive responses to the questionnaire survey on knowledge, skills, and attitudes toward pressure ulcer treatment was significantly higher after the lecture than before and highest after the practical training. In addition, students who aspired to become pharmacists tended to provide a higher percentage of positive responses after the lecture. However, the gap between aspiring and non-aspiring pharmacists tended to narrow after practical training. These results suggest that incorporating practical training on pressure ulcer treatment into lectures improves students' knowledge, skills, and attitudes toward its treatment. Including practical training in pressure ulcer education may compensate for the difference in the educational effect of lectures between students who aspire to become pharmacists and those who do not, thereby improving the educational effect for the latter.

Keywords: pressure ulcer, pharmaceutical education, practical training, career path, medical simulator

1. Introduction

Pressure ulcers, also known as decubitus ulcers, are a global concern in the therapeutic care of patients, as they have been associated with increased mortality rates in elderly patients (*1,2*). In 2009, the Japanese Society of Pressure Ulcers defines pressure ulcers as irreversible hemorrhagic injuries that appear when external force is applied to the body and blood flow in soft tissues between bones and the skin surface is continuously reduced or stopped. Pressure ulcers are a common complication of immobility among older adult patients (*3*), who are bedridden for long periods of time, and once they develop, they are known to be refractory. The number of patients with bedsores is expected to increase in Japan's super-aging society, both in hospitals and at home, highlighting the urgent need to address this issue. In fact, data from the Washington State Department of Health revealed that hospitalized patients with pressure ulcers have an average increase of 10.8 days in their length of stay (*4*). Although topical drugs have been commonly used in the topical treatment of bedsores, the Furuta Method, which involves drug selection based on the characteristics of the base agent, is also widely used (*5*). After Furuta *et al*. reported that pharmacists' participation in bedsore treatment is effective in not only shortening the duration of treatment but also reducing medical costs, expectations for the contribution of pharmacists in bedsore treatment have been high (*6*).

In 2014, the Ministry of Health, Labour and Welfare (MHLW) issued the "Handling of Practical Guidance on the Use of Medicines," allowing pharmacists to impart practical guidance on the application or injection of dispensed topical drugs without medical judgment or skill. In addition, in the 2022 revision of medical service fees, descriptions of pharmacological management and collaboration with pharmacists were added to the criteria for bedsore control, which is stipulated as a requirement for basic inpatient fees. Furthermore, the "Action Plan for Pharmacists to Play an Active Role in the Community" issued by MHLW in 2022 calls for the interdisciplinary promotion of measures for bedsores, including practical guidance by pharmacists

on how to apply topical medicines. The incidence and prevalence of pressure ulcers can be reduced through team care involving management by pharmacists (*7*). Thus, there exists a growing need for pharmacists to participate in bedsore treatment in Japan. However, active participation in pressure ulcer treatment through practical instruction in topical medications is not high. Currently, the Japanese Society of Pressure Ulcers and other organizations are imparting practical training for pharmacists using a pressure ulcer simulator to improve their skills in teaching topical medication. However, to increase the number of pharmacists engaged in bedsore treatment, approaches from pharmacy education are also deemed necessary.

In Japan, a six-year educational program has been implemented in pharmacy universities for pharmacist training. Pre-clinical training for pharmacist practice is imparted in the fourth year within the university setting and, in the fifth year, students undergo pharmacy experiential training in community pharmacies and hospitals, interacting with actual patients under the supervision of licensed pharmacists. The Model Core Curriculum for Pharmaceutical Education, revised in 2013 and 2022 does not list bedsores as a required component of pre-clinical training for pharmacist practice, although they are a required component of pharmacy experiential training. Therefore, learning about bedsores in a practical training format in addition to lectures at universities can be expected to be effective. Pressure ulcer simulators are widely used in practical training for pharmacists engaged in pressure ulcer treatment. However, the educational effect of using a similar simulator for the practical training of pharmacy students without practical experience is unknown. At the Faculty of Pharmacy, Keio University, approximately 40% of graduates are employed as pharmacists in hospitals and community pharmacies. While they are likely to be involved in pressure ulcer treatment as pharmacists, in other career paths, opportunities for involvement are almost nonexistent. A study on the motivational factors involved in nursing students' practical training revealed that acquiring the skills necessary to become a nurse was also a motivational factor (*8*). In pressure ulcer education, the aspiration, or lack thereof, to become a pharmacist may influence students' motivation to learn and the effectiveness of education. However, these details are unexplored.

In this study, we administered a questionnaire survey to clarify the educational effects of including a practical training course on the practical guidance of topical medication using a pressure ulcer simulator after the conventional lecture as part of the clinical preparatory education for bedsores for fourth-year pharmacy students. We also examined the relationship between the educational effects and whether students want to become pharmacists as a future career path.

2. Materials and Methods

2.1. Subjects and survey methods

A 90-minute lecture on pressure ulcers was given to 138 fourth-year students from the Department of Pharmacy, Faculty of Pharmaceutical Sciences (6-year course), Keio University, on April 24, 2024, in accordance with the syllabus for the 2024 academic year. The students were divided into four groups, undergoing a practical training session on pressure ulcers, which lasted 210 minutes (comprising 90 minutes of classroom lecture and 120 minutes of practical training) on one of the four days from May 20 to 23, 2024. During the practical training, students learned how to teach topical application of drugs in accordance with the Furuta Method using a pressure ulcer simulator (Japan Sleeve Scientific Co., Ltd., Niigata, Japan), which was loaned, free of charge, by Kaken Pharma Co. Students who attended the lectures and practical training were surveyed three times – before, after the lecture, and after the practical training – using a self-administered Google Form. To avoid absenteeism, the pre- and post-lecture surveys were conducted 15 minutes before and 15 minutes after the lecture, respectively. As no student was absent during the practical training, the deadline for responses after the practical training was the day after the training was completed (May 24, 2024).

2.2. Survey items

The questionnaire comprised 9 questions (Supplementary Figure S1, *https://www.ddtjournal.com/supplementaldata/254*). Questions 1–5 sought to determine students' knowledge of pressure ulcers; questions 6–8, their skills and attitudes toward pressure ulcer treatment; and question 9, their intention to pursue a career as a licensed pharmacist in the future. The post-lecture and post-practice questionnaires included a section for post-lecture comments (question 10). Questions 1–8 were five-choice questions rated on a 4-point Likert scale, with "not sure" responses being excluded.

2.3. Data analysis

The most positive responses (know/think/imagine) on the 4-point Likert scale were analyzed. The relationship between educational effectiveness and aspiration to become a pharmacist was analyzed by dichotomizing the highest rating on the scale and the rest of the responses. Simple and cross-tabulations were conducted using Microsoft® Excel® 365 MSO (16.0.18025.20160). Kruskal-Wallis tests and Mann-Whitney *U*-tests were conducted at a significance level of 0.05, using IBM® SPSS® Statistics Version 29.0.0.0 (241) (IBM Japan, Tokyo, Japan).

2.4. Ethical considerations

This study was planned in compliance with the "Ethical Guidelines for Research of the Japanese Society for Medical Education" (effective July 26, 2012) and approved by the Research Ethics Committee for Human Subjects, Faculty of Pharmaceutical Sciences, Keio University (approval number: 240222-1).

3. Results

3.1. Effectiveness of lectures and practical training on pressure ulcers

Of the 138 students enrolled in the course, 74 (53.6%), 75 (54.3%), and 100 (72.5%) responded to the pre-lecture, post-lecture, and post-practice questionnaires, respectively (response rate in parentheses).

Figure 1 depicts the results of students' knowledge (questions 1–5) related to pressure ulcer treatment in the three surveys. For all items, the percentage of positive responses tended to increase in the following order: pre-lecture, post-lecture, and post-practice. Due to the exclusion of "not sure" responses from the statistical analysis, the sample size (n) varied for each response. When analyzing the distribution of responses for knowledge, significant differences were observed after the lecture and after the practical training compared to before the lecture for all questions (Kruskal-Wallis test, $p < 0.01$). As a result of the lecture and practical training, the number of students selecting positive responses increased for not only the attitude- and skill-related categories (questions 6–8) but also other categories (Figure 2). When analyzing the distribution of responses for skills and attitudes, significant differences were observed in questions 6 and 7. The responses after the lecture and after the practical training differed significantly from those before the lecture ($p < 0.01$). In question 8, a significant difference was observed between the responses after the practical training and those before the lecture ($p < 0.05$).

3.2. Association between aspiration to become a pharmacist and educational effectiveness

Figure 3 depicts the results of the three questionnaires in terms of students' intention to work as pharmacists in the future. In the pre-lecture survey, 23% of students

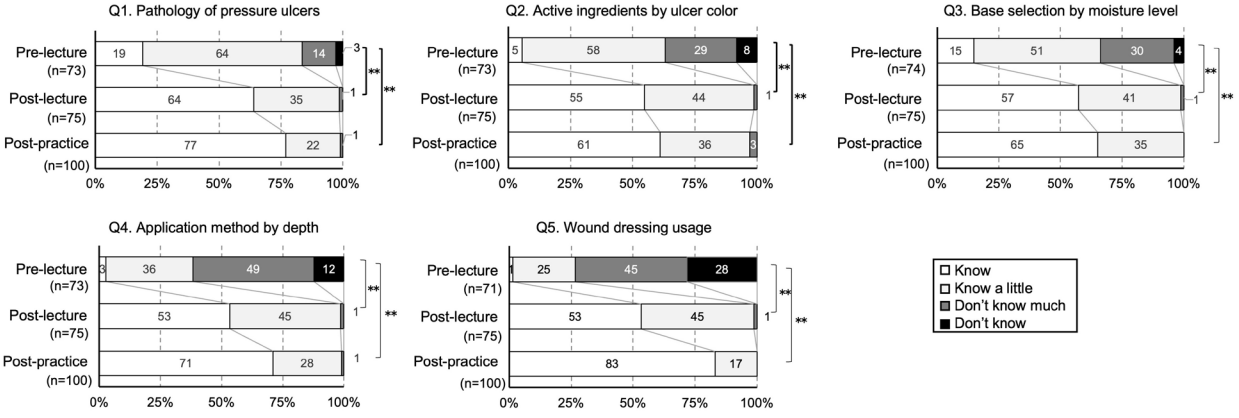

Figure 1. Student questionnaire on knowledge of pressure ulcer treatment. Comparison of the percentages for each questionnaire item (questions 1–5) at pre-lecture, post-lecture, and post-practice. The items are related to knowledge of pressure ulcer treatment. Statistical analysis was performed using the Kruskal–Wallis test. **: $p < 0.01$.

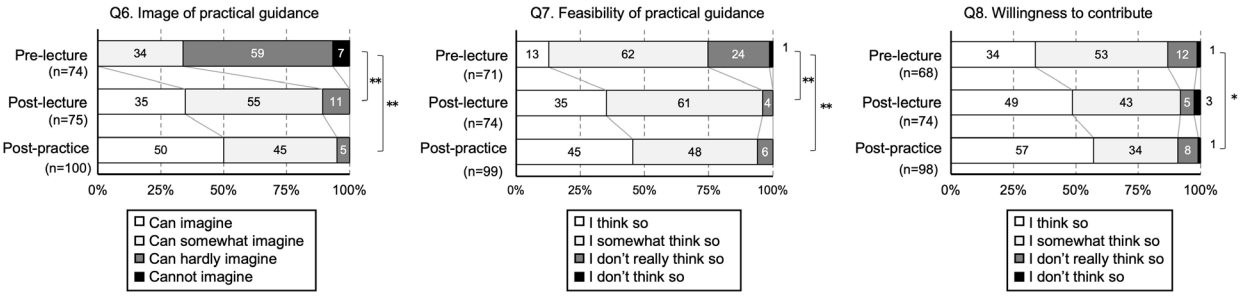

Figure 2. Student questionnaire on skills and attitudes of pressure ulcer treatment. Comparison of the percentages for each questionnaire item (questions 6–8) at pre-lecture, post-lecture, and post-practice. The items are related to skills in and attitudes towards pressure ulcer treatment. Statistical analysis was performed using the Kruskal–Wallis test. *: $p < 0.05$, **: $p < 0.01$.

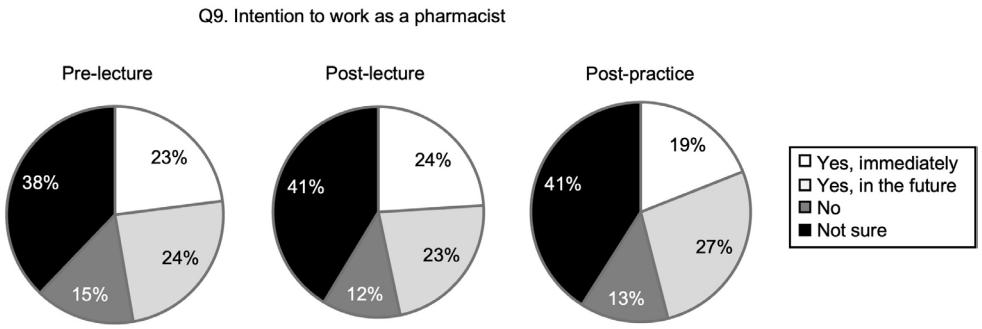

Figure 3. Student intention to work as a pharmacist in the future. The pie charts shows the results of responses to question 9, which asked whether students intended to pursue a career using their pharmacist license in the future. Responses were collected at pre-lecture, post-lecture, and post-practice. Students who answered "Yes" were classified as those aspiring to become pharmacists.

answered that they intended to work as a pharmacist immediately after graduation, 24% intended to change jobs in the future and work as a pharmacist someday, 15% did not intend to work as a pharmacist, and 38% reported they did not know at present. The percentage of students who intended to work as pharmacists, including those who wished to begin working immediately and those who planned to do so in the future, was 47%. Similar trends were observed in the post-lecture and post-practice questionnaires.

Table 1 depicts the number and percentage of positive responses for knowledge (questions 1–5) and skills and attitudes (questions 6–8) related to pressure ulcer treatment in the three surveys. Before the lecture, the percentage of positive responses was low for knowledge, skills, and attitudes, with many items below 20%. After the lecture, the percentage of positive responses for all items increased, although the percentage of positive responses for skills and attitudes remained lower than that for knowledge. After the practical training, the percentage of positive responses for skills and attitudes reached almost 50%. In the pre-lecture questionnaire, the percentage of positive responses was low for all questions, with no significant difference observed depending on whether the students wanted to become pharmacists. In the post-lecture questionnaire, the percentage of positive responses increased for all questions—especially questions 1, 2, and 4—with the percentage of positive responses from students who wanted to become pharmacists being significantly higher than that from students who did not want to become pharmacists (Mann-Whitney *U*-test, $p = 0.028$, $p = 0.002$ and $p = 0.014$). In the post-practice questionnaire, the percentage of positive responses from students who wanted to become pharmacists was significantly higher than that of students who did not want to become pharmacists in questions 2 and 3 ($p = 0.043$ and $p = 0.033$).

In addition, to confirm the relationship between the effects on knowledge (questions 1–5) and skills/attitudes (questions 6–8) in pressure ulcer education and the aspiration, or lack thereof, to become a pharmacist, the difference in positive response rates was calculated. Before the lecture, the mean difference in positive response rates between students who wanted to become pharmacists and those who did not was small (-1.9 ± 1.4 points). However, after the lecture, the difference in positive response rates increased for all questions, with a mean value of 21.5 ± 2.9 points, 10 times higher than that before the lecture. In addition, students who wanted to become pharmacists tended to give more positive responses than those who did not. After the practical training, the differences tended to be smaller than after the lecture in all items, and the mean value of the differences was reduced to 9.4 ± 2.4 points.

4. Discussion

In this study, we investigated the educational effects of including practical training on topical medication using a pressure ulcer simulator in conventional lectures for fourth-year pharmacy students in the Department of Pharmacy.

Before the lecture, the percentage of students who rated their knowledge, skills, and attitudes highly was low. After the lecture, although this percentage increased, it did not reach the majority. After the practical training, the proportion of students who rated their knowledge, skills, and attitudes highly improved to almost a majority. In addition, the students' aspirations to become pharmacists in the future was also examined in relation to the aforementioned educational effects. Although the difference in positive response rates was small before the lecture, the average difference in positive response rates increased by more than 20 points after the lecture, for students who wanted to become pharmacists compared to those who did not. We, thus, confirmed that the addition of practical training after the lecture increased the positive response rate of the non-pharmacist students and narrowed the above-mentioned difference. With regard to pressure ulcers, understanding the concepts of external forces, the shape of bony prominences, and the mobility of soft tissues is essential (*9*). However, students who do not aspire to become pharmacists seem to have difficulty

Table 1. Number of positive responses on knowledge, skills, and attitudes in pressure ulcer education by pharmacists' aspirations

Q	Pre-lecture				Post-lecture				Post-practice			
	Pharmacist aspiration		Gap	p value	Pharmacist aspiration		Gap	p value	Pharmacist aspiration		Gap	p value
	Yes, n (%)	No, n (%)			Yes, n (%)	No, n (%)			Yes, n (%)	No, n (%)		
1	6/34 (18)	8/39 (21)	-3	0.758	27/35 (77)	21/40 (53)	25	0.028*	36/46 (78)	41/54 (2.4)	2	0.783
2	0/35 (0)	4/38 (11)	-11	0.050*	26/35 (74)	15/40 (38)	37	0.002**	33/46 (72)	28/54 (52)	20	0.043*
3	6/35 (17)	5/39 (13)	4	0.604	24/35 (69)	19/40 (48)	21	0.067	35/46 (76)	30/54 (56)	21	0.033*
4	1/35 (2.9)	1/38 (2.6)	0	0.953	24/35 (69)	16/40 (40)	29	0.014*	34/46 (74)	37/54 (69)	5	0.555
5	0/34 (0)	1/37 (2.7)	-3	0.338	22/35 (63)	18/40 (45)	18	0.125	41/46 (89)	42/54 (78)	11	0.134
6	0/35 (0)	0/39 (0)	0	1.000	14/35 (40)	12/40 (30)	10	0.367	24/46 (52)	26/54 (48)	4	0.690
7	4/33 (12)	5/38 (13)	-1	0.897	14/34 (41)	12/40 (30)	11	0.319	22/46 (48)	23/53 (43)	4	0.660
8	11/34 (32)	12/34 (35)	-3	0.799	21/35 (60)	15/39 (39)	22	0.066	28/46 (61)	28/52 (54)	7	0.485

Notes: Q = Question No. Positive response: The most positive response on a 4-point Likert scale (know/think/imagine). *: $p < 0.05$, **: $p < 0.01$ (Mann-Whitney *U* test). Values = number of positive responses / number of valid responses.

grasping these concepts. Our study results suggest that students may not be deeply engaged until they see and experience these concepts firsthand through a pressure ulcer simulator.

The percentage of positive responses to all items measuring students' knowledge, skills, and attitudes in relation to the educational effects of bedsore treatment tended to increase in the following order: before the lecture, after the lecture, and after the practical training. These results indicate that the addition of practical training – using a bedsore simulator – to a lecture improves students' knowledge, skills, and attitudes (Table 1). Mizokami *et al*. reported that deep pressure ulcers require "wound fixation" (*10*); however, these concepts are difficult to fully understand through lectures alone. Pressure ulcer simulators are useful for learning practical techniques and observing wound sites. Answers to questions 6 and 7 were significantly better after the lecture than before, while answers to question 8 were significantly better after the practice than before. For question 8, which is related to attitude, 30% of the students responded positively before the lecture. This suggests that although many pharmacy students have low skills in pressure ulcer treatment, their awareness of its treatment before the lecture is high. Although the percentage of positive responses to all items increased from pre- to post-lecture, the percentage of positive responses to skills and attitudes remained at about 30%. By including practical training, the percentage of positive responses for skills and attitudes reached approximately 50%. Thus, while lectures alone are insufficient to enhance pharmacy students' skills and attitudes toward pressure ulcer treatment, practical learning through hands-on training can be expected to have a sufficient educational effect. In the context of medication counseling for topical drugs, reports indicate that community pharmacists provide inadequate patient instructions regarding the application of topical steroids (*11*). We believe that improving the skills and attitudes of pharmacists through practical training in topical drug application in pharmacy education will raise the level of topical drug instruction among pharmacists in Japan.

Differences in the positive response rates for all items of knowledge, skills, and attitudes after the lecture were observed depending on students' aspiration to become pharmacists. The students who aspired to become pharmacists tended to respond more positively to all items (Table 1). However, including practical training after the lecture tended to reduce the differences in all items of knowledge, skills, and attitudes. Although the questionnaire collection rate in this study was good (exceeding 50% before the lecture), after the lecture and the practical training, the equivalent response rates for each questionnaire could not be confirmed because students' personal information was not obtained due to ethical considerations. However, because the responses regarding students' intention to work as a pharmacist in

the future were the same in all three questionnaires, we do not believe that there exists a major problem with the equivalence of the response groups.

One limitation of this study is that matters concerning students' personal information were not collected due to ethical constraints, making it impossible to examine the educational effects of individual students across questionnaires. Another limitation is that, as the study was conducted on actual pharmacy students in an educational setting, it was not possible to validate the findings through an interventional trial with a control group.

The results of this study suggest that the knowledge, skills, and attitudes of pharmacy students can be improved by providing practical training using a pressure ulcer simulator in addition to lectures. Moreover, the inclusion of practical training to lectures in pressure ulcer education for pharmacy students compensated for differences in the educational effects of lectures depending on whether students wanted to become pharmacists, potentially increasing the educational effects of students who did not want to become pharmacists to the same level as those of students who did at the time of the course.

Acknowledgements

We would like to express our sincere gratitude to Kaken Pharmaceutical Co., Ltd. for lending us the bedsore simulator for the practical training of this study, and to the fourth-year students of our university who responded to our questionnaire survey.

Funding: None.

Conflict of Interest: The authors have no conflicts of interest to disclose.

References

1. Lyder CH. Pressure ulcer prevention and management. JAMA. 2003; 289:223-226.
2. Thomas DR, Goode PS, Tarquine PH, Allman RM. Hospital-acquired pressure ulcers and risk of death. J Am Geriatr Soc. 1996; 44:1435-1440.
3. Allman RM. Pressure ulcers among the elderly. N Engl J Med. 1989; 320:850-853.
4. Scott JR, Gibran NS, Engrav LH, Mack CD, Rivara FP. Incidence and characteristics of hospitalized patients with pressure ulcers: State of Washington, 1987 to 2000. Plast Reconstr Surg. 2006; 117:630-634.
5. Furuta K, Mizokami F, Sasaki H, Yasuhara M. Active topical therapy by "Furuta method" for effective pressure ulcer treatment: A retrospective study. J Pharm Health Care Sci. 2015; 1:21.
6. Furuta K, Mizokami F, Miyagawa T, Morikawa T, Nagata O, Nagata M, Fukuzawa E, Yuza M, Sakurai J, Shouji R, Fujii S. Effects of pressure ulcer treatment teams including physicians, pharmacists, and nurses on medical costs. Jpn J Healthc Adm. 2013; 50:199-207.
7. Granick MS, McGowan E, Long CD. Outcome assessment of an in-hospital cross-functional wound care team. Plast Reconstr Surg. 1998; 101:1243-1247.
8. Nakayoshi Y, Takase M, Niitani M, Imai T, Okada M, Yamamoto K, Takei Y. Exploring factors that motivate nursing students to engage in skills practice in a laboratory setting: A descriptive qualitative design. Int J Nurs Sci. 2020; 8:79-86.
9. Takahashi Y, Nemoto T, Mizokami F, Furuta K, Murasawa Y, Yoneda M, Isogai Z. A new concept: "Relative position between the external force and the bony prominence" explains location-specific occurrence of superficial injury over an undermining lesion. J Tissue Viability. 2017; 26:75-78.
10. Mizokami F, Takahashi Y, Nemoto T, Nagai Y, Tanaka M, Utani A, Furuta K, Isogai Z. Wound fixation for pressure ulcers: A new therapeutic concept based on the physical properties of wounds. J Tissue Viability. 2015; 24:35-40.
11. Oishi N, Iwata H, Kobayashi N, Fujimoto K, Yamaura K. A survey on awareness of the "finger-tip unit" and medication guidance for the use of topical steroids among community pharmacists. Drug Discov Ther. 2019; 13:128-132.

Received March 21, 2025; Revised April 15, 2025; Accepted April 20, 2025.

**Address correspondence to:*
Katsunori Yamaura, Division of Social Pharmacy, Center for Social Pharmacy and Pharmaceutical Sciences, Faculty of Pharmacy, Keio University, 1-5-30 Shibakoen, Minato-ku, Tokyo 105-8512, Japan.
E-mail: yamaura-kt@keio.jp

Released online in J-STAGE as advance publication April 27, 2025.

Original Article

DOI: 10.5582/ddt.2025.01013

Dietary supplementation with *Nopalea cochenillifera* enhances fecal mucin production and modulates serum immunoglobulin levels in a dose- and time-dependent manner in BALB/c mice

Sayaka Yokoyama[1,2], Hana Kozai[1], Amane Kikuchi[1], Suzuno Ota[3], Takanori Horibe[1], Mamoru Tanaka[1,*]

[1] Graduate School of Bioscience and Biotechnology, Chubu University, Aichi, Japan;
[2] Department of Food and Nutritional Environment, Kinjo Gakuin University, Aichi, Japan;
[3] Faculty of Health Science, Suzuka University of Medical Science, Mie, Japan.

SUMMARY: The aim of this study was to determine the time-dependent effects of the prickly pear (*Nopalea cochenillifera*) on the intestinal environment and immune function in BALB/c mice, which exhibit a predominant T helper 2 immune response. Five-week-old female BALB/c mice were divided into a control group and groups fed diets supplemented with 5% or 10% *N. cochenillifera* powder (NCP). Blood and feces were collected every 7 days. On day 28, in addition to blood and feces, the small intestine, cecum, and large intestine were collected. The cecum content weight, cecum content pH, and fecal mucin were examined. Serum antibody levels (total Immunoglobulin (Ig)M) were lower on days 14 and 21 in the 10% NCP group than in the control and 5% NCP groups. Total serum IgG levels were higher at all time points and total IgA levels were higher on days 7, 14, 21 and 28 in the 5% NCP and 10% NCP groups than in the control group. Total fecal IgA levels were lower in the 5% NCP and 10% NCP groups than in the control group from 14 days. Fecal mucin contents were higher in the 10% NCP group than in the control group from 7 days. These results suggest that *N. cochenillifera* supplementation exerts time-dependent effects on serum antibodies and the intestinal environment in BALB/c mice. In particular, NCP at 10% may enhance the intestinal mucosal barrier function and promote systemic immune responses. Further mechanistic studies are needed to determine the effects on immune responses.

Keywords: cactus, immune function, intestinal environment, immunoglobulins, mucin, mice

1. Introduction

The immune system consists of a diverse and complex system responsible for defense against a wide variety of pathogens and is essential for protecting the body from disease. The immune system comprises innate and adaptive immunities, which are composed of specific immune components that suppress infection. Immune function is influenced not only by genetic factors, but also by aging, lifestyle, and environmental factors related to susceptibility to disease-causing agents. Thus, weakened immune function can lead to autoimmune diseases, inflammatory diseases, and cancer (*1*). Chemical compounds in certain foods have been shown to regulate signaling and cellular phenotypes, ultimately affecting pathophysiology. Previous studies have reported that immune cells are activated when functional foods, such as *Chlorella* (*2,3*), probiotics, such as *Lactobacillus plantarum* (*4*), and prebiotics, such as guar gum and inulin (*5-7*), are consumed.

There is a growing need to develop and increase the production of various food products to address the threat of food shortages caused by global population growth. The food industry is trying to meet the standards of the Sustainable Development Goals, which aim to provide a stable supply of food containing a variety of nutrients; however, meeting these nutritional goals is proving to be a challenge. In addition, there is an urgent need to search for new products and to study their functional effects. The stem nodes of prickly pears are used as food in more than 30 countries, and in 2017, the United Nations Food and Agriculture Organization lauded prickly pear as a crop that could save the world from a food crisis. The family Cactaceae includes more than 1,450 species in about 30 genera and is divided into four subfamilies: Peireskioideae, Maihuenioideae, Opuntioideae, and Cactoideae (*8*). The subfamily Opuntioideae includes about 20 genera and 300 species, several of which

are used for food. Kasugai city in Aichi Prefecture is Japan's largest producer of seeding cactus and is using cactus to revitalize the financial and economic status of the city. Cactus is a useful vegetable that can be grown under a variety of conditions owing to its vitality, ability to thrive under different environmental regimes, and cultivation characteristics, and it has attracted attention as a self-sufficient agricultural product and food source because it is easy to grow in the Japanese climate. Furthermore, some varieties of cacti, such as prickly pear, have beneficial effects, including antioxidant effects (*9*) and regulatory effects on glucose (*10-13*) and lipid metabolism (*14*). Cactus is high in dietary fiber and various minerals (*15,16*). Although dietary fiber is a carbohydrate, most of it reaches the large intestine undigested because it cannot be broken down by digestive enzymes secreted by the human digestive tract (*17*). Dietary fiber is a potential prebiotic, and it undergoes partial or complete fermentation by the microflora in the colon, the products of which are a major source of energy for the intestinal microflora. The breakdown products of fiber are also important for the maintenance of the colonic epithelium (*18*). When food-derived, soluble dietary fiber and non-digestible polysaccharides undergo fermentation by the microflora in the gut, short-chain fatty acids (SCFAs) are produced, resulting in a decrease in pH, and they are involved in various cellular functions, including gene expression, chemotaxis, differentiation, proliferation, and apoptosis, thereby affecting the physiological functions of the host (*19,20*). Therefore, the fiber-rich prickly pear may have an effect on immune function. However, research has focused on large prickly pear (*Opuntia ficus-indica*), with relatively few studies of small prickly pear (*Nopalea cochenillifera*).

We have previously demonstrated that *N. cochenillifera* regulates innate and adaptive immune functions *via* the gut microflora in C3H/HeN mice, which exhibit a predominant T helper (Th) 1 immune response (*21*). In experiments focusing in the adaptive immune system, Th2-dominant mice, such as BALB/c mice, are commonly used. Changes in the intestinal environment, gastrointestinal tract, and systemic immune system due to continuous consumption of *N. cochenillifera* have not been studied sufficiently. In this study, we examined the time-dependent effects of *N. cochenillifera* on the intestinal environment and immune function in BALB/c mice, which exhibit a predominant Th2 immune response.

2. Materials and Methods

2.1. *N. cochenillifera* sample

N. cochenillifera cladodes were grown in a greenhouse in Chubu University in Aichi Prefecture, Japan. Young cladodes were harvested from plants aged 3 years. Harvested cladodes were cut into smaller pieces, freeze-dried, and milled for use in the following experiments.

2.2. Animals and diets

Six-week-old female BALB/cCrSlc mice (15–20 g) were obtained from Japan SLC (Hamamatsu, Shizuoka, Japan) and housed at 24 ± 3°C and 55 ± 10% relative humidity with a 12 h light-dark cycle in a specific pathogen-free facility. After acclimatization for 5 days, the mice were provided with the experimental diets and water *ad libitum*. Mice were divided into three groups: control (n = 8), 5% *N. cochenillifera* powder (NCP) (n = 8), and 10% NCP groups (n = 8). Mice were housed in groups of four per cage. The diets were prepared according to the recommendation of the American Institute of Nutrition and AIN-93G rodent diet (*22*). The control group received AIN-93G as a control diet and the 5%NCP and 10%NCP groups received AIN-93G supplemented with 5% NCP or 10% NCP, respectively (Table 1). The mice consumed the diets for 4 weeks. The experimental design was in accordance with the guidelines for animal experimentation and was approved by the Animal Experimental Committee of the Chubu University (authorization number: 202110051).

2.3. Animal protocol

Blood and fecal samples were collected every week. The serum was separated by centrifugation at 700× g for 15 min, collected, and stored at −20°C until analyses. Feces were collected on days 7, 14, 21, and 28. The feces were stored at −20°C, freeze-dried, and milled. At the end of the feeding period, the mice were anesthetized with isoflurane and the liver, spleen, small intestine, large intestine, and cecum were removed. The liver, spleen, and cecal contents were weighed, and the small and large intestines were measured for length. Cecal contents were measured for pH value.

2.4. Analyses of fecal total Immunoglobulin (Ig) A and mucin

Total IgA and mucin assays were performed as described previously (*21*). Total IgA concentrations in feces were

Table 1. Composition of the test diets (%)

Component (%)	Control	5%NCP	10%NCP
Cornstarch	63.2	5.82	53.2
Casein	20	20	20
Soy bean oil	7	7	7
cellulose powder	5	5	5
Mineral mix(AIN-93G-MX)	3.5	3.5	3.5
Vitamin mix(AIN-93G-VX)	1	1	1
L-Cystine	0.3	0.3	0.3
tert-Butylhydroqunone	0.0014	0.0013	0.0042
N. cochenillifera	0	5	10

measured using an enzyme-linked immunosorbent assay (ELISA) kit for quantitative analyses (Invitrogen, Waltham, MA, USA). Mucin levels were quantified using a fluorometric assay for quantitative analysis of fecal mucin (Cosmo Bio Co., Ltd., Koto Ward, Tokyo, Japan). Fecal total IgA and mucin levels were measured in accordance with the manufacturers' instructions.

2.5. Analyses of serum total IgM, IgG, and IgA

The total IgM, IgG, and IgA concentrations in serum were measured using an enzyme-linked immunosorbent assay (ELISA) kit for quantitative analyses (Invitrogen, Waltham, MA, USA).

2.6. Statistical analysis

Data are expressed as the mean ± SEM. All statistical analyses were performed using GraphPad Prism v10.2.3. (GraphPad Software, San Diego, CA, USA). For data that followed a normal distribution, two-way ANOVA was performed. For cecal content weight and pH, one-way ANOVA was used. For serum IgA, IgG and IgM, as well as fecal mucin and IgA, repeated measures ANOVA was performed. Data that did not follow a normal distribution were analyzed using the nonparametric Kruskal-Wallis test (one-way ANOVA). A Tukey's post hoc test was performed when a significant effect was determined by two-way ANOVA. A Games-Howell post hoc test was conducted when a significant effect was found by the Kruskal-Wallis test. Differences were considered significant when $p < 0.05$.

Table 2. Tissue and body weights and lengths of small and large intestines

	Control	5%NCP	10%NCP
Daily food intake (g)/mouse/day	2.37 ± 0.05	2.61 ± 0.09	2.49 ± 0.06
Body weight (Before)	16.3 ± 0.3	16.3 ± 0.3	16.4 ± 0.3
Body weight (28 days)	18.3 ± 0.2	18.9 ± 0.2	18.6 ± 0.4
Liver (g)	0.741 ± 0.021	0.793 ± 0.014	0.695 ± 0.039
Spleen (g)	0.102 ± 0.003	0.106 ± 0.0003	0.096 ± 0.003
Small intestine (cm)	37.3 ± 0.2	37.3 ± 0.7	38.3 ± 0.5
Large intestine (cm)	8.2 ± 0.2	8.2 ± 0.2	7.9 ± 0.2

Data are reported as the mean ± SEM ($n = 8$). *$p < 0.05$.

3. Results

3.1. Tissue and body weight and small and large intestine lengths

The body weight, tissue weight, and lengths of the small and large intestine on the 28th day of the experiment are shown in Table 2. There were no significant differences among groups in body weight, liver, and spleen weight or the length of the small and large intestine.

3.2. Dry fecal weight, cecum weight, and pH of cecal contents

To determine the effects of *N. cochenillifera* intake on the intestinal environment, the dry weight of the feces collected every 7 days and the contents of the cecum on day 28 were evaluated (Figure 1). The dry weight of feces was higher than that in the control group from day 7, with a 1.3-fold increase in the 5% group and a 1.5-fold increase in the 10% group over the total experimental period (Figure 1A). There was no significant differences in the weight of the cecal contents among the three groups (Figure 1B), and the pH values of the cecal contents in the groups given *N. cochenillifera* were significantly lower than those of the control group (Figure

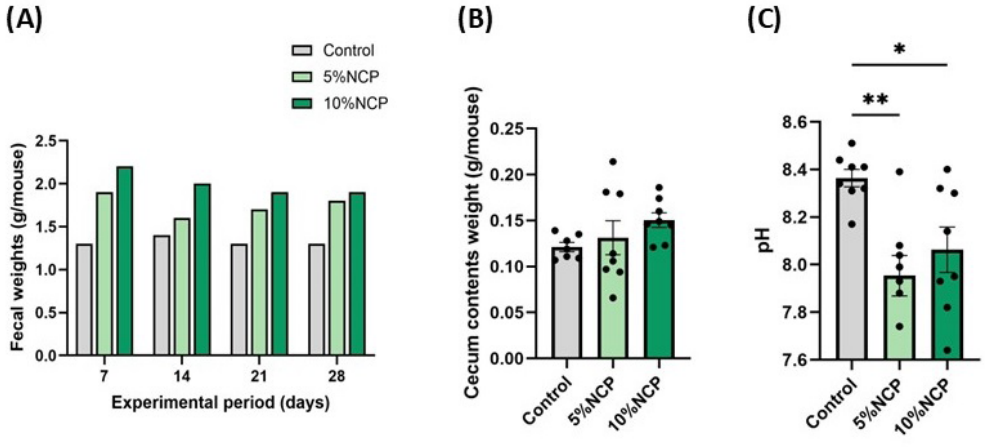

Figure 1. Dry weight of feces, cecal content weight, and pH of the cecal contents in mice fed a *Nopalea cochenillifera* diet. Dry fecal weight (**A**), weight of cecal contents (**B**), and pH of cecal contents (**C**) obtained in each 7-day period after 28 days in the control group, 5% group, and 10% group are shown. Data are expressed as the mean ± SEM ($n = 8$). *$p < 0.05$, **$p < 0.01$.

1C, $p < 0.05$).

3.3. Intestinal IgA and secreted mucins in mice fed *N. cochenillifera*

To determine the effects of *N. cochenillifera* intake on the gastrointestinal immune system, total IgA and mucin contents in feces were measured (Figure 2). Total fecal IgA was significantly lower in the 5% NCP group on days 14, 21 and 28 and in the 10% NCP group on days 14 and 28 compared with those in the control group (Figure 2A, $p < 0.05$). The total mucin content in the feces was significantly higher on day 7, 14 and 28 in the 5% NCP group and on days 7, 14, and 21 in the 10% NCP group compared with those in the control group (Figure 2B, $p < 0.05$).

3.4. Antibody concentrations in the serum

To investigate the immunostimulatory effects of *N. cochenillifera* intake on the systemic immune system, total serum IgM, IgG, and IgA were measured (Figure 3). The IgM levels in the NCP 10% group on days 14 and 21 were significantly lower than those in the control groups (Figure 3A, $p < 0.05$). Additionally, the IgG and IgA levels in the NCP 5% and NCP 10% groups on days 7, 14, 21 and 28 were higher than those in the control group. Furthermore, it was observed that both

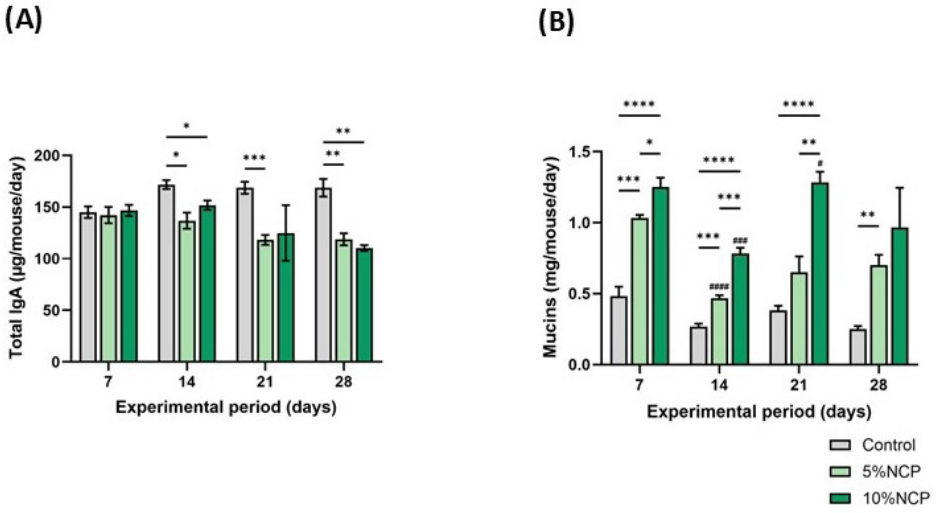

Figure 2. Effect of a diet containing *Nopalea cochenillifera* on total fecal IgA and mucin levels in mice. Amounts of total fecal IgA (**A**) and mucins (**B**) obtained over each 7-day period from the control group, NCP5%, and NCP10% are shown. Data are expressed as the mean ± SEM ($n = 6$). *$p < 0.05$, **$p < 0.01$, ***$p < 0.001$, ****$p < 0.0001$, significant difference was observed between the groups. $^{###}p < 0.001$, $^{####}p < 0.0001$, significant difference was observed compared to the previous week.

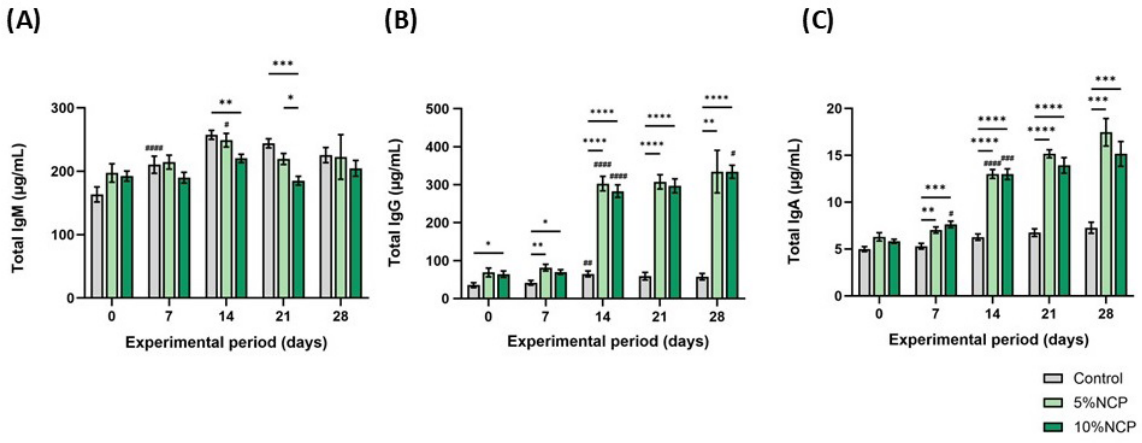

Figure 3. Effects of a diet containing *Nopalea cochenillifera* on the production of total antibodies in serum from mice. The IgM (**A**), IgG (**B**), and IgA concentrations (**C**) in the serum obtained after each 7-day period from the control group, NCP5%, and NCP10% are shown. Data are expressed as the mean ± SEM ($n = 8$). *$p < 0.05$, **$p < 0.01$, ***$p < 0.001$, ****$p < 0.0001$, significant difference was observed between the groups. $^{#}p < 0.05$, $^{##}p < 0.01$, $^{####}p < 0.0001$, significant difference was observed compared to the previous week.

had increased on day 14 compared to the previous week (Figure 3B, 3C, $p < 0.05$).

4. Discussion

In this study, we examined the effects of dietary supplementation with *N. cochenillifera* on antibody production and intestinal immune function in BALB/c mice, revealing novel functions by which the species improves the intestinal environment, intestinal barrier function, and systemic immune function in mice.

We have previously shown that approximately 50% of NCP consists of dietary fiber, of which about 80% is insoluble and 20% is soluble (*21*). Furthermore, dietary fiber in cactus is rich in cellulose, hemicellulose, and pectin (*15,16*). Cellulose, hemicellulose, and other insoluble fiber have various intestinal regulatory effects, including roles in softening stool, physically stimulating the intestinal tract, and increasing stool bulk, due to water absorption and the consequent increase in volume of the stool (*23*). Some soluble fibers, such as pectin, inulin, and guar gum, exert prebiotic effects; however, like insoluble fiber, they have large molecular sizes and are not as rapidly digested as simpler carbohydrates and sugars by intestinal bacteria (*24*). On this basis, we hypothesized that the dietary fiber-rich *N. cochenillifera* would function as a modulator of the intestinal environment. In the present study, *N. cochenillifera* consumption increased fecal weight and deceased the pH of cecal contents. Probiotic *Bifidobacteria* produces the SCFAs acetic acid and lactic acid, whereas butyric acid is produced by bacteria such as *Clostridium* and *Ruminococcus*. It is thought that enteric bacteria that produce putrefactive products that are not beneficial to the host are generally susceptible to low pH, and increased SCFAs production will limit the growth and activity of intestinal bacteria (*25*). As reported earlier, *N. cochenillifera* consumption decreases succinate and lactic acid in the cecum, increases butyrate, and lowers fecal pH. The decrease in pH in the cecal contents was likely due to fiber digestion and consequent SCFAs production by intestinal bacteria, which may have promoted intestinal regulation. The regulatory effect on the intestine was observed from the 7 days of intake, as indicated by the increase in the amount of feces. The fecal weight also increased with *N. cochenillifera* consumption, which may be attributed to its insoluble fiber. These findings suggested that both soluble and insoluble fiber in *N. cochenillifera* affect the intestinal environment.

Next, the total IgA concentration and mucin content in feces were measured to evaluate the barrier function of the gastrointestinal tract after supplementation with *N. cochenillifera*. The gastrointestinal tract is a unique tissue that is exposed not only to the threat of invasion by pathogenic microorganisms but also to the constant presence of foreign substances consumed in daily life or produced by intestinal bacteria. Therefore, immune cells in the gut lamina propria have different functions from those in the lymph nodes and spleen. The lymphoid tissue of the gut also has unique functions. Because the mucin layer exhibits a barrier function that prevents the passage of intestinal bacteria to the inside of the body (*26*) and IgA prevents bacterial contact with epithelial cells (*27*), mucin and IgA may be involved in maintaining intestinal health. Furthermore, the secretion of mucin and IgA is stimulated by SCFAs containing butyrate (*28,29*). We have reported that *N. cochenillifera* consumption increases butyrate levels in the cecum (*21*). These findings suggest that the production of fecal mucin resulting from *N. cochenillifera* consumption may be influenced by SCFAs produced by intestinal bacteria. In our study, the mucin content in feces increased significantly after the first week of *N. cochenillifera* consumption. In contrast to expectations, total fecal IgA decreased after the second week. We have previously shown that fecal mucin and IgA are increased in mice fed *N. cochenillifera* for 6 weeks. However, in the present study, similar results were not obtained for fecal IgA. This discrepancy could be attributed to differences in the mouse strain, duration of the experiments, and nature of comparisons. Although mechanism was not clarified in this study, it may involve polymeric immunoglobulin receptor (pIgR) expressed on the basement membrane of epithelial cells, as pIgR has been reported to be involved in the transcytosis of secretory IgA from inside the cells to the lumen of the gastrointestinal tract (*30*). *N. cochenillifera* may suppress the expression of pIgR, reducing IgA release into the lumen.

In further analyses of the systemic immunostimulatory effects of *N. cochenillifera* supplementation, serum IgM, IgG, and IgA concentrations were measured. Total serum IgM decreased after the 14 days in mice fed the experimental diet; in contrast, total IgG and IgA levels were significantly higher than those for the control diet. These results indicate that of the three Ig classes, *N. cochenillifera* may have the greatest effects on the production of IgG, followed by IgA. IgM is produced by B cells and is found primarily in blood. The increases in serum IgG and IgA suggest a potential contribution to enhanced immunity and infection prevention. Interestingly, IgG and IgA increased during the same period of time that IgM decreased, which may indicate that *N. cochenillifera* promoted a class switch from IgM to IgG and IgA. Although we were unable to clarify the detailed antibody production capacities in this study, an increase in antibody production in response to soluble dietary fiber has been observed in feeding experiments; however, a similar increase is not observed when lymphocytes are directly treated with fiber (*5*). Accordingly, the observed effects may be indirectly mediated by the intestinal microflora and immunomodulatory function of soluble dietary fiber. The increases in serum IgG and IgA following

N. cochenillifera consumption suggest that the species contributes to enhanced immunity and infection prevention.

In conclusion, we showed that supplementation with *N. cochenillifera* results decreases the pH of the cecal contents and increases the amount of feces and fecal mucin in mice. Furthermore, we found significant increases in total serum IgG and IgA after supplementation with *N. cochenillifera*. These findings suggest that *N. cochenillifera* has potential as a prebiotic and may modulate immune function.

Acknowledgements

We thank Paul Danielian, PhD, from Edanz (*https://jp.edanz.com/ac*) for editing a draft of this manuscript.

Funding: This study was supported by Research Institute for Biological Functions (Chubu University) (to H.K. T. H. and M.T.) and the Research and Implementation Promotion Program through open innovation grants (JPJ011937) from the Project of the Bio-oriented Technology Research Advancement Institution (BRAIN) (to H.K. T. H. and M.T.).

Conflict of Interest: The authors have no conflicts of interest to disclose.

References

1. O'Byrne KJ, Dalgleish AG. Chronic immune activation and inflammation as the cause of malignancy. Br J Cancer. 2001; 85:473-483.
2. Cheng D, Wan Z, Zhang X, Li J, Li H, Wang C. Dietary *Chlorella vulgaris* Ameliorates Altered Immunomodulatory Functions in Cyclophosphamide-Induced Immunosuppressive Mice. Nutrients. 2017; 9:708.
3. An BK, Kim KE, Jeon JY, Lee KW. Effect of dried Chlorella vulgaris and Chlorella growth factor on growth performance, meat qualities and humoral immune responses in broiler chickens. Springerplus. 2016; 5:718.
4. Lee HA, Kim H, Lee KW, Park KY. Dead *Lactobacillus plantarum* Stimulates and Skews Immune Responses toward T helper 1 and 17 Polarizations in RAW 264.7 Cells and Mouse Splenocytes. J Microbiol Biotechnol. 2016; 26:469-476.
5. Yamada K, Tokunaga Y, Ikeda A, Ohkura K, Mamiya S, Kaku S, Sugano M, Tachibana H. Dietary effect of guar gum and its partially hydrolyzed product on the lipid metabolism and immune function of Sprague-Dawley rats. Biosci Biotechnol Biochem. 1999; 63:2163-2167.
6. Ito H, Wada T, Ohguchi M, Sugiyama K, Kiriyama S, Morita T. The degree of polymerization of inulin-like fructans affects cecal mucin and immunoglobulin A in rats. J Food Sci. 2008; 73:H36-41.
7. Tanabe H, Ito H, Sugiyama K, Kiriyama S, Morita T. Dietary indigestible components exert different regional effects on luminal mucin secretion through their bulk-forming property and fermentability. Biosci Biotechnol Biochem. 2006; 70:1188-1194.
8. Hernández-Hernández T, Hernández HM, De-Nova JA, Puente R, Eguiarte LE, Magallón S. Phylogenetic relationships and evolution of growth form in Cactaceae (Caryophyllales, Eudicotyledoneae). Am J Bot. 2011; 98:44-61.
9. Budinsky A, Wolfram R, Oguogho A, Efthimiou Y, Stamatopoulos Y, Sinzinger H. Regular ingestion of opuntia robusta lowers oxidation injury. Plef. 2001; 65:45-50.
10. Ibañez-Camacho R, Roman-Ramos R. Hypoglycemic effect of Opuntia cactus. Arch Invest Med (Mex). 1979; 10:223-230.
11. Ibáñez-Camacho R, Meckes-Lozoya M. Effect of a semipurified product obtained from *Opuntia streptacantha* L. (a cactus) on glycemia and triglyceridemia of rabbit. Arch Invest Med (Mex). 1983; 14:437-443.
12. Frati Munari AC, Vera Lastra O, Ariza Andraca CR. Evaluation of nopal capsules in diabetes mellitus. Gac Med Mex. 1992; 128:431-436.
13. Trejo-González A, Gabriel-Ortiz G, Puebla-Pérez AM, Huízar-Contreras MD, Munguía-Mazariegos MR, Mejía-Arreguín S, Calva E. A purified extract from prickly pear cactus (*Opuntia fuliginosa*) controls experimentally induced diabetes in rats. J Ethnopharmacol. 1996; 55:27-33.
14. Fernandez ML, Lin EC, Trejo A, McNamara DJ. Prickly pear (*Opuntia* sp.) pectin alters hepatic cholesterol metabolism without affecting cholesterol absorption in guinea pigs fed a hypercholesterolemic diet. J Nutr. 1994; 124:817-824.
15. López-Palacios C, Peña-Valdivia CB, Rodríguez-Hernández AI, Reyes-Agüero JA. Rheological Flow Behavior of Structural Polysaccharides from Edible Tender Cladodes of Wild, Semidomesticated and Cultivated 'Nopal' (Opuntia) of Mexican Highlands. Plant Foods Hum Nutr. 2016; 71:388-395.
16. Hernández-Urbiola MI, Pérez-Torrero E, Hernández-Quevedo G, Rojas-Molina JI, Cortes ME, Rodríguez-García ME. Study of nutritional composition of nopal (*Opuntia ficus indica* cv. *Redonda*) at different maturity stages. Open Nutr J. 2010; 4:11-16.
17. Fleming SE, Marthinsen D, Kuhnlein H. Colonic function and fermentation in men consuming high fiber diets. J Nutr. 1983; 113:2535-2544.
18. Carlson JL, Erickson JM, Hess JM, Gould TJ, Slavin JL. Prebiotic Dietary Fiber and Gut Health: Comparing the *in Vitro* Fermentations of Beta-Glucan, Inulin and Xylooligosaccharide. Nutrients. 2017; 9:1316.
19. Corrêa-Oliveira R, Fachi JL, Vieira A, Sato FT, Vinolo MA. Regulation of immune cell function by short-chain fatty acids. Clin Transl Immunology. 2016; 5:e73.
20. Wong JM dSR, Kendall CW, Emam A, Jenkins DJ. Colonic health: fermentation and short chain fatty acids. J Clin Gastroenterol. 2006; 40:235-243.
21. Kozai H, Watanabe C, Kosaka R, Aoki T, Hamada H, Kawashima M, Kono T, Akagi K, Kremenik MJ, Yano H, Tanaka M, Oyanagi E. *Nopalea cochenillifera* Regulates the Immune Response and Gut Microbiota in Mice. Nutrients. 2024; 16:4376.
22. Reeves PG, Nielsen FH, Fahey GC, Jr. AIN-93 purified diets for laboratory rodents: final report of the American Institute of Nutrition ad hoc writing committee on the reformulation of the AIN-76A rodent diet. J Nutr. 1993; 123:1939-1951.
23. Ebihara K. Studies on Nutritional and Physiological

Effects of Dietary Fiber. J Jpn Soc Nutr Food Sci. 2008; 61:3-8.
24. do Carmo MM, Walker JC, Novello D, Caselato VM, Sgarbieri VC, Ouwehand AC, Andreollo NA, Hiane PA, Dos Santos EF. Polydextrose: Physiological Function, and Effects on Health. Nutrients. 2016; 8:553.
25. Martin-Gallausiaux C, Marinelli L, Blottière HM, Larraufie P, Lapaque N. SCFA: mechanisms and functional importance in the gut. Proc Nutr Soc. 2021; 80:37-49.
26. Johansson ME, Phillipson M, Petersson J, Velcich A, Holm L, Hansson GC. The inner of the two Muc2 mucin-dependent mucus layers in colon is devoid of bacteria. Proc Natl Acad Sci U S A. 2008; 105:15064-15069.
27. Childers NK, Bruce MG, McGhee JR. Molecular mechanisms of immunoglobulin A defense. Annu Rev Microbiol. 1989; 43:503-536.
28. Ebihara K, Tachibe M, Kaneko N, Kishida T. Hydroxypropylation of high-amylose maize starch changes digestion and fermentation-dependent parameters in rats. J Nutr Sci. 2013; 2:e17.
29. Gaudier E, Jarry A, Blottière HM, de Coppet P, Buisine MP, Aubert JP, Laboisse C, Cherbut C, Hoebler C. Butyrate specifically modulates MUC gene expression in intestinal epithelial goblet cells deprived of glucose. Am J Physiol Gastrointest Liver Physiol. 2004; 287:G1168-1174.
30. Wei H, Wang JY. Role of Polymeric Immunoglobulin Receptor in IgA and IgM Transcytosis. Int J Mol Sci. 2021; 22:2284.

Received February 21, 2025; Revised March 25, 2025; Accepted April 22, 2025.

**Address correspondence to:*
Mamoru Tanaka, Graduate School of Bioscience and Biotechnology, Chubu University, Kasugai, Aichi, Japan, 1200 Matsumoto-cho, Kasugai-city, Aichi 487-8501, Japan.
E-mail: m-tanaka@fsc.chubu.ac.jp

Released online in J-STAGE as advance publication April 27, 2025.

Original Article

DOI: 10.5582/ddt.2025.01023

Generation and characterization of a humanized GJB2 p.V37I knock-in mouse model for studying age-related hearing loss

Yiding Yu[1,2,3], Yue Li[1,2,3], Jingyun Li[1,2,3], Xu Zhang[1,2,3], Xuemin Chen[4,5], Pengzhao Hu[4,5], Wenjie Huang[4,5], Cheng Wen[1,2,3], Lin Deng[1,2,3], Xiaohua Cheng[1,2,3], Ning Yu[4,5,*], Lihui Huang[1,2,3,*]

[1] Otolaryngology Head and Neck Surgery, Beijing Tongren Hospital, Capital Medical University, Beijing, China;
[2] Beijing Institute of Otolaryngology, Beijing, China;
[3] Key Laboratory of Otolaryngology Head and Neck Surgery, Ministry of Education, Beijing, China;
[4] College of Otolaryngology Head and Neck Surgery, Chinese PLA General Hospital, Beijing, China;
[5] National Clinical Research Center for Otolaryngologic Diseases, Beijing, China.

SUMMARY: Age-related hearing loss (ARHL) has been closely linked to genetic factors, with studies identifying the p.V37I mutation in the *GJB2* gene as a potential contributor to ARHL. To investigate this, we generated a humanized p.V37I mutant mouse model and performed auditory brainstem response (ABR) testing, cochlear morphology assessments, and transcriptional sequence of mutant and wild-type (WT) mice at different ages. Our results indicated that this kind of *GJB2* mutation does not lead to cochlear developmental abnormalities, and aging mutant mice exhibit only mild hearing loss compared to WT mice, without significant cochlear morphological differences. However, transcriptional analyses revealed substantial differences between mutant and WT mice. GO enrichment analysis of the DEGs between aging mutant and WT mice highlights significant enrichment in biological processes related to neural and sensory functions. Notably enriched terms include "neuron-to-neuron synapse," "immune response-activating signaling pathway," "regulation of synapse structure or activity," and "sensory perception of sound." These findings suggest that the p.V37I mutation in aging mice affects synaptic and calcium signaling pathways, as well as sensory system development. Despite these molecular changes, cochlear function remains normal in early life; however, as the mice age, hearing loss accelerates, likely due to a diminished capacity for gene-mediated protection against external stimuli.

Keywords: Age-related hearing loss, genetic hearing loss, c.109G>A mutant, RNA-seq, knock-in mouse

1. Introduction

Age-related hearing loss (ARHL) is a significant public health concern, affecting over 1.5 billion people worldwide, with about one-third of those over 65 experiencing disabling hearing loss (*1*). Beyond the auditory deficits, ARHL is associated with cognitive decline, increased risks of falls, depression, loneliness, and dementia (*2-4*), collectively imposing significant social and economic burdens. These challenges underscore the urgent need for effective prevention and treatment strategies (*5,6*).

ARHL is thought to result from the interplay of multiple factors, including aging, environmental influences, and genetics, with genetic factors accounting for 30% to 70% of cases (*1,7*). Among the genetic contributors, *GJB2* is the most well-known deafness-associated gene, responsible for over 50% of sensorineural hearing loss (SNHL) cases and a primary target in newborn genetic screening (*7*). While *GJB2*'s role in congenital hearing loss is well-recognized, its contribution to hearing loss in adults, particularly in the elderly, is increasingly being appreciated. One specific mutation, p.V37I (c.109G>A), has been shown to be ethnically specific, with a high carrier rate (6.2-11.79%) in the Chinese population (*8,9*). Importantly, this mutation has been implicated in age-related hearing loss (*10*).

Although nearly all newborns in China undergo genetic and hearing screening at birth these years (*11,12*), adults are rarely tested for the genetic causes of hearing loss, even though approximately 80% of hearing loss cases are diagnosed after the second decade of life (*1*). This gap in genetic testing among adults highlights the need to better understand the genetic underpinnings of ARHL to guide future diagnostic and therapeutic strategies. Given the high carrier rate of the p.V37I (c.109G>A) mutation, its investigation holds significant

clinical relevance.

Due to the limited availability of human cochlear samples, it is essential to develop appropriate animal models to effectively investigate the pathogenesis of hearing loss caused by gene mutations. Currently, there have been studies on animal models of the *GJB2* gene c.109G>A mutation, particularly the p.V37M mouse model (*13,14*). However, a p.V37I model with the same mutation as in humans has not been established. In this study, we have successfully created a p.V37I mouse model for the first time by performing precise double-base editing at the p.V37 codon of the *GJB2* gene. This model is expected to provide a foundation for the future development of therapeutic and preventive strategies for hearing loss.

2. Materials and Methods

2.1. Generation of the p.V37I knock-in mouse model

Mice were generated from the C57BL/6J background. The p.V37I knock-in mice were generated using the CRISPR/Cas9 genome editing system. The efficacy of the target site was verified using the spCas9-gRNA Target Efficiency Assay Kit (Beijing, China). The guide RNA (gRNA) and Cas9 were expressed in the vector (Figure 1A). The mouse *GJB2* gene sequences were obtained from NCBI (National Center of Biotechnology Information,Gene ID:14619). Given that the c.109G>A mutation differ between humans and mice, a direct c.109G>A substitution in mice would result in a p.V37M amino acid change, to achieve the desired p.V37I amino acid substitution, we modified two distinct DNA bases (Figure 1B). The Cas9 Nickase mRNA, Cas9 target gRNA, and donor DNA were microinjected into mouse zygotes under standard conditions to generate the F0 generation. F1 offspring carrying the heterozygous p.V37I mutation were obtained by crossing mutant founders (F0) with C57BL/6J. After the birth of founder

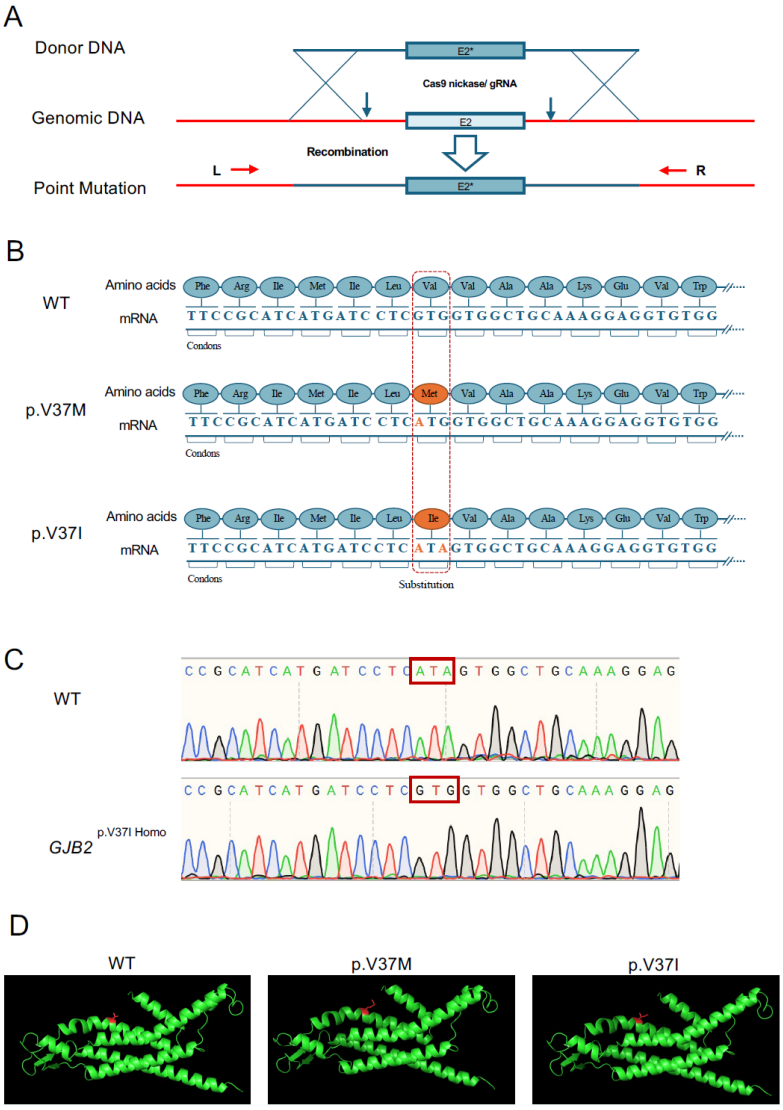

Figure 1. The generation of p.V37I mice. A: Schematic diagram of the construction of the p.V37I mutation mice. **B**: The difference of the amino acids and mRNA sequence between WT, p.V37M and p.V37I variants. **C**: Representative Sanger sequencing results confirming the p.V37I mutation in mice. **D**: Three-dimensional structural modeling and visualization of *GJB2* protein variants.

mice, tail samples were collected for DNA extraction, followed by PCR and sequencing to identify positive founders. F2 offspring with the homozygous p.V37I mutation were generated from the crossing between heterozygous F1 offspring. The genotyping of the homozygous mice we produced was confirmed using PCR analysis and Sanger sequencing of genomic DNA extracted from mouse tail clippings to detect the targeted mutation (Figure 1C). All animal procedures adhered to guidelines for animal research and were approved by the Experimental Animal Ethics Committee of Capital Medical University (Number: TRLAWEC2022-S186).

2.2. Functional predictions of *GJB2* mutations

The functional effects of the p.V37I and p.V37M mutations on the GJB2 protein were evaluated using two widely used mutation prediction tools, SIFT (*https://sift.bii.a-star.edu.sg/*) and PolyPhen-2 (*http://genetics.bwh.harvard.edu/pph2/*), with default threshold settings. The GJB2 protein sequence (UniProtKB-Q00977) was used as the query. To further investigate the structural impacts of the p.V37I and p.V37M mutations, we employed PyMOL for three-dimensional structural modeling and visualization of both mutant (p.V37I&p.V37M) and wild-type proteins. The secondary structure was rendered, with α-helices displayed in green. The mutation sites – methionine at position 37 for p.V37M and isoleucine for p.V37I – were highlighted in red to illustrate their locations within the protein and spatial relationships with surrounding residues. High-resolution rendering was performed to generate structural images for analysis and presentation.

2.3. Auditory brainstem response tests

Auditory brainstem response (ABR) tests were performed in WT ($n = 6$) and homozygous p.V37I ($n = 6$) mice every month between the ages of 1 month and the 12 months. The mice were anesthetized with 1% sodium pentobarbital (50 mg/kgb.w.) delivered intraperitoneally. The anesthetized mice were moved into the shielded room, the electrodes were connected. We use the TDT system to measure the thresholds of the auditory brainstem response (ABR) in mice. The active electrodes were inserted into the vertex and the ipsilateral retro-auricular region with a ground electrode on the back of the mouse's head. Specifically, the ABR threshold for pure-tone stimuli was measured at frequencies of 8, 16, and 24 kHz. Experimental animals were tested for ABR thresholds at each frequency of Click, 8 kHz, 16 kHz, and 24 kHz, with stimulus intensities starting at 90 dB SPL and decreasing in 10 dB increments, and thresholds were judged by the lowest stimulus intensity at which repeatable wave II could be discerned. The genotypes of the mice were kept confidential from the tester during the experiment.

2.4. Cochlear histology analysis

Fresh cochleae were perfused with 4% paraformaldehyde (Solarbio, Beijing, China) in PBS through small openings at the apex and base, repeated more than three times until lymphatic fluid mixed with blood was expelled. The cochleae were then transferred into an Eppendorf tube containing the paraformaldehyde overnight at 4°C. The 10% EDTA solution (Solarbio, Beijing, China) was used for decalcification at room temperature for 24 hours. For light microscopy studies, the samples were dehydrated and embedded in paraffin. Subsequently, serial sections (5 mm) were stained with H&E.

2.5. Immunofluorescence

After decalcification with disodium EDTA, the cochleae were dehydrated with 15% and 30% sucrose for 1.5 h each and embedded in optimal cutting temperature compound (Sakura, CA, USA) overnight at 4°C. And sections with a thickness of 10 μm were cut. Meanwhile, the sensory epitheliums of cochlea were dissected out and were incubated in blocking solution (containing 10% goat serum, 1% BSA), and 0.1% Triton X-100 in PBS for 30 minutes. The epitheliums were incubated overnight at 4°C with monoclonal mouse anti-Cx26 antibody (1:400, Invitrogen, CA, USA) prepared in the blocking solution. For double immunofluorescence staining of Cx26 and Cx30, polyclonal rabbit anti-Cx30 antibody (1:400, CA, USA) was used. After being washed with PBS three times, the epithelium sections were incubated with corresponding Alexa Fluor 488- and 568-conjugated goat anti-mouse IgG and Alexa Fluor 568-conjugated goat anti-rabbit IgG (1:500, Thermofisher, MA, USA) in the blocking solution at room temperature (25°C) for 1 hour. The sections were stained by 4′, 6-diamidino-2-phenylindole (DAPI, 0.1 mg/mL, D1306; Thermofisher, MA, USA) for 15 minutes to visualize cell nuclei. A confocal microscope (Zeiss, Germany) was used to observe the experimental results.

2.6. Scanning electron microscope

After decalcification with 10% EDTA decalcification solution, the cochlear epitheliums were exposed by dissection, and the fixed sample was rinsed three times for 15 min each in 0.1 M phosphate buffer PB (pH 7.4). 1% osmium acid prepared in 0.1 M phosphate buffer PB was fixed at room temperature and protected from light for 1.5 h. The sample was then rinsed three times for 15 min each in 0.1 M phosphate buffer PB. The cochlear tissues were then dehydrated in gradient alcohol and dried for 15 min after the transition to isoamyl acetate, and the samples were placed in a critical point dryer (Quorum, UK) and coated by ion sputtering vacuum coating. An electron microscope (Hitachi, Japan) was used for observation and photography.

2.7. RNAseq

Samples were subjected to total RNA using Trizol (Invitrogen, CA, USA) according to the protocol outlined by Chomczynski *et al.* (*15*). RNA quality was determined by A260/A280 measuring using a NanodropTM One C spectrophotometer (ThermoFisher, MA, USA). Quantification of qualifying RNAs was performed using a Qubit3.0 with a QubitTM RNA Broad Range Assay kit (Life Technologies, CA, USA). The stranded RNA sequencing library was prepared using a KC-DigitalTM Stranded mRNA Library Prep Kit for Illumina® (Seqhealth Technology Co., Ltd. Wuhan, China) following the manufacturer's instructions. Finally sequenced on an Illumina Novaseq 6000 platform.

2.8. Statistical analysis

All tests, tissue processing, quantification, and data analysis were conducted in a blinded manner throughout the study. To assess the normality of the data distribution, parametric tests (unpaired two-tailed Student's *t*-test) were used (GraphPad Prism 8.0). The data are expressed as the mean ± SEM and statistical significance was defined as $P < 0.05$.

2.9. Bioinformatic analysis

2.9.1. Screening of differentially expressed genes

The gene expression in the p.V37I mice and the wild-type (WT) mice, the sequence reads were then mapped to the mouse genome assembly (GRCm38/mm10) using STAR v2.5.3a. Following this, the differential gene expression between p.V37I and wild-type mice analysis was performed using the DESeq2 (*16*), with a screening condition of *P*-adjusted < 0.05 and the |log2FC| > 1.5.

2.9.2. Functional annotation of the DEGs

The DEGs were analyzed for enrichment using Gene Ontology (GO) through clusterProfiler (4.6.2). The corresponding biological functions related to the differentially expressed genes (DEGs) were also presented. The calculated *P*-value was adjusted through Benjamini and Hochberg's approach, using an adjusted $P < 0.05$ as a threshold. GO terms with adjusted $P < 0.05$ were regarded as significantly enriched by DEGs.

3. Results

3.1. *GJB2* p.V37I and p.V37M mutations can cause potential functional impairment

SIFT analysis predicted both two variants to be "tolerated," with output scores of 0.22 for p.V37M and 0.67 for p.V37I, indicating a relatively lower likelihood of functional disruption. In contrast, PolyPhen-2 classified both mutations as "probably damaging," with a score of 1.000 for p.V37M (sensitivity: 0.00; specificity: 1.00) and 0.999 for p.V37I (sensitivity: 0.14; specificity: 0.99), suggesting a high probability of protein function alteration. Additionally, three-dimensional structural modeling and visualization revealed notable differences between the p.V37I and wild-type proteins, indicating that the p.V37M and p.V37I mutations may affect protein stability (Figure 1D).

3.2. The aged p.V37I knock-in mice have progressive mild hearing loss

The ABR assay was performed on p.V37I mice and wild-type mice, including Click, 8 kHz,16 kHz, and 32 kHz. We observed that the response thresholds of the p.V37I mice were mildly elevated when compared to those of the wild-type mice, particularly from 8 to 12 months of age. This elevation was most pronounced at higher frequencies ($P < 0.05$), as depicted in Figure 2A.

3.3. The p.V37I knock-in mice have normal cochlear development.

In adult p.V37I mice at 1 month of age, morphological assessments showed normal cochlear development, it indicated that this kind of mutation can't induce developmental disorder. The cochlear tunnel remained open, with no visible abnormalities or loss detected in the hair cells or the structural integrity of the organ of Corti (Figure 2B). Additionally, SEM analysis revealed no significant disruptions in cilium structure or arrangement (Figure 2C). These findings suggest that the p.V37I mutation does not significantly affect the morphological development of the cochlea and does not result in pronounced hair cell abnormalities.

3.4. The expression levels of Cx26 and Cx30 showed no significant changes

Cx26 and Cx30 are the predominant gap junction proteins in the cochlea. Immunofluorescence staining of 1-month-old (when the auditory system is developed) p.V37I mice revealed the presence of foveal gap junction structures on the supporting cell membrane, in which Cx26 and Cx30 were co-localized correctly (Figure 2D, 2E). The p.V37I mice did not exhibit any significant differences in the localization or overall expression pattern of these proteins compared to the wild-type group. This suggests that the single amino acid substitution at position 37 does not result in a major alteration in the expression or distribution of the proteins. Specifically, the p.V37I mutation did not appear to affect the normal expression or localization of Cx26, nor does it lead to protein retention in the cytoplasm.

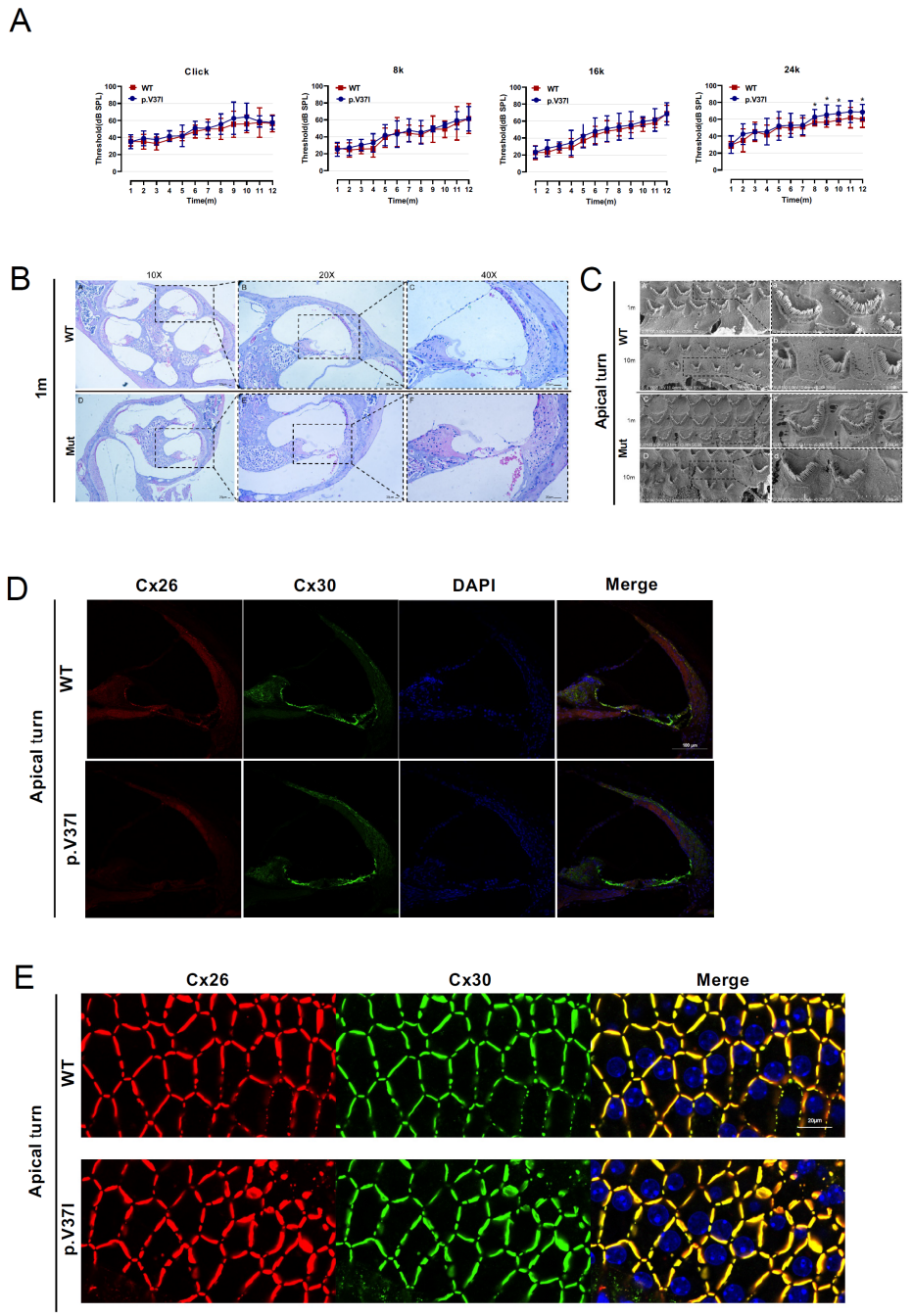

Figure 2. ABR thresholds and cochlea morphology of the p.V37I and wild-type (WT) mice. A: The averaged ABR thresholds of the wild-type and p.V37I mice at Click, 8, 16, and 24 kHz. The number of tested mice of each group is 6, asterisks indicate the statistical significance with P-values of 0.05 or lower. **B**: H&E staining showing the normal gross morphology of the p.V37I mice cochleae. Scale bars: 20 μm. **C**: Scanning electron microscopy showing normal cellular structure and arrangement of the hair cell in the p.V37I mice. **D**: Immunofluorescent staining for Cx26 (red) and Cx30 (green) in the cochlea. Scale bars: 100 μm. **E**: Immunofluorescent staining of Cx26 (red), Cx30 (green) and merged images at the age of 4 weeks from apical turns membrane. Scale bars: 20 μm.

3.5. Transcriptome analysis of the cochlea between the p.V37I mice and the WT mice.

We conducted a comparative analysis of gene expression in p.V37I and WT mice at both young (1-month) and old (8-month) ages. At 1 month, p.V37I mice exhibited 7 up-regulated and 1,311 down-regulated genes compared to wild-type mice, with an adjusted *P*-value < 0.05 and fold changes > 1.5. At 8 months, there were 1,269 up-regulated and 732 down-regulated genes in p.V37I mice relative to WT mice. Principal Component Analysis (PCA) revealed distinct clustering; at young ages, the expression profiles of p.V37I and WT mice overlapped, whereas at older ages, the profiles were clearly separable (Figure 3A). Differential expression was visualized using volcano plots (Figure 3B). GO enrichment analysis of the DEGs between aging p.V37I and WT mice highlighted significant enrichment in biological processes related to

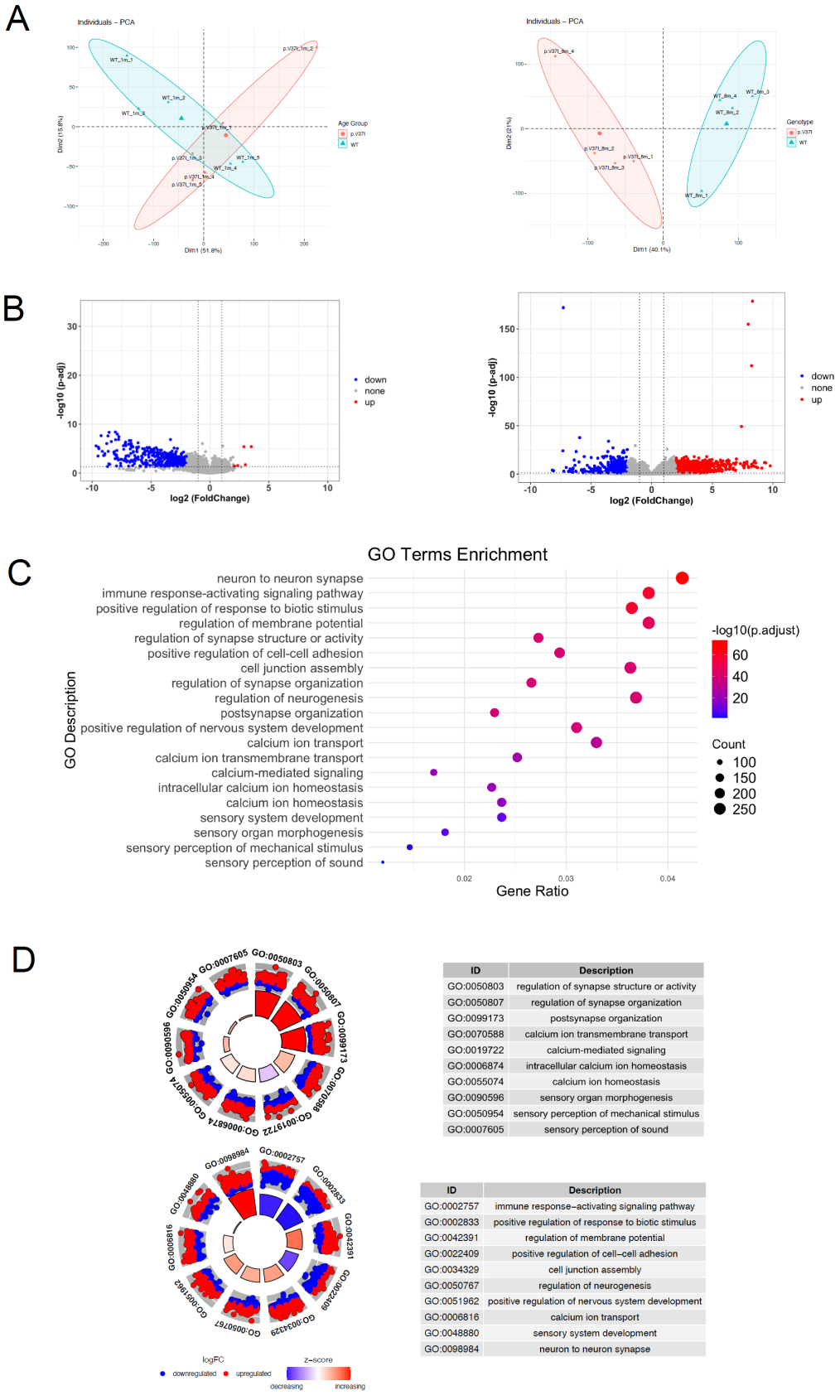

ID	Description
GO:0050803	regulation of synapse structure or activity
GO:0050807	regulation of synapse organization
GO:0099173	postsynapse organization
GO:0070588	calcium ion transmembrane transport
GO:0019722	calcium-mediated signaling
GO:0006874	intracellular calcium ion homeostasis
GO:0055074	calcium ion homeostasis
GO:0090596	sensory organ morphogenesis
GO:0050954	sensory perception of mechanical stimulus
GO:0007605	sensory perception of sound

ID	Description
GO:0002757	immune response–activating signaling pathway
GO:0002833	positive regulation of response to biotic stimulus
GO:0042391	regulation of membrane potential
GO:0022409	positive regulation of cell–cell adhesion
GO:0034329	cell junction assembly
GO:0050767	regulation of neurogenesis
GO:0051962	positive regulation of nervous system development
GO:0006816	calcium ion transport
GO:0048880	sensory system development
GO:0098984	neuron to neuron synapse

Figure 3. Transcriptome analysis of the cochlea between the p.V37I mice and the WT mice in different age. A: Principal Component Analysis (PCA) revealed the clustering of different cochlea group, at older age, the transcript profiles were clearly separable. **B**: Volcano plot with the red and blue dots representing the up and down regulation of differentially expressed genes, respectively. **C**: GO bar chart showing significant accumulation: significantly enriched GO terms based on $P \leq 0.05$; the horizontal axis shows the Gene Ratio; the vertical axis shows the description of GO terms. **D**: GO term enrichment analysis and expression patterns of differentially expressed genes (DEGs).

neural and sensory functions. Notably enriched terms include "neuron-to-neuron synapse", "immune response-activating signaling pathway", "regulation of synapse structure or activity", and "sensory perception of sound". These findings suggest that the p.V37I mutation in aging mice affects synaptic and calcium signaling pathways, as well as sensory system development (Figure 3C, 3D).

4. Discussion

The *GJB2* gene mutation is the predominant cause of deafness and hearing loss, particularly in East Asia, where the p.V37I mutation is the most prevalent variant. A comprehensive cross-sectional study involving a full life-cycle population cohort with the biallelic p.V37I mutation demonstrated a steadily progressive hearing loss that increases in prevalence with age (*10*). This suggests that the p.V37I mutation may play a significant role in ARHL in humans. It is critical to develop appropriate animal models to explore the pathogenesis of hearing loss induced by gene mutations effectively. Interestingly, the expression and functional impact of the *GJB2* gene c.109G>A mutation differ between species. In human's gene, the c.109G>A substitution results p.V37I amino acid change. However, in mice, the analogous c.109G>A substitution results in a p.V37M amino acid change (Figure 1B, 1D), which leads to progressive, mild hearing loss without significant developmental or morphological abnormalities (*13,14*). This interspecies variability limits the translational relevance of current mouse models for studying the c.109G>A (p.V37I) mutation in humans. To address this limitation, we engineered a novel mouse model with a double-base edit in the p.V37 codon of the *GJB2* gene, successfully replicating the human p.V37I amino acid sequence. This modification accurately replicates the human p.V37I amino acid sequence, thereby enhancing the model's relevance for studying the mutation's effects. The c.109G>A mutation leads to a single amino acid change, in this study, it resulted in p.V37I in humans and p.V37M in mice. This genetically modified model allows for a closer examination of the mutation's pathophysiological effects and provides a valuable tool for investigating the mechanisms underlying ARHL and related hearing disorders. Compared to models carrying the p.V37M mutation, our p.V37I model also exhibited a progressive, mild-to-moderate hearing loss. Considering the different strain background and experimental equipment difference, the difference can be reasonable. Both variants are associated with a relatively mild form of hearing loss, indicating these mutations can cause nuanced impact on the auditory function.

In our study of cochlear development and the structure of the organ of Corti, we observed that p.V37I mice exhibited a phenotype indicative of very milder auditory impairment. Morphological analysis revealed no significant abnormalities in the cochlear structure or the organ of Corti (Figure 2B). SEM further confirmed the absence of significant microstructural changes in p.V37I mice compared to WT controls (Figure 2C). Compared to the findings reported from the p.V37M model (*13,14*), no significant differences in the length of gap junction plaques were observed between p.V37M and WT mice. On the other hand, more severe cochlear disruptions have been documented in studies of other *GJB2* mutations, such as c.235delC and Cx26 knockout (KO) mice, which include structural abnormalities like closure of the tunnel of Corti (*13,14,17,18*). These observations highlight the diverse impacts of different *GJB2* mutations on cochlear architecture and auditory function. Unlike mutations associated with congenital hearing loss, such as the R75W transgenic and certain conditional knockout models, the p.V37I mutation resulted in progressive rather than congenital hearing loss (*19*). This kind of hearing loss aligned with the absence of significant structural changes in the cochlea, suggesting a more subtle impact of the p.V37I mutation on cochlear integrity.

RNA-Seq is a widely used method in both laboratory research and clinical studies, as it provides a more accurate measurement of transcript levels and their isoforms than other methods, such as microarrays. To investigate the potential mechanisms behind the gene expression changes in the p.V37I mice, we conducted RNA-Seq analyses for both p.V37I and WT mice at different ages. ARHL is characterized as a degenerative condition in which crucial genes are progressively downregulated over time. In our study, p.V37I mice began to exhibit signs of hearing loss by 8 months of age, in contrast to their WT counterparts. PCA revealed that at a younger age, the gene expression profiles in the cochlea of p.V37I mutant mice closely resembled those of wild-type mice. However, as the mice aged, the gene expression profiles diverged significantly, enabling clear differentiation into two distinct groups (Figure 3A). By 8 months of age, the number of downregulated DEGs in p.V37I mice was markedly higher than at younger ages, suggesting an accelerated decline in key gene expression (Figure 3B). This trend suggested that changes in gene expression are closely associated with the observed phenotype of hearing loss. Notably, these changes in gene expression appear to be age-dependent, indicating a potential link between aging processes and the exacerbation of auditory impairments in p.V37I mice.

The GO enrichment analysis of the DEGs between aging p.V37I and aging WT mice revealed significant enrichment in biological processes related to neural and sensory functions. Notably enriched terms included "neuron-to-neuron synapse", "immune response-activating signaling pathway", "calcium-mediated signaling pathway", and "sensory perception of sound", (Figure 3C, 3D). These findings suggest that the p.V37I mutation in aging mice influences synaptic and calcium signaling pathways, as well as the sensory

system's development and function. Calcium (Ca^{2+}) signaling in the cochlea is well-established as critical for the development and maturation of outer hair cell afferent innervation (*20,21*). In p.V37I mutant cochleae, age-related changes in calcium signaling pathways may contribute to the functional decline of hair cells, ultimately leading to auditory impairment. On the other hand, the enrichment of the "immune response-activating signaling pathway" suggests that aging p.V37I cochleae may exhibit altered immune responses, potentially impacting their ability to resist external stimuli (*22*). These age-related changes in neural, calcium, and immune signaling pathways collectively provide insights into the mechanisms underlying the progressive hearing loss observed in p.V37I mice.

In conclusion, we conducted a comparative analysis of the transcriptional profiles of cochlea tissue between *GJB2* gene p.V37I mutant and the WT mice of different ages by RNA-Seq. We aimed to identify the underlying mechanisms of gene expression before any obviously morphological changes. The transcriptomic differences between the p.V37I and wild groups were different at different time points, indicating that the p.V37I mice may experience mild cochlea function impairment throughout their lifespan without experiencing observable hearing loss during their early years. However, as they age, the p.V37I mice become more vulnerable to oxidative stress, inflammation, immune system dysregulation, and other abnormalities compared to wild mice, leading to more severe age-related hearing loss. This is reflected by increased hearing impairment or earlier aging in old mice.

Moreover, it should be noted that the cochlea comprises a quite scarce number of sensory cells, and the bulk transcriptome sequencing approach is potentially insufficient for discerning the intricate gene expression patterns related to cilia and microtubules in outer hair cells (*23,24*). These specific gene expressions may be overshadowed by the influence of environmental noise. Consequently, further investigations are warranted to augment the depth of exploration into the inner ear, with particular emphasis on elucidating the functional characteristics and gene expression profiles of various cochlear systems, such as the Corti's organ and the stria vascular system (*25*). The employment of cutting-edge technologies and sequencing methodologies, such as single-cell sequencing, can help in deciphering the intricate mechanisms underlying genetic-induced hearing loss. Single-cell sequencing, boasting superior resolution capabilities when compared to bulk-seq, stands poised to represent the subsequent stride toward conducting more comprehensive and insightful research (*22,26,27*).

Acknowledgements

We sincerely appreciate the guidance of our tutors and every member of our team.

Funding: This work was supported by the National Natural Science Foundation of China (grant numbers 81870730, 82071064), and the Capital's Funds for Health Improvement and Research (grant number, CFH 2022-2-1092).

Conflict of Interest: The authors have no conflicts of interest to disclose.

References

1. World Health Organization. World report on hearing. *https://www.who.int/publications/i/item/world-report-on-hearing* (accessed January 19, 2025).
2. Cui Q, Chen N, Wen C, Xi J, Huang L. Research trends and hotspot analysis of age-related hearing loss from a bibliographic perspective. Front Psychol. 2022; 13:921117.
3. Salvi R, Ding D, Jiang H, Chen GD, Greco A, Manohar S, Sun W, Ralli M. Hidden age-related hearing loss and hearing disorders: Current knowledge and future directions. Hear Balance Commun. 2018; 16:74-82.
4. Lin FR, Yaffe K, Xia J, Xue QL, Harris TB, Purchase-Helzner E, Satterfield S, Ayonayon HN, Ferrucci L, Simonsick EM. Hearing loss and cognitive decline in older adults. JAMA Intern Med. 2013; 173:293-299.
5. Ahmadmehrabi S, Brant J, Epstein DJ, Ruckenstein MJ, Rader DJ. Genetics of postlingual sensorineural hearing loss. Laryngoscope. 2021; 131:401-409.
6. Wells HRR, Newman TA, Williams FMK. Genetics of age-related hearing loss. J Neurosci Res. 2020; 98:1698-1704.
7. del Castillo FJ, del Castillo I. The DFNB1 subtype of autosomal recessive non-syndromic hearing impairment. Front Biosci Landmark Ed. 2011; 16:3252-3274.
8. Li L, Lu J, Tao Z, Huang Q, Chai Y, Li X, Huang Z, Li Y, Xiang M, Yang J, Yao G, Wang Y, Yang T, Wu H. The p.V37I exclusive genotype of *GJB2*: A genetic risk-indicator of postnatal permanent childhood hearing impairment. PLoS One. 2012; 7:e36621.
9. Yu X, Lin Y, Xu J, Che T, Li L, Yang T, Wu H. Molecular epidemiology of Chinese Han deaf patients with bi-allelic and mono-allelic *GJB2* mutations. Orphanet J Rare Dis. 2020; 15(1):29.
10. Chen Y, Wang Z, Jiang Y, *et al*. Biallelic p.V37I variant in GJB2 is associated with increasing incidence of hearing loss with age. Genet Med. 2022; 24:915-923.
11. Wen C, Yang X, Cheng X, *et al*. Optimized concurrent hearing and genetic screening in Beijing, China: A cross-sectional study. Biosci Trends. 2023; 17:148-159.
12. Dai P, Huang LH, Wang GJ, *et al*. Concurrent hearing and genetic screening of 180,469 neonates with follow-up in Beijing, China. Am J Hum Genet. 2019; 105:803-812.
13. Chen Y, Hu L, Wang X, Sun C, Lin X, Li L, Mei L, Huang Z, Yang T, Wu H. Characterization of a knock-in mouse model of the homozygous p.V37I variant in Gjb2. Sci Rep. 2016; 6:33279.
14. Lin X, Li G, Zhang Y, Zhao J, Lu J, Gao Y, Liu H, Li GL, Yang T, Song L, Wu H. Hearing consequences in Gjb2 knock-in mice: implications for human p.V37I mutation. Aging. 2019; 11:7416-7441.
15. Chomczynski P, Sacchi N. The single-step method of RNA isolation by acid guanidinium thiocyanate-phenol-

chloroform extraction: twenty-something years on. Nat Protoc. 2006; 1:581-585.
16. Love MI, Huber W, Anders S. Moderated estimation of fold change and dispersion for RNA-seq data with DESeq2. Genome Biol. 2014; 15:550.
17. Zhu Y, Zong L, Mei L, Zhao HB. Connexin26 gap junction mediates miRNA intercellular genetic communication in the cochlea and is required for inner ear development. Sci Rep. 2015; 5:15647.
18. Li Q, Cui C, Liao R, *et al*. The pathogenesis of common *Gjb2* mutations associated with human hereditary deafness in mice. Cell Mol Life Sci. 2023; 80:148.
19. Inoshita A, Iizuka T, Okamura H-O, Minekawa A, Kojima K, Furukawa M, Kusunoki T, Ikeda K. Postnatal development of the organ of Corti in dominant-negative *Gjb2* transgenic mice. Neuroscience. 2008; 156:1039-1047.
20. Yang Y, Murtha K, Climer LK, Ceriani F, Thompson P, Hornak AJ, Marcotti W, Simmons DD. Oncomodulin regulates spontaneous calcium signaling and maturation of afferent innervation in cochlear outer hair cells. J Physiol. 2023; 601:4291-4308.
21. Murtha KE, Yang Y, Ceriani F, Jeng JY, Climer LK, Jones F, Charles J, Devana SK, Hornak AJ, Marcotti W, Simmons DD. Oncomodulin (OCM) uniquely regulates calcium signaling in neonatal cochlear outer hair cells. Cell Calcium. 2022; 105:102613.
22. Sun G, Zheng Y, Fu X, *et al*. Single-cell transcriptomic atlas of mouse cochlear aging. Protein Cell. 2023; 14:180-201.
23. Ma X, Guo J, Tian M, Fu Y, Jiang P, Zhang Y, Chai R. Advance and application of single-cell transcriptomics in auditory research. Neurosci Bull. 2024; 40:963-980.
24. Jean P, Wong Jun Tai F, Singh-Estivalet A, *et al*. Single-cell transcriptomic profiling of the mouse cochlea: An atlas for targeted therapies. Proc Natl Acad Sci. 2023; 120:e2221744120.
25. Xu Z, Tu S, Pass C, Zhang Y, Liu H, Diers J, Fu Y, He DZZ, Zuo J. Profiling mouse cochlear cell maturation using 10× Genomics single-cell transcriptomics. Front Cell Neurosci. 2022; 16:962106.
26. Liu H, Giffen KP, Chen L, Henderson HJ, Cao TA, Kozeny GA, Beisel KW, Li Y, He DZ. Molecular and cytological profiling of biological aging of mouse cochlear inner and outer hair cells. Cell Rep. 2022; 39:110665.
27. Hoa M, Olszewski R, Li X, Taukulis I, Gu S, DeTorres A, Lopez IA, Linthicum FH Jr, Ishiyama A, Martin D, Morell RJ, Kelley MW. Characterizing adult cochlear supporting cell transcriptional diversity using single-cell RNA-seq: Validation in the adult mouse and translational implications for the adult human cochlea. Front Mol Neurosci. 2020; 13:13.

Received January 29, 2025; Revised April 21, 2025; Accepted April 23, 2025.

**Address correspondence to:*
Lihui Huang, Otolaryngology Head and Neck Surgery, Beijing Tongren Hospital, Capital Medical University, Beijing 100730, China; Beijing Institute of Otolaryngology, Beijing 100005, China; Key Laboratory of Otolaryngology Head and Neck Surgery, Ministry of Education, Beijing 100005, China.
E-mail: huangpub@126.com

Ning Yu, College of Otolaryngology Head and Neck Surgery, Chinese PLA General Hospital, Beijing 100853, China; National Clinical Research Center for Otolaryngologic Diseases, Beijing 100853, China.
E-mail: yuning@301hospital.org

Released online in J-STAGE as advance publication April 28, 2025.

Original Article

DOI: 10.5582/ddt.2025.01011

Clinical benefits of rapid initiation of antiretroviral therapy within 14 days for newly diagnosed late-presentation people living with human immunodeficiency virus (PLWH)

Xiang Zhang[1,§], Hongjing Guan[2,§], Xiaoyun Di[1], Mengqing Li[2], Jingli Peng[1], Rentian Cai[3,*], Hongxia Wei[2,3,*]

[1] Department of Infectious Disease, The Second Hospital of Nanjing, Affiliated to Nanjing University of Chinese Medicine, Nanjing, Jiangsu, China;
[2] Department of Infectious Disease, The School of Public Health of Nanjing Medical University, The Second Hospital of Nanjing, Nanjing, Jiangsu, China;
[3] Department of Infectious Disease, The Second Hospital of Nanjing, Nanjing, Jiangsu, China.

SUMMARY: This study evaluated the impact of initiating antiretroviral therapy (ART) within 14 days compared to starting after 14 days in newly diagnosed, late-presenting people living with human immunodeficiency virus (PLWH). A total of 1,538 PLWH with a baseline $CD4^+$ T-cell count < 350 cells/μL who attended our outpatient clinic from January 2017 to June 2022 were included. Participants were divided into two groups based on ART initiation timing: rapid initiation (ART within 14 days) and delayed initiation (ART after 14 days). Rapid initiation led to significantly higher virologic suppression rates at 6 months (62.5% *vs.* 52.7%, $P < 0.05$) and 1 year (81.6% *vs.* 72.1%, $P < 0.01$) compared to delayed initiation. While overall treatment retention rates were comparable, rapid initiation improved retention at 6 months for those with baseline $CD4^+$ < 200 cells/μL and at 1 year for those with baseline $CD4^+$ between 200 and 350 cells/μL. No significant differences in $CD4^+$ T-cell counts or CD4/CD8 ratio were observed. A positive correlation was found between baseline viral load and time to virologic suppression, with rapid initiation of ART leading to faster suppression, especially in those with higher baseline viral loads. Multivariate analysis confirmed that ART initiation timing and baseline viral load were key determinants of virologic suppression. In conclusion, rapid ART initiation within 14 days was associated with higher virologic suppression at 6 months and 1 year. Rapid initiation of ART and lower baseline viral load were critical for virologic suppression, with improved retention for specific subgroups.

Keywords: Rapid ART initiation, virologic suppression rate, treatment retention rate, immune recovery

1. Introduction

Acquired immunodeficiency syndrome (AIDS), caused by the human immunodeficiency virus (HIV), has been a major global health concern since 1981. As of July 2022, approximately 84.2 million people worldwide have been infected, with 40.1 million deaths due to HIV-related illnesses (*1*). In China, 1.223 million people were reported to be living with HIV/AIDS by the end of 2022 (*2*). The introduction of combination antiretroviral therapy (cART) in 1996 significantly improved outcomes for people living with HIV (PLWH) (*3*). Since 2015, the WHO has recommended initiating ART for all HIV-positive individuals regardless of $CD4^+$ T-cell count (*4,5*), and China adopted this guideline in 2016 (*6*), resulting in nearly 600,000 PLWH starting ART the following year (*7*).

Recent evidence suggests that rapid ART initiation, defined variably as starting treatment within 5 to 14 days after diagnosis(*8,9*), can further improve clinical outcomes. Studies across multiple countries have demonstrated that immediate or same-day ART initiation leads to higher rates of virologic suppression, reduced treatment dropout, and significantly lower mortality (*8-19*). For example, rapid ART initiation has been associated with a 63% reduction in mortality (*10*) and faster virologic suppression in settings such as Haiti, Atlanta (USA), San Francisco (USA), and Guangxi (China) (*13,17-20*). These benefits are particularly pronounced in patients with advanced disease or low $CD4^+$ counts (*10,19*). Despite variations in implementation across regions, the trend toward rapid initiation is supported by strong clinical evidence.

Late presentation remains a key barrier to effective HIV treatment, especially in low- and middle-income countries. In China, the proportion of late presenters

has decreased over the years, from 80% in 2008 to 29% in 2016 (*21,22*). However, many newly diagnosed individuals still present with $CD4^+$ counts below 350 or 200 cells/μL or with AIDS-defining conditions (*23*), placing them at higher risk for poor outcomes, including a tenfold increase in morbidity and mortality during the first year after diagnosis (*24,25*). Delayed diagnosis also contributes to ongoing transmission and incomplete immune recovery (*26-29*). Despite the urgency, there is a lack of focused research on late-presenting PLWH in China. This retrospective study analyzes such patients treated at Nanjing Second Hospital from 2017 to 2022, aiming to evaluate the impact of rapid versus delayed ART initiation on virologic suppression, treatment retention, and immune recovery over 1 year and 5 years.

2. Materials and Methods

2.1. Study subjects

This study is a single-center, retrospective, controlled study. The subjects were patients who visited the Infectious Diseases Department at Nanjing Second Hospital between January 1, 2017, and June 30, 2022. The study focused on treatment-naive individuals with a baseline $CD4^+$ T cell count below 350 cells/μL. Eligible patients were categorized into two groups based on the time to initiate ART after diagnosis: the rapid initiation group (ART started within 14 days of diagnosis) and the delayed initiation group (ART started more than 14 days after diagnosis).

2.1.1. Inclusion criteria

Aged 18 years or older; Diagnosed with HIV/AIDS according to the People's Republic of China health industry standard (WS293-2019) - "Diagnosis of AIDS and HIV Infection"; Received initial antiviral treatment at Nanjing Second Hospital with complete follow-up data; Baseline $CD4^+$ T cell count below 350 cells/μL.

2.1.2. Exclusion criteria

Prior receipt of any form of antiretroviral therapy; Absence of baseline viral load (VL) data; Coexisting conditions such as tuberculous meningitis, cryptococcal meningitis, or Kaposi's sarcoma that would preclude rapid initiation of ART; Patients transferred out during the follow-up period.

2.2. Study methods and data collection

2.2.1. Study design

This study employs a single-center, retrospective design. This study was approved by the Ethics Committee of The Second Hospital of Nanjing, Affiliated to Nanjing University of Chinese Medicine (Approval No: 2024-LS-ky043). All procedures were conducted in accordance with the Declaration of Helsinki (2013 revision).

2.2.2. Baseline assessment

Baseline data were collected before the initiation of ART, including general information (age, sex, marital status), immunological status ($CD4^+$ T cell count, CD4/CD8 ratio), HIV infection status (HIV-1 RNA viral load, time of HIV diagnosis, and time from diagnosis to treatment).

2.2.3. Follow-up data collection

Participants were followed at regular intervals, with data collected at 3 months, 6 months, 1 year, 2 years, 3 years, 4 years, and 5 years after initiating ART. Collected data included: HIV-1 RNA viral load; $CD4^+$ T cell count, $CD8^+$ T cell count; adherence to and interruption of treatment. Data from HIV-1 RNA and immune status tests conducted within 3 months before or after each follow-up visit were included in the analysis for that time point.

2.2.4. Data sources

Data were sourced from the following: National AIDS Basic Prevention and Treatment Information System database; Electronic Medical Record System of Nanjing Second Hospital; Laboratory Information System (LIS); Patient paper records.

2.2.5. Stratified analysis

Since the majority of late-presenting patients had $CD4^+$ T cell counts below 200 cells/μL, stratification by $CD4^+$ T cell count < 200 cells/μL was performed to account for variations in baseline $CD4^+$ T cell levels and their impact on achieving viral suppression.

2.3. Study endpoints and definitions

2.3.1. Primary endpoints

Viral suppression rate: The proportion of patients with plasma HIV-1 RNA < 50 copies/mL at 12 months post-treatment. Treatment retention rate: The ratio of actual treated patients to the number of patients eligible for treatment each year. $CD4^+$ T cell count and change from baseline: Measurement of $CD4^+$ T cell count and the difference from baseline at 12 months. CD4/CD8 ratio: The ratio of $CD4^+$ to $CD8^+$ T cells.

2.3.2. Secondary endpoints

Viral suppression rate: Proportions of patients with plasma HIV-1 RNA < 50 copies/mL at 1 year, 2 years,

3 years, 4 years, and 5 years. Treatment retention rate: Treatment adherence rates at 1 year, 2 years, 3 years, 4 years, and 5 years. $CD4^+$ T cell count and change from baseline: Changes in $CD4^+$ T cell count from baseline at the specified time points. CD4/CD8 ratio: The CD4/CD8 ratio at each follow-up interval. Mortality rate and related factors: The mortality rate during the 5-year follow-up period and factors associated with mortality.

2.4. Statistical methods

Data were collected and initially processed using Excel, and statistical analyses were conducted with R Studio 4.3.0. All graphical representations were generated using Origin. Baseline characteristics of the population were described using appropriate methods based on data types. For continuous variables, median values and interquartile ranges (IQR) were reported. Comparisons between two groups for normally distributed data were performed using the Student's *t*-test, while non-normally distributed data were analyzed using the Wilcoxon rank-sum test. Categorical data were expressed as percentages, and comparisons between two groups were made using the chi-square test or Fisher's exact test.

Correlation curves were employed to describe the relationship between baseline viral load, time to ART initiation, and the duration required to achieve viral suppression. Cox proportional hazards regression analysis was used to identify factors associated with achieving viral suppression in late-presenting HIV patients post-treatment. Kaplan-Meier (K-M) curves illustrated the time to viral suppression for the rapid initiation group compared to the delayed initiation group, under various influencing factors.

Stratified analyses were performed based on baseline $CD4^+$ T cell counts, distinguishing between those with $CD4^+$ T cell counts < 200 cells/μL and those with counts between 200 and 350 cells/μL. These analyses evaluated changes in viral suppression rates, treatment retention rates, and immune recovery. Statistical significance was set at $P < 0.05$.

3. Results

3.1. Patient enrollment and study flow

Between January 1, 2017, and June 30, 2022, a total of 1,717 individuals with a baseline $CD4^+$ T cell count below 350 cells/μL were initially enrolled at the Infectious Diseases Department of Nanjing Second Hospital. Following exclusion of 58 cases with missing baseline viral load data, 16 cases with cryptococcal meningitis, tuberculous meningitis, or Kaposi's sarcoma, and 105 cases transferred from other institutions, 1,538 patients were included in the subsequent analysis (Figure 1).

Of these, 456 patients were in the rapid initiation group, and 1,082 patients were in the delayed initiation

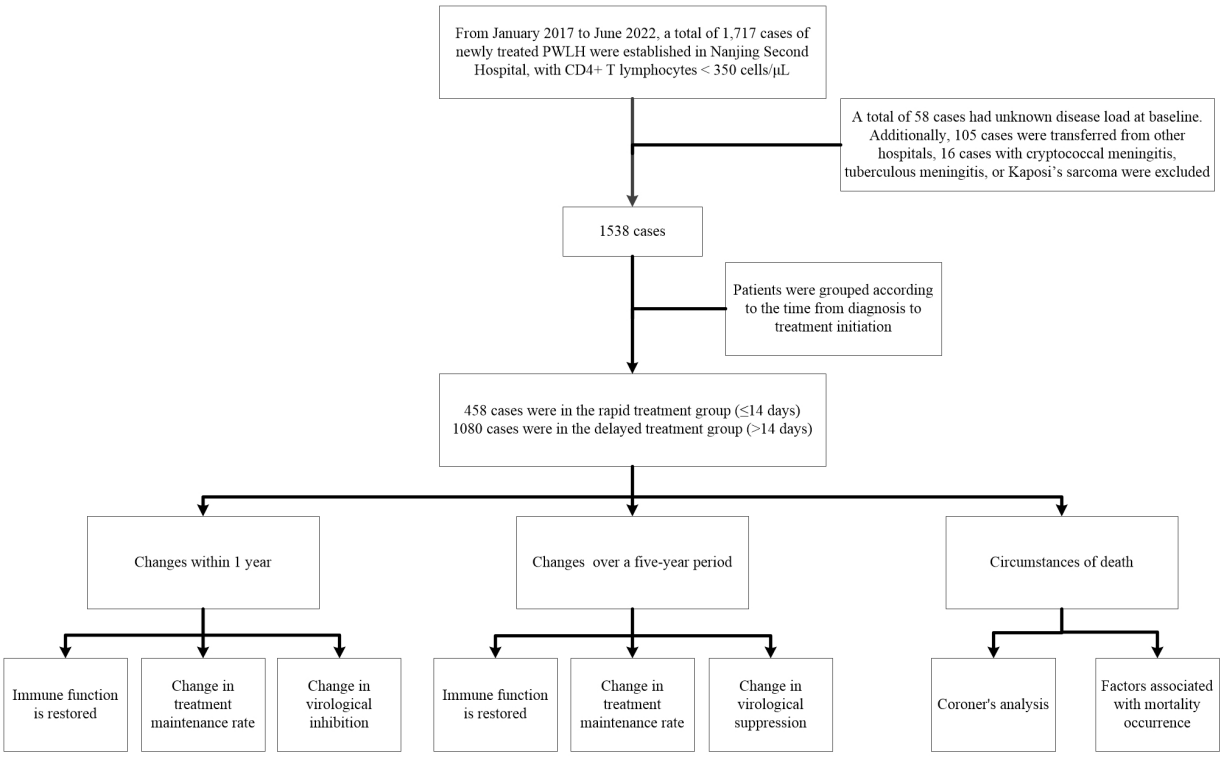

Figure 1. Baseline enrollment status.

group (Table 1). Overall, the cohort comprised 1,419 males (92.3%) and 119 females (7.7%). The median age of the patients was 38 years (IQR: 30-54 years). Education levels showed that 959 patients (62.4%) had attained a high school diploma or higher.

The median time from diagnosis to treatment initiation showed a decreasing trend over the years: 26 days (IQR: 14-69.5) in 2018; 26 days (IQR: 13-68.5) in 2019; 20 days (IQR: 13-48) in 2020; 20 days (IQR: 13-42) in 2021; and 18 days (IQR: 11-39.75) in 2022.

The median baseline $CD4^+$ T cell count for the overall cohort was 181 cells/μL (IQR: 66-266 cells/μL). The largest proportion of patients had $CD4^+$ T cell counts between 200 and 350 cells/μL (712 patients, 46.3%), followed by those with counts between 100 and 199 cells/μL (331 patients, 21.5%), counts below 50 cells/μL (309 patients, 20.1%), and counts between 50 and 99 cells/μL (186 patients, 12.1%).

The median log10 value of baseline VL was 4.8 log10 copies/mL (IQR: 4.3-5.2 log10 copies/mL). The baseline VL was significantly higher in the rapid initiation group compared to the delayed initiation group (4.8 log10 copies/mL *vs.* 4.7 log10 copies/mL, $P = 0.048$).

3.2. Viral suppression rates, treatment retention rates, and immune recovery within 1 year of ART

3.2.1. Viral suppression rates

We found that rapid ART initiation resulted in significantly higher one-year viral suppression rates than delayed initiation in patients with advanced HIV. As shown in Table 2, the overall viral suppression rate within one year for late-stage people living with HIV exhibited an increasing trend over time. The rapid initiation group demonstrated significantly higher viral suppression rates compared to the delayed initiation group at 6 months (62.5% *vs.* 52.7%, $P = 0.022$) and at 1 year (81.6% *vs.* 72.1%, $P = 0.001$).

Furthermore, the data demonstrated superior viral suppression with rapid ART in both low (< 200 cells/μL) and moderate (200-350 cells/μL) $CD4^+$ T cell count groups. When stratified by baseline $CD4^+$ T cell levels, the viral suppression rate within one year showed an increasing trend regardless of the baseline $CD4^+$ T cell count. For individuals with baseline $CD4^+$ T cell counts < 200 cells/μL, the viral suppression rate at 1 year was significantly higher in the rapid initiation group compared to the delayed initiation group (77.3% *vs.* 66.6%, $P < 0.05$). In the cohort with baseline $CD4^+$ T cell counts between 200 and 350 cells/μL, the rapid initiation group exhibited significantly higher viral suppression rates at 6 months (76.7% *vs.* 62.9%, $P < 0.05$) and at 1 year (86.0% *vs.* 77.6%, $P < 0.05$) compared to the delayed initiation group.

To identify key predictors of viral suppression, we conducted comprehensive univariate and multivariate Cox regression analyses. Univariate and multivariate Cox regression models were employed to analyze the factors influencing viral suppression, with factors

Table 1. General characteristics between the two groups

Feature	Total (n = 1538)	Rapid ART (n = 456)	Delayed ART (n = 1082)	*P*
Age, years				0.932
Median (IQR)	38 (30-54)	38 (30-55)	38 (30-54)	
Gender				0.57
Male, n (%)	1419 (92.3)	418 (91.7)	1001 (92.5)	
Female, n (%)	119 (7.7)	38 (8.3)	81 (7.5)	
Education Level				0.377
Primary and Below, n (%)	88 (5.7)	30 (6.6)	58 (5.4)	
Junior High, n (%)	189 (12.3)	50 (11.0)	139 (12.8)	
High School and Above, n (%)	959 (62.4)	278 (61.0)	681 (62.9)	
Unknown, n (%)	302 (19.6)	98 (21.5)	204 (18.9)	
Marital Status				0.191
Single, Divorced, Widowed, n (%)	989 (64.3)	282 (61.8)	707 (65.3)	
Married or Cohabiting, n (%)	549 (35.7)	174 (38.2)	375 (34.7)	
Baseline CD4+ T Cells, cells/μL				0.268
<50, n (%)	309 (20.1)	105 (23.0)	204 (18.9)	
50-99, n (%)	186 (12.1)	57 (12.5)	129 (11.9)	
100-199, n (%)	331 (21.5)	93 (20.4)	238 (22.0)	
200-349, n (%)	712 (46.3)	201 (44.1)	511 (47.2)	
Baseline VL, log10copies/ml				0.048*
Median (IQR)	4.8 (4.3-5.2)	4.8 (4.4-5.2)	4.7 (4.3-5.2)	
Time from Diagnosis to Treatment (day)				
2018, Median (IQR)	26 (14-69.5)	12 (7-12)	40 (26-230)	< 0.001***
2019, Median (IQR)	26 (13-68.5)	10 (5-12)	35 (21-154)	< 0.001***
2020, Median (IQR)	20 (13-48)	12 (7-13)	33 (21-89)	< 0.001***
2021, Median (IQR)	20 (13-42)	12 (8-13)	31 (20-114.5)	< 0.001***
2022, Median (IQR)	18 (11-39.75)	8.5 (5-12)	33 (19.25-81.5)	< 0.001***

IQR: interquartile ranges ; *: $P < 0.05$; ***: $P < 0.001$.

Table 2. Virological suppression rates at different $CD4^+$ T cell counts within one year

Population group / Time Point	Total Population			$CD4^+$ T Cells < 200 cells/μL			$CD4^+$ T Cells 200-350 cells/μL		
	≤ 14 Days	> 14 Days	*P*	≤ 14 Days	> 14 Days	*P*	≤ 14 Days	> 14 Days	*P*
3 M Viral Suppression Rate	0.327	0.31	0.759	0.276	0.24	0.366	0.402	0.393	0.875
6 M Viral Suppression Rate	0.625	0.527	0.022*	0.512	0.435	0.113	0.767	0.629	0.009**
9 M Viral Suppression Rate	0.816	0.721	0.001***	0.773	0.666	0.005**	0.86	0.776	0.021*

M: month; *: $P < 0.05$; **: $P < 0.01$; ***: $P < 0.001$.

Table 3. Factors associated with virological suppression in late-presenting PLWH: Cox regression analysis

Factors	Univariate HR (95% CI)	*P*	Multivariate HR (95% CI)	*P*
Age	0.996 (0.990, 1.000)	0.053	0.997 (0.993, 1.000)	0.079
Initial VL Measurement, copies/mL				
$< 10^5$	1			
$> 10^5$	0.623 (0.556, 0.698)	< 0.001***	0.631 (0.563, 0.708)	< 0.001***
Initial CD4+ T Cells, cells/μL				
< 50	1			
50-150	0.918 (0.889, 1.200)	0.314		
> 150	1.322 (1.208, 1.474)	< 0.001***	1.180 (0.989, 1.408)	0.066
Time from Diagnosis to Treatment, days				
Within 14 Days	1			
Greater than 14 Days	0.721 (0.777, 0.936)	< 0.001***	0.711 (0.632, 0.800)	< 0.001***
Use of Co-Trimoxazole				
No	1			
Yes	0.762 (0.724, 0.913)	< 0.001***	0.975 (0.838, 1.130)	0.739

*: $P < 0.05$; **: $P < 0.01$; ***: $P < 0.001$.

showing $P < 0.1$ in univariate analysis included in the multivariate model. The univariate analysis identified several significant factors: age ($P = 0.053$), baseline viral load ($P < 0.001$), baseline $CD4^+$ T cell count ($P < 0.001$), whether ART was initiated rapidly ($P < 0.001$), and the use of co-trimoxazole for prophylaxis ($P < 0.001$).

The multivariate Cox regression model, employing the forward likelihood ratio method, revealed that a baseline VL < 10^5 copies/mL (HR: 0.623, 95% CI: 0.556–0.698, $P < 0.001$) and ART initiation within 14 days of diagnosis (HR: 0.71, 95% CI: 0.632–0.800, $P < 0.001$) were significantly associated with a higher likelihood of achieving viral suppression (Table 3).

The survival analysis revealed two critical determinants of viral suppression timing in late-stage PLWH: treatment initiation speed and baseline viral load. As illustrated in Figures 2A1 and A2, the time to achieve viral suppression in late-stage PLWH is influenced by the time from diagnosis to treatment initiation and baseline viral load levels. The Kaplan-Meier curves demonstrate that, within the rapid initiation group, the median time to achieve 50% viral suppression is significantly shorter, indicating that earlier initiation of ART leads to quicker attainment of viral suppression ($P < 0.001$). Additionally, for treatment-naive late-stage PLWH, those with a baseline VL below 10^5 copies/mL achieve viral suppression more rapidly ($P < 0.001$).

Our correlation analysis demonstrates that baseline viral load significantly impacts the viral suppression timeline in late-stage PLWH, with differential effects across viral load strata. Overall, higher baseline viral load in late-stage PLWH is associated with a longer time to achieve viral suppression ($R = 0.24$, $P < 0.01$), as shown in Figure 2B1. Further stratification by baseline VL thresholds of 10^5 copies/mL reveals that in the group with VL < 10^5 copies/mL, there is a positive correlation between the time from diagnosis to treatment and the time to achieve viral suppression ($R = 0.099$, $P = 0.0027$). This correlation is more pronounced in the group with VL > 10^5 copies/mL ($R = 0.17$, $P < 0.001$), indicating a stronger relationship (Figures 2B2 and 2B3).

Additionally, a positive correlation was observed between the time to initiate ART and the time to achieve viral suppression, meaning that earlier initiation of ART is associated with a shorter time to achieve viral suppression ($R = 0.16$, $P < 0.001$) (Figure 2B4).

3.2.2. Treatment retention rates

For late-stage PLWH undergoing ART, treatment retention rates were assessed at various time points. At 3 months, the retention rates were 98.7% in the rapid initiation group and 96.1% in the delayed initiation group ($P = 0.316$) (Table 4). At 6 months, retention rates were 98.1% in the rapid initiation group compared to 95.7% in the delayed initiation group ($P = 0.563$). At 1 year, the treatment retention rates were 96.8% for the rapid initiation group and 93.6% for the delayed initiation

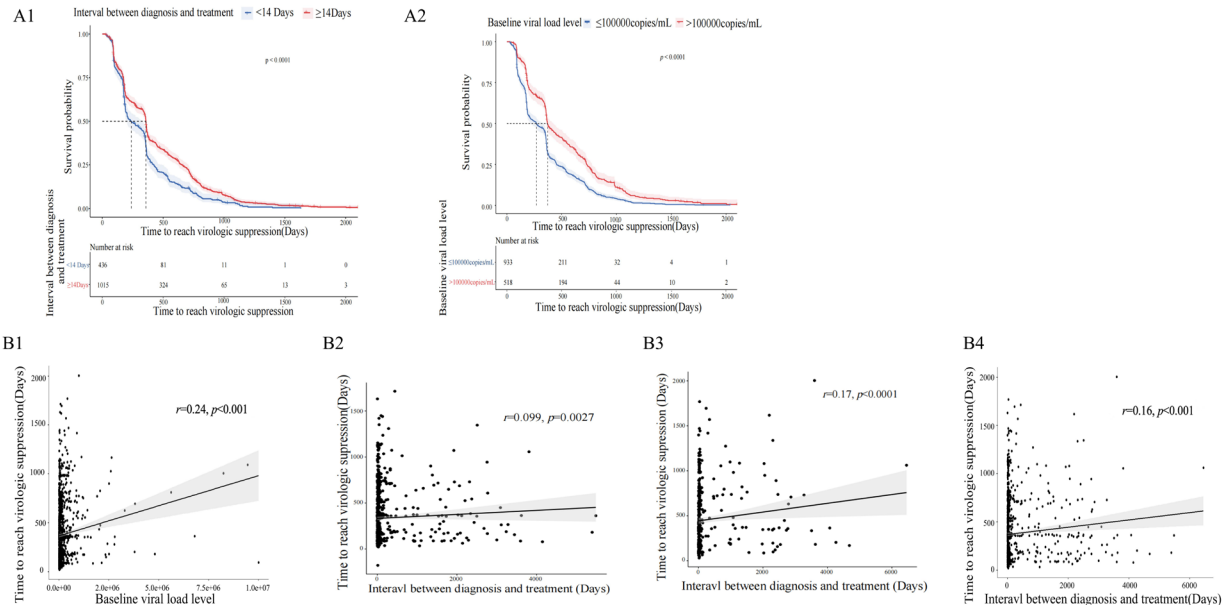

Figure 2. Kaplan-Meier (K-M) curves for achieving virological suppression and correlations with achieving virological suppression after treatment. (**A1**) K-M curves for the rapid start and delayed start treatment groups. (**A2**) K-M curves for different baseline viral loads. (**B1**) Correlation between baseline viral load and achieving virological suppression after treatment. (**B2**) Correlation between baseline viral load < 10^5 copies/mL and achieving virological suppression after treatment. (**B3**) Correlation between baseline viral load > 10^5 copies/mL and achieving virological suppression after treatment. (**B4**) Correlation between time from diagnosis to initiation of antiretroviral therapy and achieving virological suppression after treatment.

Table 4. Treatment maintenance rates at different CD4$^+$ T cell counts within one year

Population group	Total Population			Baseline CD4$^+$ T Cell Count < 200 cells/μL			Baseline CD4$^+$ T Cell Count: 200-350 cells/μL		
Time Point	≤ 14 Days	> 14 Days	*P*	≤ 14 Days	> 14 Days	*P*	≤ 14 Days	> 14 Days	*P*
3 M Treatment Retention Rate	0.987	0.961	0.316	0.988	0.954	0.084	0.986	0.969	0.880
6 M Treatment Retention Rate	0.981	0.951	0.563	0.983	0.937	< 0.001***	0.979	0.966	0.218
12 M Treatment Retention Rate	0.968	0.936	0.510	0.973	0.924	0.160	0.962	0.951	0.009**

M: month; **: $P < 0.01$; ***: $P < 0.001$.

group ($P = 0.510$). Differences between the groups were not statistically significant.

Further stratification by baseline CD4$^+$ T cell count revealed differences in retention rates. For individuals with a baseline CD4$^+$ T cell count < 200 cells/μL, the treatment retention rate at 6 months was significantly higher in the rapid initiation group compared to the delayed initiation group (98.3% *vs.* 93.7%, $P < 0.001$). For those with baseline CD4$^+$ T cell counts between 200 and 350 cells/μL, the retention rate at 1 year was notably higher in the rapid initiation group compared to the delayed initiation group (96.2% *vs.* 95.1%, $P < 0.05$).

3.2.3. Immune recovery

Longitudinal immune reconstitution monitoring demonstrated substantial post-treatment improvements in both quantitative and functional immunological parameters for late-stage PLWH. As illustrated in Figure 3A, the recovery of CD4$^+$ T cell counts and related metrics in late-stage PLWH post-treatment shows a marked improvement. Overall, CD4$^+$ T cell counts increased from a baseline of 183 cells/μL to 342 cells/μL within one year, representing a rise of 159 cells/μL over this period. The most rapid increase in CD4$^+$ T cell counts was observed at 3 months post-treatment (Figure 3A1 and A2).

The CD4/CD8 ratio also exhibited an upward trend over the year, increasing from a baseline of 0.17 to 0.39 by the end of the year, reflecting an improvement of 0.22 (Figure 3A3).

The comparative analysis revealed comparable immune recovery including CD4$^+$ T cell counts and CD4/CD8 ratio between rapid and delayed ART initiation groups in late-stage PLWH at one-year follow-up. Immune recovery in late-stage PLWH improved following treatment. However, at one year, there were no significant statistical differences between the rapid initiation and delayed initiation groups in terms of CD4$^+$ T cell counts (336 cells/μL *vs.* 347 cells/μL; *P*

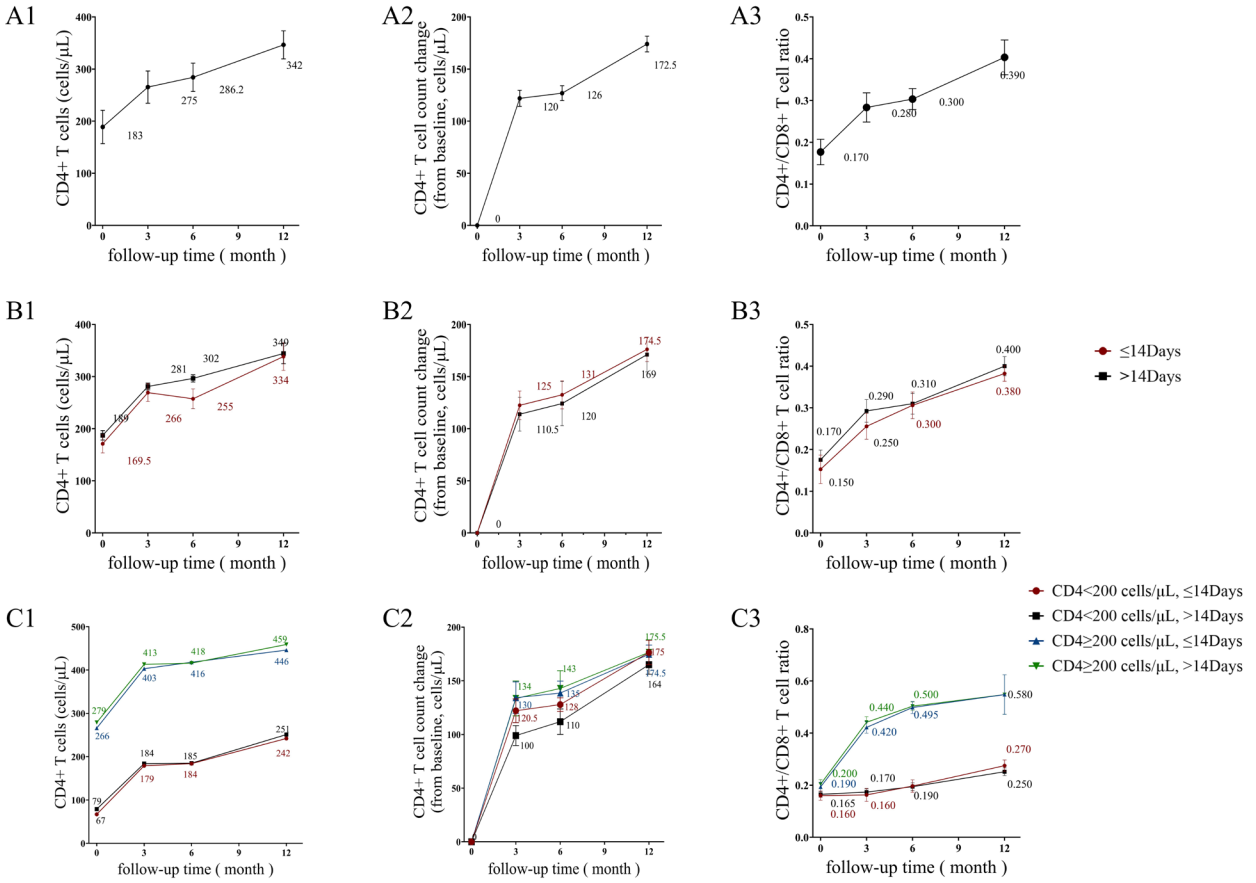

Figure 3. Immune reconstitution in late-presenting PLWH within one year of treatment. (**A1**) $CD4^+$ T cell recovery in late-presenting PLWH within one year of treatment. (**A2**) Increase in $CD4^+$ T cells from baseline in late-presenting PLWH within one year of treatment. (**A3**) CD4/CD8 ratio recovery in late-presenting PLWH within one year of treatment. (**B1**) Changes in $CD4^+$ T cell count in late-presenting PLWH within one year after treatment. (**B2**) Increase in $CD4^+$ T cells in late-presenting PLWH within one year after treatment. (**B3**) Changes in the CD4/CD8 ratio in late-presenting PLWH within one year after treatment. (**C1**) Changes in $CD4^+$ T cell count in late-presenting PLWH with baseline $CD4^+$ T cells < 200/μL, and $CD4^+$ T cells 200-350/μL under different treatment initiation groups within one year of treatment. (**C2**) Increase in $CD4^+$ T cells in late-presenting PLWH with baseline $CD4^+$ T cells < 200/μL, and $CD4^+$ T cells 200-350/μL under different treatment initiation groups within one year of treatment. (**C3**) Changes in CD4/CD8 ratio in late-presenting PLWH with baseline CD4+ T cells < 200/μL, and $CD4^+$ T cells 200-350/μL under different treatment initiation groups within one year of treatment.

> 0.05), the increase from baseline (174.5 cells/μL *vs.* 169 cells/μL; $P > 0.05$), or the CD4/CD8 ratio (0.40 *vs.* 0.38; $P > 0.05$). Similar to the overall trend, both groups experienced the most rapid increase in $CD4^+$ T cell counts at 3 months post-treatment, with increases of 125 cells/μL and 110.5 cells/μL, respectively, although the differences between the groups were not statistically significant (Figures 3B).

We compared $CD4^+$ T cell recovery between rapid and delayed ART initiation groups stratified by baseline CD4+ levels (< 200 *vs.* 200-350 cells/μL) in late-stage PLWH. In the < 200 cells/μL subgroup, the rapid initiation group showed numerically higher but statistically non-significant improvements in $CD4^+$ counts (251 *vs.* 242 cells/μL) and CD4/CD8 ratio (0.27 *vs.* 0.25) at one year ($P > 0.05$). Similarly, in the 200-350 cells/μL subgroup, no significant differences were observed in final $CD4^+$ counts (446 *vs.* 459 cells/μL), absolute increases (174.5 *vs.* 175.5 cells/μL), or CD4/CD8 ratio (0.58 *vs.* 0.58) between initiation strategies ($P > 0.05$). Both subgroups demonstrated comparable immune reconstitution regardless of treatment initiation timing (Figures 3C).

3.3. Viral suppression rates, treatment retention rates, and immune recovery within 5 years of ART

The follow-up period for this study extended up to five years, with a decreasing number of participants over time. Specifically, the number of patients followed up at 1 year, 2 years, 3 years, 4 years, and 5 years were 1,402, 1,143, 837, 601, and 337, respectively.

3.3.1. Viral suppression rates

This five-year longitudinal study of late-stage PLWH revealed progressive viral suppression improvements, with rates rising from first-year levels to 88.2% by year five. The rapid initiation group demonstrated significantly higher 1-year suppression rates (81.6% *vs.* 72.1%, $P = 0.001$), with subsequent annual rates of

84.4% (*vs.* 83.6%, $P > 0.05$) at year 2, 89.3% (*vs.* 88.7%, $P > 0.05$) at year 3, and 90.8% (*vs.* 87.4%, $P > 0.05$) at year 5 (Table 5). Stratified analyses showed consistent temporal patterns: for $CD4^+ < 200$ cells/μL patients, rapid initiation achieved 77.3% *vs.* 66.6% ($P = 0.005$) at year 1, 81.6% *vs.* 78.2% at year 2, 85.9% *vs.* 85.0% at year 3, 86.7% *vs.* 86.5% at year 4, and 88.9% *vs.* 85.5% at year 5 (all $P > 0.05$ beyond year 1); while the $CD4^+$ 200-350 cells/μL cohort showed 86.0% *vs.* 77.6% ($P = 0.021$) at year 1, 95.3% *vs.* 92.6% at year 3, and 95.2% *vs.* 92.4% at year 5 (all $P > 0.05$ post-year 1). These results demonstrate that rapid ART initiation's early virological advantage (particularly during the first year) gradually converges with delayed initiation outcomes across all $CD4^+$ strata by year 2-5.

3.3.2. Treatment retention rates

Our study evaluated ART retention rates among late-stage PLWH, finding an overall 5-year retention rate of 75.64% with declining adherence over time. While rapid ART initiation showed significantly higher retention only at year 2 (97.7% *vs.* 92.5%, $P = 0.011$), trends favored this approach across all years (96.8% *vs.* 93.6% at year 1; 96.4% *vs.* 91.5% at year 3; 96.2% *vs.* 91.4% at year 4; 96.4% *vs.* 91.9% at year 5; all $P > 0.05$ except year 2) (Table 6). Stratified analysis revealed distinct patterns: in the $CD4^+ < 200$ cells/μL subgroup, retention gradually declined from 97.3% (rapid) *vs.* 92.4% (delayed) at year 1 to 94.0% *vs.* 93.3% at year 5 (all $P > 0.05$), while the $CD4^+$ 200-350 cells/μL subgroup showed significantly better 1-year retention with rapid initiation (96.2% *vs.* 95.1%, $P = 0.009$) but comparable subsequent rates. These findings suggest that while rapid initiation may offer early retention benefits, particularly in less immunocompromised patients, long-term adherence challenges persist across all subgroups.

3.3.3. Immune recovery

Five-year immunological monitoring of late-stage PLWH demonstrated progressive immune recovery under ART, with both $CD4^+$ T cell counts and CD4/CD8 ratio showing sustained improvement. $CD4^+$ counts increased from 342 cells/μL at year 1 to 442 cells/μL at year 5, representing median gains of 172 cells/μL (year 1), 213 (year 2), 241 (year 3), 257 (year 4), and 373 (year 5) above baseline. Parallel improvements occurred in CD4/CD8 ratio, rising from 0.39 (year 1) to 0.57 (year 5), with median annual increases of 0.22, 0.28, 0.32, 0.38, and 0.40 respectively above the baseline ratio of 0.17. These quantitative and functional immune parameters showed consistent year-over-year enhancement throughout the observation period (Figure 4A).

Comparative analysis of immune recovery between ART initiation strategies revealed that while both groups showed progressive improvements in $CD4^+$ counts and CD4/CD8 ratio over five years, the rapid initiation group maintained consistently lower absolute $CD4^+$ counts at all annual follow-ups despite starting with lower baseline values. Notably, the magnitude of $CD4^+$ count increases from baseline showed no statistically significant differences between groups. By year 5, the rapid initiation group achieved a marginally higher CD4/CD8 ratio (0.706 *vs.* 0.674), though intergroup differences remained non-significant at all timepoints (Figure 4B),

Table 5. Changes in virological suppression rates within five years after antiviral treatment

Population group	Total Population			Baseline $CD4^+$ T cell count < 200 cells/μL			Baseline CD4+ T cell count: 200-350 cells/μL		
Time Point	≤ 14 Days	> 14 Days	*P*	≤ 14 Days	> 14 Days	*P*	≤ 14 Days	> 14 Days	*P*
1 Year	81.60%	72.10%	0.001***	77.30%	66.60%	0.005**	86.00%	77.60%	0.021*
2 Years	84.40%	83.60%	0.733	81.60%	78.20%	0.342	88.50%	89.70%	0.727
3 Years	89.30%	88.70%	0.818	85.90%	85.00%	0.801	95.30%	92.60%	0.377
4 Years	87.80%	88.70%	0.74	86.70%	86.50%	0.976	90.50%	91.80%	0.796
5 Years	90.80%	87.40%	0.499	88.90%	85.50%	0.564	95.20%	89.70%	0.424

*: $P < 0.05$; **: $P < 0.01$; ***: $P < 0.001$.

Table 6. Treatment maintenance rates within five years after ART

Population group	Total Population			Baseline $CD4^+$ T cell count < 200 cells/μL			Baseline CD4+ T cell count: 200-350 cells/μL		
Time Point	≤ 14 Days	> 14 Days	*P*	≤ 14 Days	> 14 Days	*P*	≤ 14 Days	> 14 Days	*P*
1 Year	96.80%	93.60%	0.510	97.30%	92.40%	0.160	96.20%	95.10%	0.009**
2 Years	97.70%	92.50%	0.011*	96.10%	94.60%	0.299	96.40%	97.00%	0.916
3 Years	96.40%	91.50%	0.056	95.70%	93.60%	0.266	94.40%	95.90%	0.593
4 Years	96.20%	91.40%	0.155	95.00%	93.40%	0.715	92.70%	95.80%	0.307
5 Years	96.40%	91.90%	0.380	94.00%	93.30%	1.000	89.30%	95.10%	0.204

*: $P < 0.05$; **: $P < 0.01$.

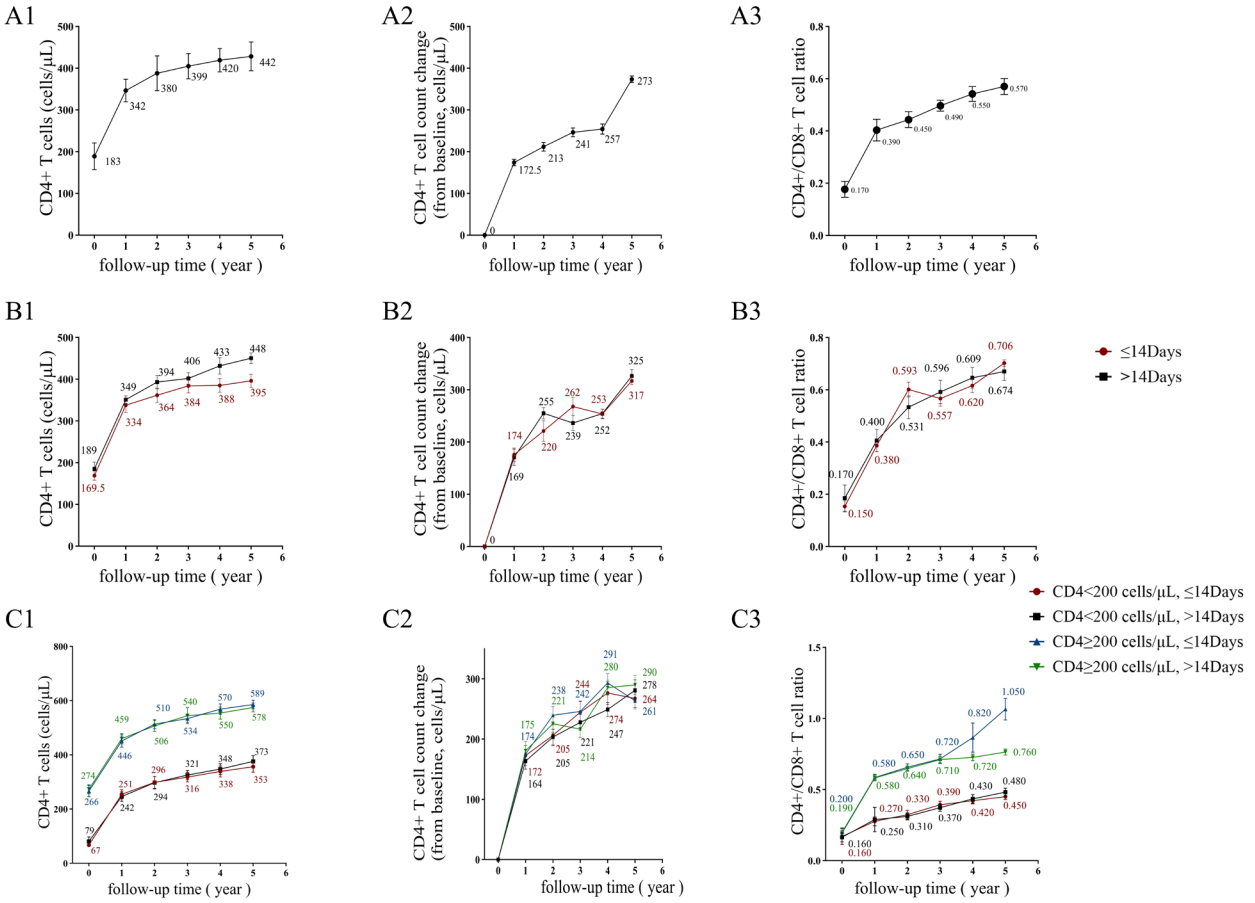

Figure 4. Immune reconstitution in late-presenting PLWH within five year of treatment. (**A1**) Changes in CD4$^+$ T cell count in late-presenting PLWH within five years of ART. (**A2**) Change in CD4$^+$ T cell count from baseline in late-presenting PLWH within five years of ART. (**A3**) Changes in CD4/CD8 ratio in late-presenting PLWH within five years of ART. (**B1**) CD4$^+$ T cell recovery in late-presenting HIV patients in the rapid start and delayed treatment groups within five years of treatment. (**B2**) Increase in CD4$^+$ T cells in late-presenting HIV patients in the rapid start and delayed treatment groups within five years of treatment. (**B3**) CD4/CD8 ratio recovery in late-presenting HIV patients in the rapid start and delayed treatment groups within five years of treatment. (**C1**) CD4$^+$ T cell recovery in late-presenting HIV patients with different CD4$^+$ T cell stratifications in the rapid start and delayed treatment groups within five years of treatment. (**C2**) Increase in CD4$^+$ T cells in late-presenting HIV patients with different CD4$^+$ T cell stratifications in the rapid start and delayed treatment groups within five years of treatment. (**C3**) CD4/CD8 ratio recovery in late-presenting HIV patients with different CD4$^+$ T cell stratifications in the rapid start and delayed treatment groups after five years of treatment.

suggesting comparable long-term immune reconstitution regardless of initiation timing.

Stratified by baseline CD4$^+$ levels (< 200 *vs.* 200-350 cells/μL), both rapid and delayed ART initiation groups demonstrated similar five-year immune recovery trajectories, with comparable improvements in CD4$^+$ T cell counts, absolute increases from baseline, and CD4/CD8 ratio (Figure 4C). While all immunological parameters showed sustained upward trends regardless of initiation timing, no statistically significant differences emerged between the treatment strategies in either CD4$^+$ stratum, indicating equivalent long-term immune reconstitution across different baseline immunological statuses (Figure 4C).

4. Discussion

Our study highlights several clinical benefits of initiating ART rapidly, including a reduction in time to achieve virological suppression, increased virological suppression rates, and higher treatment adherence rates.

Our findings indicate that rapid ART initiation significantly shortens the time to achieve virological suppression for late-presenting individuals with HIV, regardless of their baseline HIV RNA levels. The time to suppression is positively correlated with baseline viral load. These results corroborate previous studies. For example, research by Christopher D Pilcher *et al.* in the United States demonstrated that initiating ART on the same day of diagnosis reduced the median time to virological suppression (defined as HIV RNA < 200 copies/mL) to 56 days, compared to 79 days for standard ART (*18*). A similar retrospective study in Taiwan showed that starting ART within 7 days of diagnosis decreased the median time to virological suppression from 138 days to 47 days (*30*).

Moreover, our study found that the rapid ART initiation group had significantly higher virological

suppression rates at both 6 months and 1 year compared to the delayed initiation group. This supports previous findings. For instance, Serena P Koenig *et al.* in Haiti reported that among individuals aged 18 and older, those who started ART on the same day of diagnosis had a 1-year virological suppression rate (HIV-1 RNA < 50 copies/mL) of 53%, while those starting ART 3 weeks after diagnosis had a rate of 44% (*13*). In our study, despite a rapid initiation period within 14 days, the 1-year virological suppression rate was 81.6% for the rapid initiation group, compared to 72.1% for the delayed initiation group. Although both rates exceeded those reported in Haiti, they underscore that rapid ART initiation can achieve higher 1-year suppression rates. Similarly, a study in Lesotho found that initiating ART on the same day of an HIV-positive diagnosis resulted in a 1-year virological suppression rate of 50.4%, compared to 34.3% for standard ART (*31*). Additional studies support these findings, such as a multicenter retrospective study in Taiwan showing that 88% of late-presenting HIV patients (with a baseline CD4 count < 200 cells/μL) who started ART within 14 days had a 48-week virological suppression rate of 84% (*32*). The Rainbow study in Italy, which included 30 late-presenting HIV patients (with a baseline CD4 count < 200 cells/μL) who began ART within 7 days, reported a 48-week virological suppression rate of 90% (*33*). Rapid ART initiation not only accelerates HIV suppression but also enhances virological suppression rates. Compared to standard ART, same-day initiation can increase the virological suppression rate by 9.2-16% by months 10-12 (*13,17,34,35*).

Although our study did not examine HIV transmission risks at different time points for the rapid and delayed initiation groups, existing research indicates that lower HIV viral loads correlate with reduced transmission risk. Therefore, rapid ART initiation, by shortening the time to virological suppression and achieving higher suppression rates, likely reduces the risk of HIV transmission to others.

Treatment adherence is crucial for achieving sustained virological suppression and immune recovery in HIV-infected individuals. Our study found that the 1-year treatment adherence rate was 96.8% in the rapid initiation group, compared to 93.6% in the delayed initiation group. Although this difference was not statistically significant, subgroup analysis based on baseline $CD4^+$ T cell counts revealed that for individuals with a baseline $CD4^+$ count < 200 cells/μL, the rapid initiation group had a significantly higher treatment adherence rate at 6 months (97.3% *vs.* 92.4%). For individuals with a baseline $CD4^+$ count between 200 and 350 cells/μL, the 1-year treatment adherence rate was 96.2% in the rapid initiation group, compared to 95.1% in the delayed initiation group. A retrospective study in Taiwan also analyzed treatment adherence, finding that the 7-day rapid ART group had an adherence rate of 88.3%, significantly higher than the 79.0% for the standard initiation group (*30*). Jason Halperin's prospective study in the United States found that patients who initiated ART within 3 days of diagnosis had a 12-month adherence rate of 92%, compared to 80% for those starting ART after 3 days (*36*). Although the grouping methods differed, these studies suggest that earlier ART initiation may be associated with higher adherence rates, potentially due to improved patient compliance. At Nanjing Second Hospital, both rapid and delayed initiation groups had high treatment adherence rates, likely attributable to both patient compliance and high-quality HIV chronic disease management.

Theoretically, rapid ART initiation should facilitate faster and better immune recovery, given its ability to shorten the time to virological suppression and achieve higher suppression rates. We assessed immune recovery using changes in $CD4^+$ T cell counts and CD4/CD8 ratio. Our results show that while $CD4^+$ T cell counts increased over time with ART, there were no statistically significant differences in absolute $CD4^+$ T cell counts between the rapid and delayed initiation groups at various follow-up points. This suggests that late-presenting PLWH, particularly those receiving long-term treatment, experience the most rapid recovery of $CD4^+$ T cell counts and CD4/CD8 ratio within the first or second year of treatment, with stabilization occurring after more than four years. Recent research indicates that from baseline to week 48, the average $CD4^+$ T cell count increased from 133 to 309 cells/μL, and the average CD4/CD8 ratio increased from 0.18 to 0.44 ($P < 0.001$) (*33*). Previous studies have reported that 28% of patients achieved normalization of the CD4/CD8 ratio during a median follow-up of 2.6 years, with a 5-year probability of normalization at 0.44 (*37*). The lack of significant differences in $CD4^+$ T cell counts and CD4/CD8 ratio between the rapid and delayed initiation groups may be attributed to various influencing factors, such as thymic regeneration, microbiome shifts, cellular apoptosis, age, and comorbidities, which were not examined in our study. However, rapid ART initiation at least mitigates the impact of HIV infection, a key factor influencing immune recovery. Our study also found that the rapid initiation group had lower $CD4^+$ T cell counts compared to the delayed initiation group over the 5-year follow-up period, possibly due to higher baseline $CD4^+$ T cell counts in the delayed initiation group.

In summary, our study confirms that rapid ART initiation can shorten the time to virological suppression and achieve higher suppression and adherence rates. These outcomes are critical for evaluating ART efficacy, benefiting HIV-infected individuals, and reducing the risk of HIV transmission in the population. Although rapid ART did not show clear advantages in immune recovery metrics such as $CD4^+$ T cell counts and CD4/CD8 ratio, the numerous influencing factors warrant further investigation into additional factors affecting

immune recovery in both groups.

Limitations and future directions

As a single-center study, our results may not be generalizable to other settings with different HIV care practices and ART regimens. The retrospective nature of this study and missing follow-up data limit the sample size. Future studies with larger sample sizes are needed. The study did not analyze comorbidities in late-presenting PLWH. This single-center study did not track HIV transmission rates, so the benefits of rapid ART initiation in reducing population-level HIV transmission cannot be directly confirmed.

Acknowledgements

We thank Dr. Zhilang Hu for his insightful and guiding comments on this paper.

Funding: This work was supported by a grant from 2022 Annual Key Project supported by Medical Science and Technology Development Foundation, Nanjing Department of Health, (Grant number: ZKX 22040) and Phase I Reserve Talent of The Second Hospital of Nanjing (Grant number: HBRCYL01)

Conflict of Interest: The authors have no conflicts of interest to disclose.

References

1. World Health Organization. HIV/AIDS. Available at *https://www.who.int/data/gho/data/themes/hiv-aids.* 2022.
2. Han M. Analysis of the HIV/AIDS Epidemic Situation in China and Prospects for Prevention and Control. Zhongguo Ai Zi Bing Xing Bing. 2023; 29:247-250 (in Chinese).
3. WHO Guidelines Approved by the Guidelines Review Committee. Guidelines for Managing Advanced HIV Disease and Rapid Initiation of Antiretroviral Therapy. World Health Organization. 2017.
4. UNAIDS_Global HIV & AIDS Statistics-2019 Fact Sheet: Latest Statistics on the Status of the AIDS Epidemic, World Aids Day. *https://www.unaids.org/sites/default/files/media_asset/UNAIDS_FactSheet_en.pdf.* 2020.
5. WHO Guidelines Approved by the Guidelines Review Committee, Guideline on When to Start Antiretroviral Therapy and on Pre-Exposure Prophylaxis for HIV. Geneva, 2015.
6. Yang X, Li X, Qiao S, Zhang Q, Shen Z, Zhou Y. Immunological and virologic outcomes of people living with HIV in Guangxi, China: 2012-2017. PLoS One. 2019; 14:e0213205.
7. Zhang F-G, Ma Y. Progress and challenges in China's free ART programme. Lancet HIV. 2019; 6:e8-e9.
8. Ford N, Migone C, Calmy A, Kerschberger B, Kanters S, Nsanzimana S, Mills EJ, Meintjes G, Vitoria M, Doherty M, Shubber Z. Benefits and risks of rapid initiation of antiretroviral therapy. AIDS. 2018; 32:17-23.
9. Jiao J, Dai L, Chen X. Research progress on rapid antiviral treatment strategies for HIV/AIDS. Zhongguo Ai Zi Bing Xing Bing. 2020; 26:660-663.
10. Zhao Y, Wu Z, McGoogan JM, Shi CX, Li A, Dou Z, Ma Y, Qin Q, Brookmeyer R, Detels R, Montaner JSG. Immediate antiretroviral therapy decreases mortality among patients with high CD4 counts in China: A nationwide, retrospective cohort study. Clin Infect Dis. 2018; 66:727-734.
11. Girometti N, Nwokolo N, McOwan A, Whitlock G. Outcomes of acutely HIV-1-infected individuals following rapid antiretroviral therapy initiation. Antivir Ther. 2017; 22:77-80.
12. Hoenigl M, Chaillon A, Moore DJ, Morris SR, Mehta SR, Gianella S, Amico KR, Little SJ. Rapid HIV viral load suppression in those initiating antiretroviral therapy at first visit after HIV diagnosis. Sci Rep. 2016; 6:32947.
13. Koenig SP, Dorvil N, Dévieux JG*, et al.* Same-day HIV testing with initiation of antiretroviral therapy versus standard care for persons living with HIV: A randomized unblinded trial. PLoS Med. 2017; 14:e1002357.
14. Bacon O, Chin J, L. H. The Rapid ART Program Initiative for HIV Diagnoses (RAPID) in San Francisco. In: Conference on Retroviruses and Opportunistic Infections; 2018 Mar 4-7; Boston, MA.
15. Dijkstra M, van Rooijen MS, Hillebregt MM, *et al.* Decreased time to viral suppression after implementation of targeted testing and immediate initiation of treatment of acute human immunodeficiency virus infection among men who have sex with men in Amsterdam. Clin Infect Dis. 2021; 72:1952-1960.
16. Halperin J, Butler I, Conner K, Myers L, Holm P, Bartram L, Van Sickels N. Linkage and antiretroviral therapy within 72 hours at a federally qualified health center in New Orleans. AIDS Patient Care STDS. 2018; 32:39-41.
17. Labhardt ND, Ringera I, Lejone TI, Klimkait T, Muhairwe J, Amstutz A, Glass TR. Effect of offering same-day ART vs usual health facility referral during home-based HIV testing on linkage to care and viral suppression among adults with HIV in Lesotho: The CASCADE randomized clinical trial. JAMA. 2018; 319:1103-1112.
18. Pilcher CD, Ospina-Norvell C, Dasgupta A, Jones D, Hartogensis W, Torres S, Calderon F, Demicco E, Geng E, Gandhi M, Havlir DV, Hatano H. The effect of same-day observed initiation of antiretroviral therapy on HIV viral load and treatment outcomes in a US public health setting. J Acquir Immune Defic Syndr. 2017; 74:44-51.
19. Wu Z, Zhao Y, Ge X*, et al.* Simplified HIV testing and treatment in China: Analysis of mortality rates before and after a structural intervention. PLoS Med. 2015; 12:e1001874.
20. Colasanti J, Sumitani J, Mehta CC, Zhang Y, Nguyen ML, Del Rio C, Armstrong WS. Implementation of a rapid entry program decreases time to viral suppression among vulnerable persons living with HIV in the Southern United States. Open Forum Infect Dis. 2018; 5:ofy104.
21. Sun J, Liu L, Shen J, Chen P, Lu H. Trends in baseline CD4 cell counts and risk factors for late antiretroviral therapy initiation among HIV-positive patients in Shanghai, a retrospective cross-sectional study. BMC Infect Dis. 2017; 17:285.
22. Lin KY, Cheng CY, Li CW, *et al.* Trends and outcomes of late initiation of combination antiretroviral therapy driven by late presentation among HIV-positive Taiwanese patients in the era of treatment scale-up. PloS One. 2017;

12:e0179870.
23. Antinori A, Coenen T, Costagiola D, *et al.* Late presentation of HIV infection: a consensus definition. HIV Med. 2011; 12:61-64.
24. Sobrino-Vegas P, Moreno S, Rubio R, Viciana P, Bernardino JI, Blanco JR, Bernal E, Asensi V, Pulido F, del Amo J, Hernando V. Impact of late presentation of HIV infection on short-, mid- and long-term mortality and causes of death in a multicenter national cohort: 2004-2013. J Infect. 2016; 72:587-596.
25. Sabin CA, Smith CJ, Gumley H, Murphy G, Lampe FC, Phillips AN, Prinz B, Youle M, Johnson MA. Late presenters in the era of highly active antiretroviral therapy: uptake of and responses to antiretroviral therapy. AIDS. 2004; 18:2145-2151.
26. Kelley CF, Kitchen CM, Hunt PW, Rodriguez B, Hecht FM, Kitahata M, Crane HM, Willig J, Mugavero M, Saag M, Martin JN, Deeks SG. Incomplete peripheral CD4+ cell count restoration in HIV-infected patients receiving long-term antiretroviral treatment. Clin Infect Dis. 2009; 48:787-794.
27. Jevtović D, Vanovac V, Veselinović M, Salemović D, Ranin J, Stefanova E. The incidence of and risk factors for HIV-associated cognitive-motor complex among patients on HAART. Biomed Pharmacother. 2009; 63:561-565.
28. Marks G, Crepaz N, Janssen RS. Estimating sexual transmission of HIV from persons aware and unaware that they are infected with the virus in the USA. AIDS. 2006; 20:1447-1450.
29. van Opstal SEM, van der Zwan JS, Wagener MN, Been SK, Miedema HS, Roelofs P, van Gorp ECM. Late presentation of HIV infection in the Netherlands: Reasons for late diagnoses and impact on vocational functioning. AIDS Behav. 2018; 22:2593-2603.
30. Huang YC, Sun HY, Chuang YC, Huang YS, Lin KY, Huang SH, Chen GJ, Luo YZ, Wu PY, Liu WC, Hung CC, Chang SC. Short-term outcomes of rapid initiation of antiretroviral therapy among HIV-positive patients: real-world experience from a single-centre retrospective cohort in Taiwan. BMJ Open. 2019; 9:e033246.
31. Labhardt ND, Ringera I, Lejone TI, Klimkait T, Muhairwe J, Amstutz A, Glass TR. Effect of offering same-day ART vs usual health facility referral during home-based HIV testing on linkage to care and viral suppression among adults with HIV in Lesotho: The CASCADE randomized clinical trial. JAMA. 2018; 319:1103-1112.
32. Lee CY, Lee CH, Tang HJ, Tsai HC, Yang CH, Lin YP, Wang SF, Lu PL. Comparison of Virological Efficacy of DTG/ABC/3TG and B/F/TAF Regimens and Discontinuation Patterns in Persons Living with Advanced HIV in the Era of Rapid ART: A Retrospective Multicenter Cohort Study. Infect Dis Ther. 2023; 12:843-861.
33. Camici M, Gagliardini R, Lanini S, *et al.* Rapid ART initiation with bictegravir/emtricitabine/tenofovir alafenamide in individuals presenting with advanced HIV disease (Rainbow study). Int J Antimicrob Agents. 2024; 63:107049.
34. Rosen S, Maskew M, Fox MP, Nyoni C, Mongwenyana C, Malete G, Sanne I, Bokaba D, Sauls C, Rohr J, Long L. Initiating antiretroviral therapy for HIV at a patient's first clinic visit: The RapIT randomized controlled trial. PLoS Med. 2016; 13:e1002015.
35. Seekaew P, Phanuphak N, Teeratakulpisarn N, Amatavete S, Lujintanon S, Teeratakulpisarn S, Pankam T, Nampaisan O, Jomja P, Prabjunteuk C, Plodgratoke P, Ramautarsing R, Phanuphak P. Same-day antiretroviral therapy initiation hub model at the Thai Red Cross Anonymous Clinic in Bangkok, Thailand: An observational cohort study. J Int AIDS Soc. 2021; 24:e25869.
36. Halperin J, Conner K, Butler I, Zeng P, Myers L, Clark R, Van Sickels N. A care continuum of immediate ART for newly diagnosed patients and patients presenting later to care at a federally qualified health center in New Orleans. Open Forum Infect Dis. 2019; 6:ofz161.
37. Zhabokritsky A, Szadkowski L, Cooper C, Loutfy M, Wong A, McClean A, Hogg RS, Walmsley SL. Increased CD4:CD8 ratio normalization with implementation of current ART management guidelines. J Antimicrob Chemother. 2021; 76:729-737.

Received February 18, 2025; Revised April 24, 2025; Accepted April 25, 2025.

[§]These authors contributed equally to this work.

**Address correspondence to:*
Hongxia Wei and Rentian Cai, Department of Infectious Disease, The Second Hospital of Nanjing, Affiliated to Nanjing University of Chinese Medicine, 210000, No. 1-1, Kangfu road, Nanjing, China.
E-mail: njyy019@njucm.edu.cn (HW); cairentian@163.com (RC)

Correspondence

DOI: 10.5582/ddt.2025.01032

Can the herpes zoster vaccination be a strategy against dementia?

Ya-nan Ma[1], Kenji Karako[2], Peipei Song[3,4,*], Ying Xia[1,5,*]

[1] Department of Neurosurgery, Haikou Affiliated Hospital of Central South University Xiangya School of Medicine, Haikou, China;
[2] Department of Surgery, Graduate School of Medicine, The University of Tokyo, Tokyo, Japan;
[3] Center for Clinical Sciences, Japan Institute for Health Security, Tokyo, Japan;
[4] National College of Nursing Japan, Tokyo, Japan;
[5] Integrated Neuroscience Center, Geriatric Hospital of Hainan, Haikou, China.

SUMMARY: Herpes Zoster (HZ), caused by the reactivation of the varicella-zoster virus (VZV), is a common infectious disease. Recent studies suggest a potential association between HZ and the development of dementia, particularly Alzheimer's disease and other neurodegenerative disorders. Epidemiological evidence indicates that HZ infection, especially in individuals with central nervous system involvement, may increase the risk of dementia. Pathologically, VZV may contribute to neuronal dysfunction and degeneration by inducing chronic neuroinflammation, infection-related cerebrovascular lesions, and direct central nervous system toxicity. HZ vaccines, particularly novel recombinant subunit vaccines (*e.g.*, Shingrix), not only effectively prevent HZ but may also confer cognitive protection through mechanisms such as "trained immunity" activation and anti-inflammatory response modulation. Multiple natural experiments and retrospective cohort studies have found that HZ vaccination is significantly associated with a reduced risk of dementia, with particularly pronounced protective effects in women and older adults. Although most evidence currently stems from observational studies and is subject to potential confounding factors, the biological plausibility and consistent findings support the potential of HZ vaccination as an adjunctive strategy for dementia prevention. Future prospective randomized controlled trials are needed to further clarify the causal relationship and underlying neuroimmune mechanisms, providing a stronger evidence base for establishing scientific vaccination strategies for older adults and dementia prevention systems.

Keywords: Alzheimer's disease, vaccine, neuroinflammation, recombinant vaccine, immunosenescence, neurodegenerative diseases

1. Vaccines and dementia

As the aging population grows, dementia, particularly Alzheimer's disease (AD), has become one of the most pressing global public health challenges (*1*). With no curative treatments available, identifying modifiable risk factors and preventive strategies has become a research priority. In recent years, clinical studies have revealed a potential link between varicella-zoster virus (VZV) and dementia onset (Table 1) (*2-8*). This raises the question: could vaccines that prevent herpes zoster (HZ) also inadvertently protect the brain?

A nationwide cohort study in South Korea found that individuals with HZ had a significantly higher risk of dementia (adjusted hazard ratio, HR = 1.12), while antiviral treatment reduced this risk (adjusted HR = 0.76) (*9*). However, a UK CPRD database study found no significant association between HZ and dementia (*10*). A Danish national cohort study indicated that HZ involving the central nervous system (CNS) nearly doubled the risk of dementia (HR = 1.94). This suggests that direct viral invasion of the brain may be a key risk factor (*11*).

2. Vaccination: More than just preventing HZ?

The most exciting findings come from vaccine research. In a "natural experiment" conducted in Wales, UK, Eyting *et al.* used birth date cutoffs to determine vaccine eligibility and found a 20% reduction in dementia incidence among those vaccinated with the live vaccine (*11*). A U.S. natural experiment based on electronic medical records revealed that Shingrix, a recombinant vaccine, delayed dementia diagnosis by an average of 164 days compared to unvaccinated individuals, demonstrating a significant neuroprotective effect (*4*). Retrospective cohort studies and systematic reviews further support this view (*6,12*). HZ vaccines not only prevent disease but may also "prevent dementia".

Table 1. Characteristics and key findings of studies investigating HZ vaccination as a protective factor against dementia

Author (Ref)	Study design	Age (years)	Female : male	Vaccine(s) employed	Vaccinated (n)	Unvaccinated (n)	Dementia definition	Results
Eyting *et al.* (*2*)	A natural experiment	80 (Mean)	55:45	Zostavax	84,071	198,470	Read/ICD-9/ICD-10 codes	HZ vaccination was associated with a 20.0% relative reduction in the incidence of newly diagnosed dementia over a 7-year follow-up period, with a stronger protective effect observed in females than in males.
Harris *et al.* (*3*)	Retrospective cohort study	72 (Mean)	59:41	Zostavax/Shingrix	16,106	21,417	ICD-9/ICD-10 codes	During follow-up, 8.1% of vaccinated individuals and 10.7% of unvaccinated individuals developed AD, corresponding to a relative risk of 0.75 and an absolute risk reduction of 2%.
Taquet *et al.* (*4*)	A natural experiment	71 (Mean)	53:42	recombinant vaccine/ live vaccine	200,405	7269	ICD-10 codes	Recombinant zoster vaccine was associated with a significantly reduced risk of dementia within six years post-vaccination and a 164-day delay in dementia diagnosis.
Tang *et al.* (*5*)	Retrospective cohort study	62 (Mean)	49:51	RZV/Shingrix	666,710	3,835,968	ICD-10 codes	Adjusted analyses showed that both two-dose (HR 0.68) and single-dose (HR 0.89) vaccination were associated with reduced dementia risk, while prior HZ diagnosis increased the risk (HR 1.47). Antiviral treatment was linked to lower dementia incidence.
Lophatananon *et al.* (*6*)	Retrospective cohort study	≥70	52:48	Varicella/Shingles/ Zostavax	854,745	8,490,813	ICD-10 codes	Zoster vaccination was associated with reduced risk of all-cause dementia (HR 0.78), AD (HR 0.91), and other dementias (HR 0.71).
Lophatananon *et al.* (*7*)	Case-control study	≥70	55:45	Zostavax	35,116	193,020	ICD-9/ICD-10 codes	Shingles history ≥3 years prior showed no significant association with dementia risk (OR 1.09), while Zostavax vaccination was linked to a significantly reduced risk (OR 0.81).
Lehrer *et al.* (*8*)	Cross-sectional, interviewed	70 (Mean)	37:33	Zostavax/Shingrix	99	176	Social activities hampered by disorientation or memory loss	In BRFSS 2017 data, HZ vaccination was associated with a lower prevalence of social impairment due to disorientation or memory loss (61.6% *vs.* 46.6%). Multivariate analysis confirmed a significant protective effect of vaccination.

Abbreviations: AD, Alzheimer's disease; ARR, Absolute risk reduction; BRFSS, Behavioral Risk Factor Surveillance System; CI, Confidence interval; HR, Hazard ratio; HZ, Herpes zoster; ICD-9/10, International Classification of Diseases, 9th/10th Revision; OR, Odds ratio; RZV, Recombinant zoster vaccine; VHA, Veterans Health Administration.

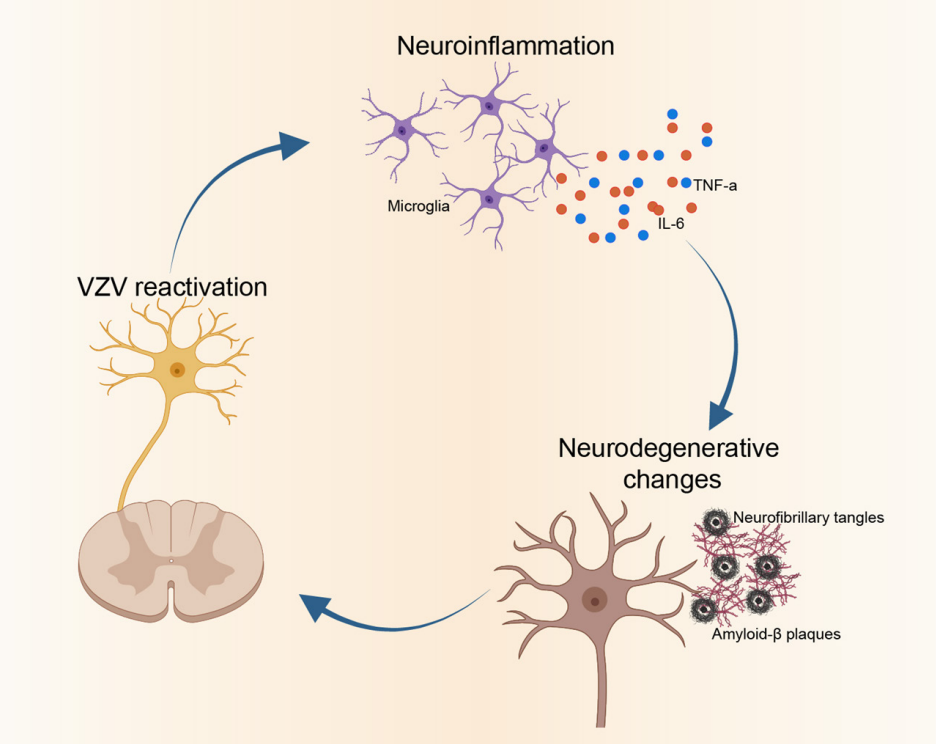

Figure 1. Proposed mechanism linking VZV reactivation to neurodegenerative processes. Abbreviations: VZV, varicella-zoster virus.

3. Pathogenic mechanisms

Current research suggests that VZV may contribute to or accelerate neurodegenerative processes through multiple pathways, including neural invasion, amplified inflammatory responses, and vascular damage (*13-16*). Additionally, the "off-target" immunomodulatory effects of vaccines may underlie their ability to reduce dementia risk (*17*). (Figure 1)

3.1. VZV latent infection and neural reactivation

Following primary infection, VZV establishes latency in the dorsal root ganglia (DRG) or cranial nerve ganglia, where it can persist for decades (*18,19*). Under conditions such as immunosenescence, immunosuppression, or acute stress, the virus can reactivate, spreading *via* anterograde transport to infect the peripheral or CNS (*18*). Studies have detected VZV DNA and proteins in the cerebrospinal fluid and serum of some patients without skin symptoms, indicating its ability to breach the blood-brain barrier (BBB) (*20*). Such subclinical or focal reactivation may not present as typical rashes but can induce localized inflammation or vascular lesions in the brain, leading to long-term neurological damage (*11*).

3.2. Neuroinflammation

VZV infection can activate resident immune cells in the brain, particularly microglia and astrocytes, leading to upregulated expression of pro-inflammatory cytokines such as interleukin (IL)-1β, IL-6, and tumor necrosis factor-alpha (TNF-α) (*21,22*). These inflammatory signals not only directly induce neuronal apoptosis but also contribute to AD pathology by promoting β-amyloid (Aβ) deposition and Tau protein hyperphosphorylation (*23*). Animal studies and autopsies have shown that viral infections significantly enhance the cleavage of amyloid precursor protein (APP) and the accumulation of phosphorylated Tau, triggering synaptic dysfunction and neuronal loss (*24*). In addition, VZV can amplify central immune responses by activating the NLRP3 inflammasome pathway, creating a "low-grade, chronic" neuroinflammatory environment (*25*).

3.3. Vascular damage

VZV can directly infect endothelial cells of cerebral small vessels, inducing vasculitis, smooth muscle cell damage, and thrombosis, leading to perfusion deficits and white matter degeneration, thereby increasing the risk of vascular cognitive impairment (*10,11*). This mechanism is particularly pronounced in HZ ophthalmicus (*11*). This "HZ-associated vasculopathy" may present with subacute or chronic progression and can manifest on imaging as features similar to small vessel dementia, such as periventricular white matter hyperintensities (*16*).

3.4. Direct CNS infection

Compared to individuals with normal immune function, those with compromised immunity face a 51% higher

risk of developing HZ, a 25% higher recurrence rate, and a 2.37-fold increased likelihood of HZ complications(*16*). This may explain the elevated HZ risk in older adults, particularly in those with immunocompromised (IC) conditions due to diseases or treatments that alter immune responses (*e.g.*, immunodeficiency disorders, autoimmune diseases, HIV, cancer, organ transplantation) (*26*). In immunocompromised individuals, VZV can breach the BBB and invade the brain parenchyma, causing meningitis, encephalitis, or even myelitis (*27*). Although such CNS infections are rare, they can result in long-term neurocognitive sequelae even after recovery. Long-term follow-up data indicate a significantly increased dementia risk in patients with central nervous system HZ, supporting the direct neurotoxic effects of the virus (*11*).

3.5. Vaccine-induced "trained immunity" and systemic immune reprogramming

HZ vaccines, particularly the recombinant subunit vaccine Shingrix, not only induce specific $CD4^+$ T-cell responses and neutralizing antibodies but also promote a "trained immunity" state by activating innate immune components such as monocytes and natural killer cells (*28,29*). This epigenetic reprogramming-driven, non-specific immune enhancement has been shown to improve the body's ability to regulate responses to various pathogens and chronic inflammatory conditions (*30*). In older adults, this vaccine effect may facilitate "anti-inflammatory reprogramming," mitigating systemic low-grade inflammation associated with immunosenescence (inflammaging), thereby indirectly slowing the progression of neurodegenerative diseases (*2,4*).

4. From "viral risk" to "vaccine opportunity"

Although most current studies are observational and have not fully ruled out confounding factors, their findings are biologically plausible and have been consistently validated across diverse populations. Given the global accessibility, safety, and established benefits of HZ vaccines, their "additional neuroprotective effects" hold significant public health implications.

However, confirming their true efficacy in dementia prevention requires further evidence from long-term, prospective, randomized controlled trials. In the context of persistent vaccine hesitancy and suboptimal vaccination rates among older adults, clearly communicating the potential of HZ vaccines to "reduce dementia risk" to the public, clinicians, and policymakers could be a critical step in challenging entrenched perceptions and improving vaccine uptake.

The link between vaccines and neurodegenerative diseases was once considered an "unexpected discovery," but with accumulating evidence, we may be on the cusp of a new preventive pathway. It is time to reconsider the role of infectious factors in dementia and the strategic value of vaccines in an aging society.

5. Conclusion

In summary, VZV reactivation may contribute to dementia pathogenesis through chronic neuroinflammation, vascular damage, and direct neurotoxicity. Concurrently, HZ vaccination demonstrates neuroprotective potential beyond its role in preventing HZ. Although current studies are primarily observational, their biological plausibility and consistency across populations underscore the need for further research. As dementia prevalence rises and therapeutic options remain limited, incorporating HZ vaccination into broader preventive strategies may offer a feasible and cost-effective approach to supporting cognitive health in aging populations.

Funding: This work was supported by grants from National Natural Science Foundation of China (82460268), the Hainan Province Clinical Medical Research Center (No. LCYX202309), the Hainan Province Postdoctoral Research Project (403254), and Grants-in-Aid from the Ministry of Education, Science, Sports, and Culture of Japan (24K14216).

Conflict of Interest: The authors have no conflicts of interest to disclose.

References

1. Ma YN, Xia Y, Karako K, Song P, Tang W, Hu X. Serum proteomics reveals early biomarkers of Alzheimer's disease: The dual role of APOE-ε4. Biosci Trends. 2025; 19:1-9.
2. Eyting M, Xie M, Michalik F, Hess S, Chung S, Geldsetzer P. A natural experiment on the effect of herpes zoster vaccination on dementia. Nature. 2025. doi:10.1038/s41586-025-08800-x
3. Harris K, Ling Y, Bukhbinder AS, Chen L, Phelps KN, Cruz G, Thomas J, Kim Y, Jiang X, Schulz PE. The impact of routine vaccinations on Alzheimer's disease risk in persons 65 years and older: a claims-based cohort study using propensity score matching J Alzheimers Dis. 2023; 95:703-718.
4. Taquet M, Dercon Q, Todd JA, Harrison PJ. The recombinant shingles vaccine is associated with lower risk of dementia. Nat Med. 2024; 30:2777-2781.
5. Tang E, Ray I, Arnold BF, Acharya NR. Recombinant zoster vaccine and the risk of dementia. Vaccine. 2025; 46:126673.
6. Lophatananon A, Carr M, McMillan B, Dobson C, Itzhaki R, Parisi R, Ashcroft DM, Muir KR. The association of herpes zoster and influenza vaccinations with the risk of developing dementia: A population-based cohort study within the UK Clinical Practice Research Datalink. BMC Public Health. 2023; 23:1903.
7. Lophatananon A, Mekli K, Cant R, Burns A, Dobson C, Itzhaki R, Muir K. Shingles, Zostavax vaccination and risk of developing dementia: A nested case-control study-results from the UK Biobank cohort. BMJ Open. 2021;

11:e045871.
8. Lehrer S, Rheinstein PH. Herpes zoster vaccination reduces risk of dementia. In Vivo. 2021; 35:3271-3275.
9. Bae S, Yun SC, Kim MC, Yoon W, Lim JS, Lee SO, Choi SH, Kim YS, Woo JH, Kim SY, Kim SH. Association of herpes zoster with dementia and effect of antiviral therapy on dementia: A population-based cohort study. Eur Arch Psychiatry Clin Neurosci. 2021; 271:987-997.
10. Warren-Gash C, Williamson E, Shiekh SI, Borjas-Howard J, Pearce N, Breuer JM, Smeeth L. No evidence that herpes zoster is associated with increased risk of dementia diagnosis. Ann Clin Transl Neurol. 2022; 9:363-374.
11. Schmidt SAJ, Veres K, Sorensen HT, Obel N, Henderson VW. Incident herpes zoster and risk of dementia: a population-based Danish cohort study Neurology. 2022; 99:e660-e668.
12. Shah S, Dahal K, Thapa S, Subedi P, Paudel BS, Chand S, Salem A, Lammle M, Sah R, Krsak M. Herpes zoster vaccination and the risk of dementia: A systematic review and meta-analysis. Brain Behav. 2024; 14:e3415.
13. Wozniak MA, Itzhaki RF, Shipley SJ, Dobson CB. Herpes simplex virus infection causes cellular beta-amyloid accumulation and secretase upregulation. Neurosci Lett. 2007; 429:95-100.
14. Wozniak MA, Frost AL, Itzhaki RF. Alzheimer's disease-specific tau phosphorylation is induced by herpes simplex virus type 1. J Alzheimers Dis. 2009; 16:341-350.
15. Wang JP, Kurt-Jones EA, Shin OS, Manchak MD, Levin MJ, Finberg RW. Varicella-zoster virus activates inflammatory cytokines in human monocytes and macrophages *via* Toll-like receptor 2. J Virol. 2005; 79:12658-12666.
16. Shoji H, Umeda S, Kanazawa M, Koga N, Takaki H, Kitsuki S, Matsuoka M, Matsushita T, Fukushima Y, Fukuda K. Herpes zoster central nervous system complication: An increasing trend of acute limbic encephalitis. Intractable Rare Dis Res. 2025; 14:81-84.
17. Benn CS, Netea MG, Selin LK, Aaby P. A small jab - a big effect: Nonspecific immunomodulation by vaccines. Trends Immunol. 2013; 34:431-439.
18. Hakami MA, Khan FR, Abdulaziz O, Alshaghdali K, Hazazi A, Aleissi AF, Abalkhail A, Alotaibi BS, Alhazmi AYM, Kukreti N, Binshaya AS. Varicella-zoster virus-related neurological complications: From infection to immunomodulatory therapies. Rev Med Virol. 2024; 34:e2554.
19. Kennedy PG. Varicella-zoster virus latency in human ganglia. Rev Med Virol. 2002; 12:327-334.
20. Kimura H, Futamura M, Kito H, Ando T, Goto M, Kuzushima K, Shibata M, Morishima T. Detection of viral DNA in neonatal herpes simplex virus infections: Frequent and prolonged presence in serum and cerebrospinal fluid. J Infect Dis. 1991; 164:289-293.
21. Yue J, Yao M. Humoral cytokine levels in patients with herpes zoster: A meta-analysis. J Pain Res. 2024; 17:887-902.
22. Carpenter JE, Clayton AC, Halling KC, Bonthius DJ, Buckingham EM, Jackson W, Dotzler SM, Card JP, Enquist LW, Grose C. Defensive perimeter in the central nervous system: Predominance of astrocytes and astrogliosis during recovery from varicella-zoster virus encephalitis. J Virol. 2016; 90:379-391.
23. Bubak AN, Como CN, Coughlan CM, Johnson NR, Hassell JE, Mescher T, Niemeyer CS, Mahalingam R, Cohrs RJ, Boyd TD, Potter H, Russ HA, Nagel MA. Varicella-zoster virus infection of primary human spinal astrocytes produces intracellular amylin, amyloid-beta, and an amyloidogenic extracellular environment. J Infect Dis. 2020; 221:1088-1097.
24. Itzhaki RF, Lathe R. Herpes viruses and senile dementia: First population evidence for a causal link. J Alzheimers Dis. 2018; 64:363-366.
25. Nour AM, Reichelt M, Ku CC, Ho MY, Heineman TC, Arvin AM. Varicella-zoster virus infection triggers formation of an interleukin-1beta (IL-1beta)-processing inflammasome complex. J Biol Chem. 2011; 286:17921-17933.
26. Chen SY, Suaya JA, Li Q, Galindo CM, Misurski D, Burstin S, Levin MJ. Incidence of herpes zoster in patients with altered immune function. Infection. 2014; 42:325-334.
27. Alvarez JC, Alvarez J, Tinoco J, Mellado P, Miranda H, Ferres M, Forero J, Alvarez C. Varicella-zoster virus meningitis and encephalitis: An understated cause of central nervous system infections. Cureus. 2020; 12:e11583.
28. Jang SO, Lee JH, Chung YJ, Oh HS, Shin M, Kim SO, Hong SP. Chimeric adenovirus-based herpes zoster vaccine with the tPA signal peptide elicits a robust T-cell immune response. Virology. 2024; 600:110243.
29. Voic H, de Vries RD, Sidney J, Rubiro P, Moore E, Phillips E, Mallal S, Schwan B, Weiskopf D, Sette A, Grifoni A. Identification and characterization of $CD4^+$ T cell epitopes after Shingrix vaccination. J Virol. 2020; 94.
30. Vuscan P, Kischkel B, Joosten LAB, Netea MG. Trained immunity: General and emerging concepts. Immunol Rev. 2024; 323:164-185.

Received April 9, 2025; Revised April 27, 2025; Accepted April 30, 2025.

**Address correspondence to:*
Peipei Song, Center for Clinical Sciences, Japan Institute for Health Security, Tokyo 162-8655, Japan; National College of Nursing Japan, Tokyo, Japan.
E-mail: psong@jihs.go.jp

Ying Xia, Department of Neurosurgery, Haikou Affiliated Hospital of Central South University Xiangya School of Medicine, Haikou 570208, China; Integrated Neuroscience Center, Geriatric Hospital of Hainan, Haikou 571100, China.
E-mail: xiaying008@163.com

Correspondence

DOI: 10.5582/ddt.2025.01028

Gepotidacin: The first-in-class triazaacenaphthylene antibiotic approved for the treatment of uncomplicated urinary tract infections

Shasha Hu[1], Haizhou Yu[2], Jianjun Gao[3,*]

[1] Department of Pathology, The Affiliated Hospital of Qingdao University, Qingdao, Shandong, China;
[2] Department of Anesthesiology, Weihai Central Hospital Affiliated with Qingdao University, Weihai, Shandong, China;
[3] Department of Pharmacology, School of Pharmacy, Qingdao University, Qingdao, Shandong, China.

SUMMARY: Uncomplicated urinary tract infection (uUTI) is a common bacterial infection in women. While the condition typically has a favorable prognosis, the widespread use of antibiotics has led to increasingly bacterial resistance, reducing the efficacy of traditional antibiotics. On March 25, 2025, the US Food and Drug Administration approved gepotidacin for the treatment of uUTIs caused by susceptible bacteria in female adult and pediatric patients 12 years of age and older weighing at least 40 kg. Gepotidacin is the first triazaacenaphthylene antibiotic approved for clinical use. It selectively binds to and inhibits both bacterial DNA gyrase and topoisomerase IV, disrupting bacterial DNA replication through a unique mechanism and thereby killing the pathogen. Results of clinical trials indicated the non-inferiority of gepotidacin compared to the current standard therapy, nitrofurantoin. The most frequently reported adverse reaction to gepotidacin was mild to moderate diarrhea. The approval of gepotidacin represents a progress in antibiotic innovation, offering novel perspectives on drug development while spurring global efforts to tackle the escalating challenge of antimicrobial resistance.

Keywords: gepotidacin, triazaacenaphthylene, uncomplicated urinary tract infection, DNA gyrase, topoisomerase IV

Uncomplicated urinary tract infection (uUTI) refers to a urinary tract infection in patients without functional or anatomical abnormalities of the urinary tract, renal impairment, or other underlying conditions that may predispose to infection or lead to severe complications (*1*). uUTI is a common infectious disease and is particularly prevalent among women, with approximately 50% of women experiencing at least one uUTI in their lifetime (*1*). While uUTI generally has a favorable prognosis, the increasing resistance of bacteria to first-line antibiotics like nitrofurantoin has raised the risk of treatment failure (*2*). The development of innovative therapies is critical to addressing challenges in uUTI management, and especially in cases involving drug-resistant infections.

On March 25, 2025, the US Food and Drug Administration approved gepotidacin for the treatment of female adult and pediatric patients 12 years of age and older weighing at least 40 kg with uUTI caused by the following susceptible microorganisms: *Escherichia coli, Klebsiella pneumoniae, Citrobacter freundii complex, Staphylococcus saprophyticus, and Enterococcus faecalis* (*3*). Gepotidacin is the first triazaacenaphthylene antibiotic approved that has bactericidal action by simultaneously inhibiting DNA gyrase and topoisomerase IV — two enzymes critical to bacterial DNA replication (*4*). Due to balanced dual-target inhibition by gepotidacin, bacteria require concurrent mutations in both enzymes to significantly reduce their susceptibility, thereby lowering the likelihood of resistance development.

The FDA approval was primarily based on positive data from two pivotal Phase III trials, EAGLE-2 and EAGLE-3 (*5*). Both were randomized, double-blind, non-inferiority studies evaluating gepotidacin (1,500 mg twice daily for 5 days) versus nitrofurantoin (100 mg twice daily for 5 days) for efficacy and safety in treating uUTI (*5*). The primary endpoint was the therapeutic response rate (clinical and microbiological) at the test-of-cure visit (days 10-13). In EAGLE-2, gepotidacin demonstrated non-inferiority with a treatment success rate of 50.6% versus 47.0% for nitrofurantoin (*5*). In EAGLE-3, gepotidacin achieved statistical superiority with a 58.5% success rate compared to 43.6% for the control (*5*). The most frequently reported adverse event (AE) due to gepotidacin was diarrhea (14% in EAGLE-2

and 18% in EAGLE-3) that was predominantly mild to moderate in severity, and no life-threatening or fatal events were observed (*5*).

Gepotidacin is the first novel oral antibiotic approved to treat uUTI in over two decades, offering a new treatment option, particularly in cases of suboptimal efficacy or emerging resistance to existing therapies. A point worth noting is that in a Phase III trial (EAGLE-1) to treat uncomplicated urogenital gonorrhea, gepotidacin demonstrated non-inferiority to the widely used combination therapy of intravenous ceftriaxone and oral azithromycin, suggesting its potential in treating this condition as well (*6*). More clinical studies need to be conducted to demonstrate the safety and efficacy of gepotidacin in the real world, but the approval of gepotidacin represents a progress in antibiotic innovation, offering novel perspectives on drug development while spurring global efforts to tackle the escalating challenge of antimicrobial resistance.

Funding: None.

Conflict of Interest: The authors have no conflicts of interest to disclose.

References

1. Medina M, Castillo-Pino E. An introduction to the epidemiology and burden of urinary tract infections. Ther Adv Urol. 2019; 11:1756287219832172.
2. Hadidi MF, Alhamami N, Alhakami M, Abdulhamid AS, Alsharif A, Alomari MS, Alghamdi YA, Alshehri S, Ghaddaf AA, Alsenani FM, Almadani H. Antibiotics efficacy in clinical and microbiological cure of uncomplicated urinary tract infection: A systematic review and network meta-analysis. World J Urol. 2024; 42:221.
3. FDA-approved Drugs. *https://www.accessdata.fda.gov/drugsatfda_docs/appletter/2025/218230Orig1s000ltr.pdf* (accessed March 28, 2025)
4. BLUJEPA (gepotidacin) tablets. *https://www.accessdata.fda.gov/drugsatfda_docs/label/2025/218230s000lbl.pdf* (accessed March 28, 2025).
5. Wagenlehner F, Perry CR, Hooton TM, Scangarella-Oman NE, Millns H, Powell M, Jarvis E, Dennison J, Sheets A, Butler D, Breton J, Janmohamed S. Oral gepotidacin versus nitrofurantoin in patients with uncomplicated urinary tract infection (EAGLE-2 and EAGLE-3): Two randomised, controlled, double-blind, double-dummy, phase 3, non-inferiority trials. Lancet. 2024; 403:741-755.
6. GSK News. EAGLE-1 phase III data show potential for gepotidacin as a new oral treatment option for uncomplicated urogenital gonorrhoea (GC) amid growing resistance to existing treatments. *https://www.gsk.com/en-gb/media/press-releases/eagle-1-phase-iii-data-show-potential-for-gepotidacin-as-a-new-oral-treatment-option-for-uncomplicated-gc/* (accessed March 28, 2025).

Received March 29, 2025; Accepted April 5, 2025.

**Address correspondence to:*
Jianjun Gao, Department of Pharmacology, School of Pharmacy, Qingdao University, Qingdao, Shandong, China.
E-mail: gaojj@qdu.edu.cn

Released online in J-STAGE as advance publication April 11, 2025.

Correspondence

DOI: 10.5582/ddt.2025.01031

Fitusiran: The first approved siRNA therapy for hemophilia *via* reducing plasma antithrombin levels

Daoran Lu, Fangzhou Dou, Jianjun Gao*

Department of Pharmacology, School of Pharmacy, Qingdao University, Qingdao, Shandong, China.

SUMMARY: Hemophilia is a coagulation disorder caused by deficiencies in clotting factors and is primarily classified into hemophilia A (factor VIII deficiency) and hemophilia B (factor IX deficiency). Current treatment relies predominantly on replacement therapy, where patients receive clotting factor concentrates either episodically or prophylactically to achieve hemostasis or mitigate bleeding risks. Despite its efficacy, this approach presents limitations, including suboptimal treatment accessibility due to high costs, reduced patient compliance from frequent intravenous administration, and therapeutic failure in patients developing plasma inhibitors. These challenges underscore the need for novel therapeutics addressing unmet clinical demands. On March 28, 2025, the US Food and Drug Administration (FDA) approved fitusiran, a small interfering RNA (siRNA) therapeutic for hemophilia. This first-in-class agent demonstrates pan-hemophilia efficacy by targeting antithrombin to enhance thrombin activity, irrespective of factor VIII/IX deficiency status or plasma inhibitor presence. By pioneering a mechanism of antithrombin suppression, enabling sustained therapeutic action, and facilitating precision monitoring protocols, fitusiran has the potential to redefine hemophilia treatment paradigms.

Keywords: fitusiran, siRNA, replacement therapy, hemophilia, clotting factors

Hemophilia is a genetic bleeding disorder primarily caused by deficiencies in clotting factors, leading to impaired blood coagulation. Based on the specific clotting factor deficiency, it is mainly classified into hemophilia A (factor VIII deficiency) and hemophilia B (factor IX deficiency), accounting for 80-85% and 15-20% of cases, respectively (*1*). The disease follows an X-chromosome-linked recessive inheritance pattern, predominantly affecting males, while females are typically carriers. Globally, the estimated prevalence of hemophilia A is 17.1 per 100,000 males (with severe cases at 6.0 per 100,000 males), and hemophilia B has a prevalence of 3.8 per 100,000 males (*2*).

Current treatment for hemophilia relies on replacement therapy, where patients receive clotting factor concentrates either on-demand or prophylactically to control or prevent bleeding (*3*). While effective, replacement therapy has limitations, including high costs limiting accessibility, poor patient compliance due to frequent intravenous infusions, and treatment failure in cases where plasma inhibitors (neutralizing antibodies) develop (*3*). These challenges highlight the need for novel therapies to address unmet clinical needs.

On March 28, 2025, the US FDA approved fitusiran, the first small interfering RNA (siRNA) therapy for hemophilia (*4*). Administered via subcutaneous injection, fitusiran delivers siRNA targeting the *SERPINC1* gene in liver cells to suppress antithrombin synthesis (*5*). By reducing plasma antithrombin levels, fitusiran enhances thrombin activity to restore hemostasis, regardless of whether patients have a factor VIII (type A) or IX (type B) deficiency or plasma inhibitors. A key advantage is the reduced frequency of dosing compared to traditional clotting factor replacement. The initial dose is 50 mg every two months, with adjustments based on the INNOVANCE antithrombin assay, a companion diagnostic that monitors antithrombin activity to maintain levels within a target range (15-35%), balancing prevention of bleeding and the risk of thrombosis (*6*).

The approval was based on positive results from randomized controlled Phase III clinical trials, including **ATLAS-INH**, **ATLAS A/B**, and **ATLAS-OLE**. The **ATLAS-INH** trial involved 57 adult and pediatric males (age ≥ 12 years) with hemophilia A or B and neutralizing antibodies against factor VIII or factor IX (*6*). Patients in the treatment group received prophylactic fitusiran at a fixed monthly dose of 80 mg, while the control group received on-demand bypassing agents (BPAs) for bleeding events over 9 months (*6*). The **ATLAS A/B** trial involved 120 adult and pediatric

males (age ≥ 12 years) with hemophilia A or B without inhibitory antibodies (*6*). The treatment group received prophylactic fitusiran at a fixed monthly dose of 80 mg, while the control group received on-demand clotting factor concentrates over 9 months (*6*). Due to increased risks of severe thrombotic events, gallbladder disorders, and hepatotoxicity associated with the fixed monthly dose of 80 mg in these trials, the **ATLAS-OLE** study was conducted with a modified dosing regimen (*6*). This study included patients from ATLAS-INH, ATLAS A/B, and a crossover study (ATLAS-PPX) involving patients previously receiving clotting factor concentrates or BPAs. An antithrombin activity-guided dosing strategy (targeting antithrombin activity of 15% to 35%) for fitusiran prophylaxis was adopted for a total of 223 patients who underwent a 6-month dose adjustment period and a 7-month primary efficacy observation period. Results indicated an overall median annualized bleeding rate (ABR) of 3.7 (1.9 for inhibitor-positive patients and 3.8 for inhibitor-negative patients) (*6*). Compared to control group data from ATLAS-INH, the antithrombin-guided dosing strategy significantly reduced ABR in the treatment group (5.1 *vs*. 19.1), indicating that fitusiran prophylaxis is superior to on-demand BPAs in patients with inhibitors (*6*). Similarly, compared to ATLAS A/B control data, the treatment group had a significant reduction in the ABR (9.0 *vs*. 31.4), demonstrating fitusiran's superiority over on-demand clotting factor concentrates in patients without inhibitors (*6*). In terms of safety, fitusiran carries potential risks of thrombotic events, gallbladder disorders, and hepatotoxicity (*6*). Other common adverse reactions included viral infections, common cold symptoms (nasopharyngitis), and bacterial infections (*6*).

Capitalizing on its innovative mechanism of antithrombin suppression, sustained pharmacological activity, and precision monitoring framework, fitusiran has the potential to redefine therapeutic paradigms for hemophilia. Nevertheless, comprehensive validation of its real-world efficacy and safety necessitates further longitudinal clinical evaluation across diverse patient populations.

Funding: None.

Conflict of Interest: The authors have no conflicts of interest to disclose.

References

1. Srivastava A, Brewer AK, Mauser-Bunschoten EP, Key NS, Kitchen S, Llinas A, Ludlam CA, Mahlangu JN, Mulder K, Poon MC, Street A, Treatment Guidelines Working Group on Behalf of The World Federation Of Hemophilia. Guidelines for the management of hemophilia. Haemophilia. 2013; 19:e1-47.
2. Iorio A, Stonebraker JS, Chambost H, Makris M, Coffin D, Herr C, Germini F, Data, Demographics Committee of the World Federation of Hemophilia. Establishing the prevalence and prevalence at birth of hemophilia in males: A meta-analytic approach using national registries. Ann Intern Med. 2019; 171:540-546.
3. Marchesini E, Morfini M, Valentino L. Recent advances in the treatment of hemophilia: A review. Biologics. 2021; 15:221-235.
4. FDA Approves Novel Treatment for Hemophilia A or B, with or without Factor Inhibitors. *https://www.fda.gov/news-events/press-announcements/fda-approves-novel-treatment-hemophilia-or-b-or-without-factor-inhibitors* (Accessed April 1, 2025).
5. Pasi KJ, Rangarajan S, Georgiev P, *et al*. Targeting of antithrombin in hemophilia A or B with RNAi therapy. N Engl J Med. 2017; 377:819-828.
6. QFITLIA (fitusiran) injection, for subcutaneous use. *https://www.accessdata.fda.gov/drugsatfda_docs/label/2025/219019s000lbl.pdf* (Accessed March 30, 2025).

Received April 2, 2025; Accepted April 10, 2025.

**Address correspondence to:*
Jianjun Gao, Department of Pharmacology, School of Pharmacy, Qingdao University, Qingdao, Shandong, China.
E-mail: gaojj@qdu.edu.cn

Released online in J-STAGE as advance publication April 13, 2025.

Correspondence

DOI: 10.5582/ddt.2025.01012

Effects of patient age on the therapeutic effects of GIP/GLP-1 receptor agonists (tirzepatide)

Atsushi Ishimura[1,*], Yutaka Shimizu[2], Naohiro Yabuki[2]

[1] Laboratory of Clinical Pharmacy Assessment, Hoshi University, Tokyo, Japan;
[2] Pharmaceutical Department of Sainokuni Higashi Omiya Medical Center, Saitama, Japan.

SUMMARY: Glucagon-like peptide-1 receptor agonist (GLP-1RA) has attracted attention owing to its hypoglycemic and weight-loss effects, and various dosage forms are available in the market. Recently, glucose-dependent insulin secretion-stimulating polypeptide (GIP), an incretin hormone in the same family as GLP-1, has attracted attention, and tirzepatide, a GIP/GLP-1RA, has been launched. Given the short duration of tirzepatide on the market and the fact that its therapeutic effects in patients of different ages have not been reported, we conducted this study. HbA1c improved significantly in patients aged ≥ 65 years, whereas HbA1c, weight, and LDL cholesterol also improved significantly in patients aged ≤ 64 years when compared between the beginning of use and 3 months following use. Tirzepatide has a hypoglycemic effect regardless of age; however, its weight loss effect may be more pronounced in younger age groups. Therefore, optimal diabetes treatment with tirzepatide should consider the age and weight of patients.

Keywords: tirzepatide, HbA1c, weight

As the global diabetes population continues to increase, prevention and treatment strategies are attracting attention. Type 2 diabetes mellitus (T2DM), in particular, is associated with various factors such as dietary habits and lack of exercise, which not only increase the incidence of the disease but can also lead to social problems such as increased medical costs. In recent years, drug therapy for diabetes mellitus has included, in addition to biguanides and other drugs, dipeptidyl peptidase-4 (DPP-4) inhibitors, sodium glucose cotransporter 2 (SGLT2) inhibitors, and the incretin-related drug glucagon-like peptide-1 (GLP-1). The development and approval of drugs with new mechanisms of action, such as GLP-1 receptor agonists (GLP-1RAs), have led to a dramatic improvement in therapeutic efficacy. Specifically, GLP-1 is rapidly secreted into the blood from L cells in the lower part of the small and large intestines upon stimulation by lipids and carbohydrates in the diet and binds to GLP-1 receptors expressed on the pancreatic beta cell membrane. This promotes insulin secretion in a glucose concentration-dependent manner and lowers blood glucose levels. GLP-1 has been shown not only to improve blood glucose levels but also to have extrapancreatic effects, such as weight loss, improvement of lipid levels (*1*), and hepatoprotective effects (*2*). Therefore, various dosage regimens (daily or weekly) and formulations (injectable or oral) of GLP-1RA are available. In contrast, glucose-dependent insulin secretion-stimulating polypeptide (GIP), an incretin hormone in the same family as GLP-1, is not a target for diabetic drugs because of its lack of insulin secretion-promoting effects and concerns about weight gain due to its fat storage effect (*3*). However, a chimeric peptide that combines elements of both GLP-1 and GIP and can activate both receptors has been demonstrated to exhibit significant weight loss and hypoglycemic effects in patients with obesity and T2DM (*4*), and tirzepatide of GIP/GLP-1RA was recently launched. Tirzepatide has been reported to improve blood glucose levels and weight loss (*5*), which are important in the conventional treatment of diabetes, as well as blood pressure and lipid levels (*6*). However, since tirzepatide is a drug launched in 2023, and there are no reports of its therapeutic effects in patients of different ages, we conducted a study.

The study subjects were patients with T2DM who visited the Department of Diabetes and Metabolism at Sainokuni Higashi Omiya Medical Center as outpatients between April 1, 2024, and September 30, 2024, and were using tirzepatide (Manjaro®). The study population consisted of individuals whose medication remained unchanged for 3 months prior to 3 months following the initiation of tirzepatide use. The age groups for

Table 1. Laboratory results of patients using tirzepatide

	Project	Three months before	Beginning of use	Three months after	*p*-value
Young	Weight (kg)	89.0 ± 15.3	89.1 ± 15.8	86.8 ± 15.5	0.039
(*n* = 14)	HbA1c (%)	8.8 ± 1.7	8.6 ± 1.6	7.3 ± 1.6	< 0.001
	eGFR (mL/min/1.73m^2)	86.7 ± 22.4	82.2 ± 21.4	80.1 ± 17.3	0.304
	HDL cholesterol (mg/dL)	48.8 ± 9.1	52.1 ± 13.0	49.2 ± 11.5	0.108
	LDL cholesterol (mg/dL)	115.6 ± 32.9	104.0 ± 27.0	87.4 ± 25.1	0.006
	Triglycerides (mg/dL)	236.1 ± 145.7	201.6 ± 185.8	186.8 ± 146.4	0.636
Eldrly	Weight (kg)	71.6 ± 14.9	71.6 ± 15.8	70.3 ± 14.3	0.093
(*n* = 12)	HbA1c (%)	8.6 ± 1.1	8.7 ± 1.2	7.9 ± 1.0	< 0.001
	eGFR (mL/min/1.73m^2)	64.7 ± 19.6	62.8 ± 18.6	63.9 ± 17.8	0.665
	HDL cholesterol (mg/dL)	61.6 ± 18.4	61.0 ± 15.7	59.1 ± 14.4	0.304
	LDL cholesterol (mg/dL)	109.5 ± 19.3	106.5 ± 20.4	103.1 + 16.0	0.451
	Triglycerides (mg/dL)	172.3 ± 99.0	202.5 ± 122.5	188.1 + 106.0	0.543

(*p*-value: beginning of use *vs* 3 months after)

comparison were elderly (65 years and older) and young (64 years and younger), according to the World Health Organization (WHO) definition of the elderly. The variables assessed in this study were weight (kg), HbA1c (%), eGFR (mL/min/1.73 m^2), HDL cholesterol (mg/dL), LDL cholesterol (mg/dL), and triglycerides (mg/dL) 3 months before, at the beginning of tirzepatide use, and following 3 months of tirzepatide use. This study was conducted retrospectively. Test values are shown as mean ± standard deviation, and statistical analysis was performed by paired-samples t-test with a significance level of 5%. This study conformed to the provisions of the Declaration of Helsinki, and which was approved by the Ethics Committee of Sainokuni Higashi Omiya Medical Center (Approval number: 65).

Twenty-six patients received tirzepatide during the study period: 14 in the young group and 12 in the elderly group. The dose of tirzepatide was 2.5 mg for all patients. Table 1 presents the survey results. There were no significant differences in any of the measured variables between the 3 months before and at the beginning of use in both the young and elderly groups (p-values not shown). However, a comparison between the beginning of use and 3 months following use showed significant improvements in weight, HbA1c, and LDL in the young group, whereas only HbA1c improved in the elderly group.

The results of this study show that the elderly group only showed an improvement in blood glucose levels, whereas the young group showed an improvement not only in blood glucose levels but also in weight and LDL, thus suggesting that the drug may be more effective in younger age groups. Although it has been reported that the appetite suppression effect of tirzepatide is responsible for the reduction in weight and body fat mass (*7*), the difference in weight improvement between the older and younger groups in this study may be due to the difference in weight of the study subjects. Although not shown in the data, 11 of 14 (78.6%) patients at the young age group weighed 80 kg or more compared with 4 of 11 (36.4%) patients in the elderly group. This may be due to the fact that the young age group ate more than the elderly, and thus the appetite suppression effect of tirzepatide may have resulted in a significant reduction in weight. Regarding the difference in the improvement of LDL cholesterol, a decrease in weight and LDL cholesterol occurred simultaneously with the intake of high doses of green tea extract (*8*), suggesting a close relationship between weight loss and LDL reduction. This suggests that LDL cholesterol may have been improved by a decrease in food intake (weight loss) due to the appetite suppression effect of tirzepatide. In contrast, an improvement in blood glucose levels was observed in the elderly group, although there was no significant decrease in weight, suggesting that tirzepatide is a useful drug for treating diabetes mellitus. Tirzepatide (Manjaro®) has been reported to improve blood glucose and reduce weight better than dulaglutide (*9*), the most widely prescribed GLP-1RA in Japan (*10*). We also reported that tirzepatide may be more effective than dulaglutide in inhibiting the progression of renal impairment (*11*). Furthermore, tirzepatide, like dulaglutide, is a formulation that can be administered once a week and uses a dedicated, single-use injector, Ateos®, thus making it unnecessary to set doses or attach needles, and it can be used regardless of age. These aforementioned results suggest that tirzepatide has a hypoglycemic effect regardless of age, but that weight loss may be more pronounced in heavier young patients. Therefore, it is desirable to select a drug that considers not only the patient's age but also his or her weight.

This study is limited by the small number of cases obtained from a single medical institution and the lack of detailed patient backgrounds. Therefore, the results of this study may not reflect the overall picture of T2DM during tirzepatide use. It is necessary to conduct ongoing studies at multiple institutions with a large

number of patients to further improve the reliability of the study.

Acknowledgements

We thank all study participants.

Funding: None.

Conflict of Interest: The authors have no conflicts of interest to disclose.

References

1. Nambu T, Murakami T, Matsuda Y, Matsuo K, Yonemitsu S, Muro S, Oki S. Long-term efficacy of liraglutide in the treatment of patients with type 2 diabetes. J Jpn Diabetes Soc. 2014; 57:153-161.
2. Oshinoi T, Saito M, Oshinoi Y, Nakata M, Ofuchi K, Katoh M. Long-term administration of a GLP-1 receptor agonist liraglutide improves hepatic function and fibrosis in Japanese patients with type 2 diabetes mellitus. Med Consult New Rem. 2019; 56:729-735.
3. Bailey CJ. GIP analogues and the treatment of obesity-diabetes. Peptides. 2020; 125:170202.
4. Holst JJ, Rosenkilde MM. GIP as a therapeutic target in diabetes and obesity: Insight from incretin co-agonists. J Clin Endocrinol Metab. 2020; 105:e2710-e2716.
5. Dutta D, Surana V, Singla R, Aggarwal S, Sharma M. Efficacy and safety of novel twincretin tirzepatide a dual GIP and GLP-1 receptor agonist in the management of type-2 diabetes: A Cochrane meta-analysis. Indian J Endocrinol Metab. 2021; 25:475-489.
6. Kanbay M, Copur S, Siriopol D, Yildiz AB, Gaipov A, Raalte DH, Tuttle KR. Effect of tirzepatide on blood pressure and lipids: A meta-analysis of randomized controlled trials. Diabetes Obes Metab. 2023; 25:3766-3778.
7. Yabe D, Kawamori D, Seino Y, Oura T, Takeuchi M. Change in pharmacodynamic variables following once-weekly tirzepatide treatment versus dulaglutide in Japanese patients with type 2 diabetes (SURPASS J-mono substudy). Diabetes Obes Metab. 2023; 25:398-406.
8. Chen I, Liu C, Chiu J, Hsu C. Therapeutic effect of high-dose green tea extract on weight reduction: A randomized, double-blind, placebo-controlled clinical trial. Clin Nutr. 2016; 35:592-599.
9. Ishimura A, Takizawa Y. Glucagon-like peptide-1 (GLP-1) receptor agonist usage and safety study. Jpn J Appl Ther. 2024; 19:36-42.
10. Kubota M, Yamamoto K, Yoshiyama S. Effect on hemoglobin A1c (HbA1c) and body weight after discontinuation of tirzepatide, a novel glucose-dependent insulinotropic peptide (GIP) and glucagon-like peptide-1 (GLP-1) receptor agonist: A single-center case series study. Cureus. 2023; 15:e46490.
11. Ishimura A, Kumakura H. Effect of switching from dulaglutide to tirzepatide on blood glucose and renal function. Drug Discov Ther. 2024; 18:323-324.

Received February 19, 2025; Revised March 23, 2025; Accepted April 22, 2025.

**Address correspondence to:*
Atsushi Ishimura, Laboratory of Clinical Pharmacy Assessment, Hoshi University, 2-4-41 Ebara, Shinagawa-ku, Tokyo 142-8501, Japan.
E-mail: ishimura.atsushi@hoshi.ac.jp

Released online in J-STAGE as advance publication April 27, 2025.

DD&T
Drug Discoveries & Therapeutics

Guide for Authors

1. Scope of Articles

Drug Discoveries & Therapeutics (Print ISSN 1881-7831, Online ISSN 1881-784X) welcomes contributions in all fields of pharmaceutical and therapeutic research such as medicinal chemistry, pharmacology, pharmaceutical analysis, pharmaceutics, pharmaceutical administration, and experimental and clinical studies of effects, mechanisms, or uses of various treatments. Studies in drug-related fields such as biology, biochemistry, physiology, microbiology, and immunology are also within the scope of this journal.

2. Submission Types

Original Articles should be well-documented, novel, and significant to the field as a whole. An Original Article should be arranged into the following sections: Title page, Abstract, Introduction, Materials and Methods, Results, Discussion, Acknowledgments, and References. Original articles should not exceed 5,000 words in length (excluding references) and should be limited to a maximum of 50 references. Articles may contain a maximum of 10 figures and/or tables. Supplementary Data are permitted but should be limited to information that is not essential to the general understanding of the research presented in the main text, such as unaltered blots and source data as well as other file types.

Brief Reports definitively documenting either experimental results or informative clinical observations will be considered for publication in this category. Brief Reports are not intended for publication of incomplete or preliminary findings. Brief Reports should not exceed 3,000 words in length (excluding references) and should be limited to a maximum of 4 figures and/or tables and 30 references. A Brief Report contains the same sections as an Original Article, but the Results and Discussion sections should be combined.

Reviews should present a full and up-to-date account of recent developments within an area of research. Normally, reviews should not exceed 8,000 words in length (excluding references) and should be limited to a maximum of 10 figures and/or tables and 100 references. Mini reviews are also accepted, which should not exceed 4,000 words in length (excluding references) and should be limited to a maximum of 5 figures and/or tables and 50 references.

Policy Forum articles discuss research and policy issues in areas related to life science such as public health, the medical care system, and social science and may address governmental issues at district, national, and international levels of discourse. Policy Forum articles should not exceed 3,000 words in length (excluding references) and should be limited to a maximum of 5 figures and/or tables and 30 references.

Case Reports should be detailed reports of the symptoms, signs, diagnosis, treatment, and follow-up of an individual patient. Case reports may contain a demographic profile of the patient but usually describe an unusual or novel occurrence. Unreported or unusual side effects or adverse interactions involving medications will also be considered. Case Reports should not exceed 3,000 words in length (excluding references).

Communications are short, timely pieces that spotlight new research findings or policy issues of interest to the field of global health and medical practice that are of immediate importance. Depending on their content, Communications will be published as "Comments" or "Correspondence". Communications should not exceed 1,500 words in length (excluding references) and should be limited to a maximum of 2 figures and/or tables and 20 references.

Editorials are short, invited opinion pieces that discuss an issue of immediate importance to the fields of global health, medical practice, and basic science oriented for clinical application. Editorials should not exceed 1,000 words in length (excluding references) and should be limited to a maximum of 10 references. Editorials may contain one figure or table.

News articles should report the latest events in health sciences and medical research from around the world. News should not exceed 500 words in length.

Letters should present considered opinions in response to articles published in *Drug Discoveries & Therapeutics* in the last 6 months or issues of general interest. Letters should not exceed 800 words in length and may contain a maximum of 10 references. Letters may contain one figure or table.

3. Editorial Policies

For publishing and ethical standards, *Drug Discoveries & Therapeutics* follows the Recommendations for the Conduct, Reporting, Editing, and Publication of Scholarly Work in Medical Journals issued by the International Committee of Medical Journal Editors (ICMJE, *https://icmje.org/recommendations*), and the Principles of Transparency and Best Practice in Scholarly Publishing jointly issued by the Committee on Publication Ethics (COPE, *https://publicationethics.org/resources/guidelines-new/principles-transparency-and-best-practice-scholarly-publishing*), the Directory of Open Access Journals (DOAJ, *https://doaj.org/apply/transparency*), the Open Access Scholarly Publishers Association (OASPA, *https://oaspa.org/principles-of-transparency-and-best-practice-in-scholarly-publishing-4*), and the World Association of Medical Editors (WAME, *https://wame.org/principles-of-transparency-and-best-practice-in-scholarly-publishing*).

Drug Discoveries & Therapeutics will perform an especially prompt review to encourage innovative work. All original research will be subjected to a rigorous standard of peer review and will be edited by experienced copy editors to the highest standards.

Ethical Approval of Studies and Informed Consent: For all manuscripts reporting data from studies involving human participants or animals, formal review and approval, or formal review and waiver, by an appropriate institutional review board or ethics committee is required and should be described in the Methods section. When your manuscript contains any case details, personal information and/or images of patients or other individuals, authors must obtain appropriate written consent, permission and release in order to comply with all applicable laws and regulations concerning privacy and/or security of personal information. The consent form needs to comply with the relevant legal requirements of your particular jurisdiction, and please do not send signed consent form to *Drug Discoveries & Therapeutics* to respect your patient's and any other individual's privacy. Please instead describe the information clearly in the Methods (patient consent) section of your manuscript while retaining copies of the signed forms in the event they should be needed. Authors should also state that the study conformed to the provisions of the Declaration of Helsinki (as revised in 2013, *https://wma.net/what-we-do/medical-ethics/declaration-of-helsinki*). When reporting experiments on animals, authors should indicate whether the institutional and national guide for the care and use of laboratory animals was followed.

Reporting Clinical Trials: The ICMJE (*https:// icmje.org/recommendations/browse/publishing-and-editorial-issues/clinical-trial-registration.html*) defines a clinical trial as any research project that prospectively assigns people or a group of people to an intervention, with or without concurrent comparison or control groups, to study the relationship between a health-related intervention and a health outcome. Registration of clinical trials in a public trial registry

at or before the time of first patient enrollment is a condition of consideration for publication in *Drug Discoveries & Therapeutics*, and the trial registration number will be published at the end of the Abstract. The registry must be independent of for-profit interest and publicly accessible. Reports of trials must conform to CONSORT 2010 guidelines (*https://consort-statement.org/consort-2010*). Articles reporting the results of randomized trials must include the CONSORT flow diagram showing the progress of patients throughout the trial.

Conflict of Interest: All authors are required to disclose any actual or potential conflict of interest including financial interests or relationships with other people or organizations that might raise questions of bias in the work reported. If no conflict of interest exists for each author, please state "There is no conflict of interest to disclose".

Submission Declaration: When a manuscript is considered for submission to *Drug Discoveries & Therapeutics*, the authors should confirm that 1) no part of this manuscript is currently under consideration for publication elsewhere; 2) this manuscript does not contain the same information in whole or in part as manuscripts that have been published, accepted, or are under review elsewhere, except in the form of an abstract, a letter to the editor, or part of a published lecture or academic thesis; 3) authorization for publication has been obtained from the authors' employer or institution; and 4) all contributing authors have agreed to submit this manuscript.

Initial Editorial Check: Immediately after submission, the journal's managing editor will perform an initial check of the manuscript. A suitable academic editor will be notified of the submission and invited to check the manuscript and recommend reviewers. Academic editors will check for plagiarism and duplicate publication at this stage. The journal has a formal recusal process in place to help manage potential conflicts of interest of editors. In the event that an editor has a conflict of interest with a submitted manuscript or with the authors, the manuscript, review, and editorial decisions are managed by another designated editor without a conflict of interest related to the manuscript.

Peer Review: *Drug Discoveries & Therapeutics* operates a single-anonymized review process, which means that reviewers know the names of the authors, but the authors do not know who reviewed their manuscript. All articles are evaluated objectively based on academic content. External peer review of research articles is performed by at least two reviewers, and sometimes the opinions of more reviewers are sought. Peer reviewers are selected based on their expertise and ability to provide quality, constructive, and fair reviews. For research manuscripts, the editors may, in addition, seek the opinion of a statistical reviewer. Every reviewer is expected to evaluate the manuscript in a timely, transparent, and ethical manner, following the COPE guidelines (*https://publicationethics.org/files/cope-ethical-guidelines-peer-reviewers-v2_0.pdf*). We ask authors for sufficient revisions (with a second round of peer review, when necessary) before a final decision is made. Consideration for publication is based on the article's originality, novelty, and scientific soundness, and the appropriateness of its analysis.

Suggested Reviewers: A list of up to 3 reviewers who are qualified to assess the scientific merit of the study is welcomed. Reviewer information including names, affiliations, addresses, and e-mail should be provided at the same time the manuscript is submitted online. Please do not suggest reviewers with known conflicts of interest, including participants or anyone with a stake in the proposed research; anyone from the same institution; former students, advisors, or research collaborators (within the last three years); or close personal contacts. Please note that the Editor-in-Chief may accept one or more of the proposed reviewers or may request a review by other qualified persons.

Language Editing: Manuscripts prepared by authors whose native language is not English should have their work proofread by a native English speaker before submission. If not, this might delay the publication of your manuscript in *Drug Discoveries & Therapeutics*.

The Editing Support Organization can provide English proofreading, Japanese-English translation, and Chinese-English translation services to authors who want to publish in *Drug Discoveries & Therapeutics* and need assistance before submitting a manuscript. Authors can visit this organization directly at *https://www.iacmhr.com/iac-eso/support.php?lang=en. IAC-ESO* was established to facilitate manuscript preparation by researchers whose native language is not English and to help edit works intended for international academic journals.

Copyright and Reuse: Before a manuscript is accepted for publication in *Drug Discoveries & Therapeutics*, authors will be asked to sign a transfer of copyright agreement, which recognizes the common interest that both the journal and author(s) have in the protection of copyright. We accept that some authors (*e.g.*, government employees in some countries) are unable to transfer copyright. A JOURNAL PUBLISHING AGREEMENT (JPA) form will be e-mailed to the authors by the Editorial Office and must be returned by the authors by mail, fax, or as a scan. Only forms with a hand-written signature from the corresponding author are accepted. This copyright will ensure the widest possible dissemination of information. Please note that the manuscript will not proceed to the next step in publication until the JPA Form is received. In addition, if excerpts from other copyrighted works are included, the author(s) must obtain written permission from the copyright owners and credit the source(s) in the article.

4. Cover Letter

The manuscript must be accompanied by a cover letter prepared by the corresponding author on behalf of all authors. The letter should indicate the basic findings of the work and their significance. The letter should also include a statement affirming that all authors concur with the submission and that the material submitted for publication has not been published previously or is not under consideration for publication elsewhere. The cover letter should be submitted in PDF format. For an example of Cover Letter, please visit: Download Centre (*https://www.ddtjournal.com/downcentre)*.

5. Submission Checklist

The Submission Checklist should be submitted when submitting a manuscript through the Online Submission System. Please visit Download Centre (*https://www.ddtjournal.com/downcentre)* and download the Submission Checklist file. We recommend that authors use this checklist when preparing your manuscript to check that all the necessary information is included in your article (if applicable), especially with regard to Ethics Statements.

6. Manuscript Preparation

Manuscripts are suggested to be prepared in accordance with the "Recommendations for the Conduct, Reporting, Editing, and Publication of Scholarly Work in Medical Journals", as presented at *http://www.ICMJE.org*.

Manuscripts should be written in clear, grammatically correct English and submitted as a Microsoft Word file in a single-column format. Manuscripts must be paginated and typed in 12-point Times New Roman font with 24-point line spacing. Please do not embed figures in the text. Abbreviations should be used as little as possible and should be explained at first mention unless the term is a well-known abbreviation (*e.g.* DNA). Single words should not be abbreviated.

Title page: The title page must include 1) the title of the paper (Please note the title should be short, informative, and contain the major key words); 2) full name(s) and affiliation(s) of the author(s), 3) abbreviated names of the author(s), 4) full name, mailing address, telephone/fax numbers, and e-mail address of the corresponding author; 5) author contribution statements to specify the individual contributions of all authors to this manuscript, and 6) conflicts of interest (if you have an actual or potential conflict of interest to disclose, it must be included as a footnote on the title page of the manuscript; if no conflict of interest

exists for each author, please state "There is no conflict of interest to disclose").

Abstract: The abstract should briefly state the purpose of the study, methods, main findings, and conclusions. For article types including Original Article, Brief Report, Review, Policy Forum, and Case Report, a one-paragraph abstract consisting of no more than 250 words must be included in the manuscript. For Communications, Editorials, News, or Letters, a brief summary of main content in 150 words or fewer should be included in the manuscript. For articles reporting clinical trials, the trial registration number should be stated at the end of the Abstract. Abbreviations must be kept to a minimum and non-standard abbreviations explained in brackets at first mention. References should be avoided in the abstract. Three to six key words or phrases that do not occur in the title should be included in the Abstract page.

Introduction: The introduction should provide sufficient background information to make the article intelligible to readers in other disciplines and sufficient context clarifying the significance of the experimental findings.

Materials/Patients and Methods: The description should be brief but with sufficient detail to enable others to reproduce the experiments. Procedures that have been published previously should not be described in detail but appropriate references should simply be cited. Only new and significant modifications of previously published procedures require complete description. Names of products and manufacturers with their locations (city and state/country) should be given and sources of animals and cell lines should always be indicated. All clinical investigations must have been conducted in accordance with the Declaration of Helsinki (as revised in 2013, *https://wma.net/what-we-do/medical-ethics/declaration-of-helsinki*). All human and animal studies must have been approved by the appropriate institutional review board(s) and a specific declaration of approval must be made within this section.

Results: The description of the experimental results should be succinct but in sufficient detail to allow the experiments to be analyzed and interpreted by an independent reader. If necessary, subheadings may be used for an orderly presentation. All Figures and Tables should be referred to in the text in order, including those in the Supplementary Data.

Discussion: The data should be interpreted concisely without repeating material already presented in the Results section. Speculation is permissible, but it must be well-founded, and discussion of the wider implications of the findings is encouraged. Conclusions derived from the study should be included in this section.

Acknowledgments: All funding sources (including grant identification) should be credited in the Acknowledgments section. Authors should also describe the role of the study sponsor(s), if any, in study design; in the collection, analysis, and interpretation of data; in the writing of the report; and in the decision to submit the paper for publication. If the funding source had no such involvement, the authors should so state.

In addition, people who contributed to the work but who do not meet the criteria for authors should be listed along with their contributions.

References: References should be numbered in the order in which they appear in the text. Citing of unpublished results, personal communications, conference abstracts, and theses in the reference list is not recommended but these sources may be mentioned in the text. In the reference list, cite the names of all authors when there are fifteen or fewer authors; if there are sixteen or more authors, list the first three followed by *et al*. Names of journals should be abbreviated in the style used in PubMed. Authors are responsible for the accuracy of the references. The EndNote Style of *Drug Discoveries & Therapeutics* could be downloaded at **EndNote** (*https://www.ddtjournal.com/examples/Drug_Discoveries_Therapeutics.ens*).

Examples are given below:

Example 1 (Sample journal reference):

Nakata M, Tang W. Japan-China Joint Medical Workshop on Drug Discoveries and Therapeutics 2008: The need of Asian pharmaceutical researchers' cooperation. Drug Discov Ther. 2008; 2:262-263.

Example 2 (Sample journal reference with more than 15 authors):

Darby S, Hill D, Auvinen A, *et al*. Radon in homes and risk of lung cancer: Collaborative analysis of individual data from 13 European case-control studies. BMJ. 2005; 330:223.

Example 3 (Sample book reference):

Shalev AY. Post-traumatic stress disorder: Diagnosis, history and life course. In: Post-traumatic Stress Disorder, Diagnosis, Management and Treatment (Nutt DJ, Davidson JR, Zohar J, eds.). Martin Dunitz, London, UK, 2000; pp. 1-15.

Example 4 (Sample web page reference):

World Health Organization. The World Health Report 2008 – primary health care: Now more than ever. *https://apps.who.int/iris/handle/10665/43949* (accessed September 23, 2022).

Tables: All tables should be prepared in Microsoft Word or Excel and should be arranged at the end of the manuscript after the References section. Please note that tables should not in image format. All tables should have a concise title and should be numbered consecutively with Arabic numerals. If necessary, additional information should be given below the table.

Figure Legend: The figure legend should be typed on a separate page of the main manuscript and should include a short title and explanation. The legend should be concise but comprehensive and should be understood without referring to the text. Symbols used in figures must be explained. Any individually labeled figure parts or panels (A, B, *etc*.) should be specifically described by part name within the legend.

Figure Preparation: All figures should be clear and cited in numerical order in the text. Figures must fit a one- or two-column format on the journal page: 8.3 cm (3.3 in.) wide for a single column, 17.3 cm (6.8 in.) wide for a double column; maximum height: 24.0 cm (9.5 in.). Please make sure that artwork files are in an acceptable format (TIFF or JPEG) at minimum resolution (600 dpi for illustrations, graphs, and annotated artwork, and 300 dpi for micrographs and photographs). Please provide all figures as separate files. Please note that low-resolution images are one of the leading causes of article resubmission and schedule delays.

Units and Symbols: Units and symbols conforming to the International System of Units (SI) should be used for physicochemical quantities. Solidus notation (*e.g*. mg/kg, mg/mL, mol/mm^2/min) should be used. Please refer to the SI Guide *www.bipm.org/en/si/* for standard units.

Supplemental data: Supplemental data might be useful for supporting and enhancing your scientific research and *Drug Discoveries & Therapeutics* accepts the submission of these materials which will be only published online alongside the electronic version of your article. Supplemental files (figures, tables, and other text materials) should be prepared according to the above guidelines, numbered in Arabic numerals (*e.g*., Figure S1, Figure S2, and Table S1, Table S2) and referred to in the text. All figures and tables should have titles and legends. All figure legends, tables and supplemental text materials should be placed at the end of the paper. Please note all of these supplemental data should be provided at the time of initial submission and note that the editors reserve the right to limit the size

and length of Supplemental Data.

7. Online Submission

Manuscripts should be submitted to *Drug Discoveries & Therapeutics* online at *https://www.ddtjournal.com/login*. Receipt of your manuscripts submitted online will be acknowledged by an e-mail from Editorial Office containing a reference number, which should be used in all future communications. If for any reason you are unable to submit a file online, please contact the Editorial Office by e-mail at *office@ddtjournal.com*

8. Accepted Manuscripts

Page Charge: Page charges will be levied on all manuscripts accepted for publication in *Drug Discoveries & Therapeutics* (Original Articles / Brief Reports / Reviews / Policy Forum / Communications: $140 per page for black white pages, $340 per page for color pages; News / Letters: a total cost of $600). Under exceptional circumstances, the author(s) may apply to the editorial office for a waiver of the publication charges by stating the reason in the Cover Letter when the manuscript online.

Misconduct: *Drug Discoveries & Therapeutics* takes seriously all allegations of potential misconduct and adhere to the ICMJE Guideline (*https://icmje.org/recommendations*) and COPE Guideline (*https://publicationethics.org/files/Code_of_conduct_for_journal_editors.pdf*). In cases of suspected research or publication misconduct, it may be necessary for the Editor or Publisher to contact and share submission details with third parties including authors' institutions and ethics committees. The corrections, retractions, or editorial expressions of concern will be performed in line with above guidelines.

(As of December 2022)

Drug Discoveries & Therapeutics
Editorial and Head Office
Pearl City Koishikawa 603,
2-4-5 Kasuga, Bunkyo-ku,
Tokyo 112-0003, Japan.
E-mail: office@ddtjournal.com